AXONAL GROWTH, NEURONAL DAMAGE AND EPILEPTOGENESIS

by

Bin Xu

Graduate Program in

Psychology

Submitted in partial fulfillment

Of the requirements for the degree of

Doctor of Philosophy

Faculty of Graduate Studies

McMaster University

Hamilton, Ontario

July 2001-07-17

DOCTOR OF PHYLOSOPHY (2001)
(psychology)

McMaster University
Hamilton, Ontario

TITLE: Axonal growth, neuronal damage and epileptogenesis

AUTHOR: Bin Xu, B. M. (Beijing Medical University)

SUPERVISOR: Professor R.J. Racine

Number of Pages: (xvii), 218

ABSTRACT

Neuronal damage and synaptic reorganization are two common neuropathological changes repeatedly detected in human epilepsy patients and animal models of epilepsy. To date, the relationship between cell loss, axonal growth, and epileptogenesis remains unclear. However, it is proposed that neuronal damage within the hilar area and mossy fiber sprouting alter the balance of excitation and inhibition within the epileptic brain, and contribute to the development of seizures. The axonal sprouting is suggested to be triggered by either cell loss or by excessive neuronal activity, or both.

In the present study, we tested epileptogenesis and seizure-related morphological changes in several rat strains, including the Wistar strain and Long-Evans hooded strains, and the kindling-prone (FAST) and kindling-resistant strains (SLOW) created at McMaster University. These strains were tested using both KA- and pilocarpine-induced status epilepticus models.

Although the Wistar and the Long-Evans hooded strains respond similarly to KA or pilocarpine-induced SE, we found that the Wistar rat strain showed a reliable neuronal loss and more severe neuronal growth, while the Long-Evans strain showed no detectable neuron damage and moderate axonal sprouting. The mossy fiber system was also significantly different between the FAST and the SLOW strains, and responded differently to seizure activity. This evidence suggests that genetic factors might be important for the induction of seizure-related morphological changes.

In addition to the strain differences in seizure development, axonal growth and neuronal loss, it has been shown that epilepsy and synaptic reorganization can be developed independently of gross neuronal loss within the hilar area. Thus, it is clear that

neuronal damage within the hilus is neither a crucial prerequisite, nor a necessary consequence of epileptogenesis or axonal growth. Our results favour the postulate that epilepsy-related axonal growth is at least partly triggered by excessive neuronal activity and contributes to the development of seizures.

We have also tested the modulation of axonal growth and kindling development by infusing factors that affect axonal patterning and pathway finding during neuronal development, such as Neurotrophin-3 (NT-3), or axonal guidance molecules, the Eph receptors and the ephrins, into adult CNS. Continuous infusion of NT-3, or agents that affect the function of EphA receptors and ephrins, alters kindling epileptogenesis and the extent and pattern of mossy fiber sprouting in adult rats. Thus, we have shown that such factors preserve their functions into adulthood, and regulate activity-dependent axonal growth in the kindling model. Agents that affect the function of these molecules dramatically alter both kindling induction and mossy fiber sprouting. Therefore, it is likely that neurotrophic factors and axonal guidance molecules preserve their function into adulthood, modulating neuronal plasticity, epileptogenesis and synaptic reorganization in adult CNS.

ACKNOWGEDGEMENTS

I am grateful to Dr. Ronald Racine for his excellent supervision, generous support, insightful advice, and constant encouragement over the past few years. The opportunity to work and study in his laboratory has been enjoyable and rewarding. I would also like to express my sincere appreciation to the members of my advisory committee, Dr. S. Becker and Dr. K. Murphy, for their advice.

I am also indebted to Dr. Margaret Fahnestock for her valuable insights, patience and encouragement.

I wish to express my sincere appreciation to Ms. B Michalski, who assisted in preparing the western blotting in the NT-3 project, Dr. S. Li and Dr. A. Brown who helped me with in situ hybridization and double blinded dark-field measurements in the Eph project, and Dr. R. Gerlai for his advice on the Eph manuscript.

Finally, my husband Jian Zhao shared the difficulty and successes, and supported me throughout the entire course of this project.

TABLE OF CONTENTS

LIST OF TABLES

LIST OF FIGURES

LIST OF ABBREVIATIONS

AD: afterdischarge

BDNF: brain derived neurotrophic factor

CNS: central nervous system

DG: dentate gyrus

EEG: electroencephalogram

GABA: γ-aminobutyric acid

GAD: glutamic acid decarboxylase

GC: granule cell

GDNF: glial cell line-derived neurotrophic factor

IML: inner molecular layer

KA: kainic acid

LTP: long-term potentiation

MES: maximal electroshock

MFS: mossy fiber sprouting

NGF: nerve growth factor

NMDA: N-methyl-D-aspartate

NT-3: neurotrophin-3

SE: status epilepticus

SRS: spontaneous recurrent seizure

TLE: temporal lobe epilepsy

Trk: tyrosine kinase receptor

CHAPTER 1 GENERAL INTRODUCTION

1 Clinical Epilepsy

1. 1 Basic Concepts of Epilepsy

Epilepsy is one of the most common chronic disorders of the central nervous system (CNS). Approximately 1-2% of the world population, and about 300,000 Canadians have epilepsy (McNamara, 1999). Epilepsy is not a disease, but a collection of diverse syndromes, characterized by sudden, excessive and temporary discharge of certain population(s) of neurons. It can be either hereditary (primary epilepsy), or secondary to other brain dysfunctions (secondary epilepsy). A wide range of serious brain injuries, such as major head trauma, stroke, hemorrhage, infection, tumors and vascular malformations, can lead to epilepsy.

1. 2 Classification of Seizures

Epileptic seizures can be classified into two basic types: partial (focal) and generalized seizures (Table 1). If only part of one cerebral hemisphere is involved in the early stages of the seizure, it is classified as partial. If both hemispheres are involved at the onset, the seizure is classified as generalized.

The manifestation of a partial seizure can be motor, sensory, autonomic or cognitive, depending on which brain structures are engaged in the abnormal discharge (Table 1). For example, a discharge in the motor cortex results in uncontrolled rhythmical contraction of body muscles, while discharge in occipital cortex induces visual illusions and hallucinations (Dreifuss, 1997). Partial seizures can be further

Table 1. 1 International classification of seizures [adapted from Dreifuss et al. (1997)].

I. PARTIAL
A. Simple Partial Seizures
1. Motor
2. Somatosensory or sensory
3. Autonomic
4. With psychic symptoms (cognitive)
B. Complex Partial Seizures
C. Partial Seizures Evolving to Secondarily Generalized Seizures
II. GENERALIZED SEIZURES
A. Absence Seizures (Petit Mal)
B. Myoclonic Seizures
C. Clonic Seizures
D. Tonic Seizures
E. Atonic Seizures
F. Tonic-Clonic Seizures (Grand Mal)
III. UNCLASSFIED EPILEPTIC SEIZURES

classified as simple partial seizures, in which consciousness is not impaired, and complex partial seizures, with impairment of consciousness. The complex partial seizure is the most common type in human patients. It is also referred to as "temporal lobe seizures" or "limbic seizures", since the initial discharge usually arises from limbic structures of the temporal lobes (Gloor et al., 1982). See Figure 1.2 for the anatomy of the limbic system. Partial seizures may eventually spread to a wide range of brain areas and evolve into generalized seizures, which, in this case; are called "secondary generalized seizures" (Dreifuss, 1997).

The generalized seizures can also be further divided into several subtypes, including absence (petit mal), myoclonic, clonic, tonic, tonic-clonic (grand mal), and atonic seizures (Table 1). The *absence seizures* involve a sudden loss of consciousness, which is manifested by a blank stare and a brief interruption of ongoing activities. The absence seizures may or may not be accompanied by other symptoms. The *myoclonic seizures* are characterized by sudden, brief jerks of a group of muscles, once or multiple times. This type of seizure is different from the *clonic seizures*, in which the muscular contractions (jerks) are prolonged, repetitive, and rhythmical. The *tonic seizures* involve muscle contractions that are sustained, resulting in a stiffening of the body. The *atonic seizures*, on the other hand, consist of a sudden diminution of muscle tone, leading to the relaxation and dropping of jaw and limbs. The *tonic-clonic seizures*, also called grand mal, are the most frequently observed type of generalized seizures. A typical grand mal usually starts with loss of consciousness, and tonic contraction of the body (the tonic phase), followed by rhythmical limb contraction (the clonic phase). Around 10 to 25% of

seizures fail to fit into any of the seizure types described above, and therefore are categorized as unclassified (Dreifuss, 1997, Table 1).

Most epileptic seizures last only a few seconds to a few minutes. During an isolated seizure episode, the human brain rapidly recruits seizure suppressing mechanisms, which terminate the epilepsy and result in a refractory period (Treiman and Heinemann, 1997). Under certain circumstances, however, the seizure-terminating mechanisms fail, and the pathophysiologic changes from the previous seizures run into the onset of the next seizure. As a consequence, a prolonged seizure state, called status epilepticus (SE), occurs. The clinical definition of status epilepticus is continuous seizures, or intermittent seizure activities without regaining of consciousness, lasting more than 30 minutes (DeLorenzo, 1990). SE is one of the most common and severe forms of epilepsy (DeLorenzo et al., 1995).

1. 3 The Electroencephalogram of the Epileptic Patient

The electroencephalogram (EEG) records the difference of electrical potentials (voltage) between two points of the scalp. During seizures, a group of neurons synchronously fire and depolarize. When depolarizating, positive ions, such as sodium (Na^+) and potassium (K^+), flow into these neurons, leaving an electrically negative extracellular space in the active region. The scalp electrodes can detect the differences in electrical potential between the discharge region (negative) and adjacent tissue (positive). A transient, large, and abnormally synchronous depolarization across a large population of cells is recorded in the EEG as a sudden change in the voltage difference, typically referred to as a "spike". The rhythmic repetition of these transients are seen in the EEG

as an epileptic discharge, or episode, which serves as a landmark of epileptiform activity (Fisher, 1989; Niedermeyer, 1987). Note that the frequency and the pattern of the EEG discharges vary in correspondence with the subtypes of seizures. Absence seizures are associated with symmetrical 2 to 4 Hz slow spike-wave discharges, while the frequency of the bilateral spike-wave can increase up to 10 or more cycles per second during tonic-clonic seizures. In partial seizures, the initial epileptic discharges are generated within a specific brain region and cannot always be detected on the scalp (Dreifuss, 1997). Nevertheless, the EEG remains the primary clinical tool for diagnosing epilepsy, locating the site of seizure discharges, and assessing the requirement for neurosurgical treatment.

2 Animal Models of Seizures

A large number of animal models of epilepsy have been developed over the last century (Fisher, 1989, Table 2). These models serve as important tools for the investigation of the basic mechanisms of epilepsy and the search for new therapeutic approaches. In these models, seizure activity or sensitivity can be established by chemical or electrical stimulation, or by gene manipulation.

2. 1 Epilepsy Induced by Electrical Stimulation

Electrical stimulation can generate either focal or generalized seizures in intact animals. The maximal electroshock (MES) model is widely used for the screening of anticonvulsants (Fisher, 1989). Typically, high-intensity (50-150 mA), high-frequency electrical pulses are delivered to experimental animals via ear-clip or corneal electrodes, resulting in a seizure response ranging from facial clonus to representative tonic-clonic

seizures. Less intense or shorter electrical stimuli can induce epileptiform discharge and partial seizures, with or without secondary generalized tonic-clonic seizures (Ajmone-marsan and Abraham, 1965).

2. 1. 1 Kindling

Kindling is another model that employs electrical stimulations. Unlike the MES model, the kindling stimuli are applied to specific brain structures via implanted electrodes. Initially, the electrical stimulation may trigger a brief epileptiform discharge, as monitored by EEG recording, without behavioral convulsions. These evoked discharges are usually called afterdischarges (ADs, Figure 1.1). With subsequent stimuli, the ADs become prolonged and more complex. Behavioral seizures begin to occur during the ADs and become increasingly severe over time. Ultimately, the same low-intensity stimulation that was initially subconvulsive now results in intense partial and secondary generalized clonic seizures (Goddard, 1967). This kindling effect was discovered by Delgado and colleagues in 1958 and subsequently became the focus of investigation in hundreds of laboratories around the world. It has become a well-established animal model for human complex partial seizures and has also served as a popular model for long-term plastic changes.

Kindling is usually initiated by electrical stimulation of the amygdala, but most regions of forebrain can be kindled. Typically, bipolar stimulating electrodes are implanted in the amygdala or elsewhere in the brain. Daily electrical stimulus trains are applied via the electrodes, using parameters such as 0.2- 1.0 mA at 60 Hz for 1-2 seconds (Adams et al., 1997). The initial stimulus usually does not evoke any detectable

Table 2 Animal models of the epilepsies [adapted from Fisher, 1989].

Simple Partial Seizures	**Generalized Absence Seizures**
Topical convulsants (e.g. GABA antagonists, anticholinergics, and cholinergics)	Thalamic Stimulation
Electrical stimulation	Systemic penicillin
Cortically implanted metals (e.g. aluminum hydroxide, cobalt, and zinc)	Intraventricular opiates
Complex Partial Seizures	**Generalized Tonic-Clonic Seizures**
Kindling	Genetic models (e.g. photosensitive baboons, genetically epilepsy-prone rats)
Kainic acid	Maximal electroshock
Tetanus toxin	Chemical Convulsants (e.g. GABA antagonists, adenosine antagonists, glutamate agonists, and acetylcholine agonists)
Pilocarpine	Metabolic derangements (e.g. hypoxia, hypoglycemia, hypercarbia, uremia, drug withdrawal, high temperature)
Status Epilepticus	
Systemic administration of chemical convulsants	
Recurrent electrical stimulation	

Figure 1.1 Afterdischarges elicited by kindling stimulation. The initial epileptiform afterdischarge triggered by the first stimulation (day 1) is short and simple. With subsequent stimuli (day 11), the ADs become prolonged and complex. Sti. : kindling stimulation; AD: afterdischarge.

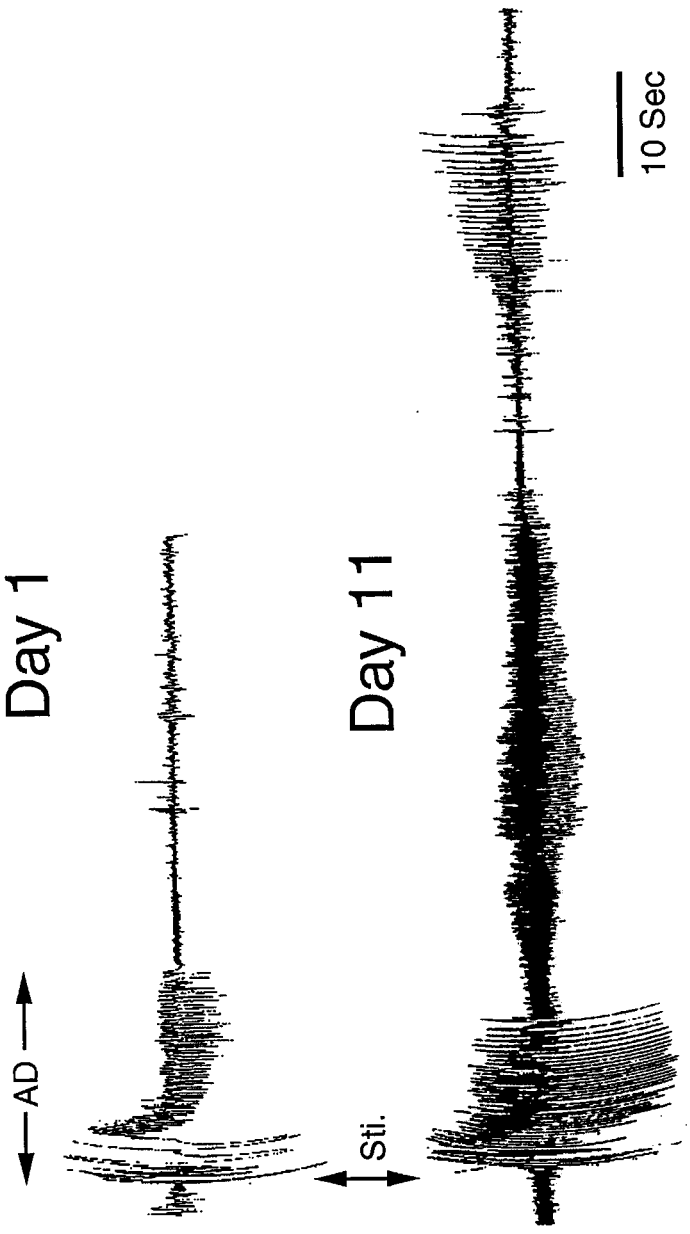
Day 1
Day 11
AD
Sti.
10 Sec

behavioral change, although it may be sufficient to induce an epileptiform afterdischarge. The afterdischarge is recorded by electroencephalography (EEG), providing a graphical recording of the focal electrical seizure. After a few days of stimulation, the kindling stimulus begins to elicit behavioral seizures, and the afterdischarges become progressively more complex and prolonged. Racine (1972) has classified kindling-induced behavioral seizure into 5 stages: Class 1 = facial clonus (mouth and facial twitches); Class 2 = facial clonus and rhythmic head nodding; Class 3 = facial clonus, head nodding and contralateral forelimb clonus; Class 4 = facial clonus, head nodding, forelimb clonus and clonic rearing; Class 5 =facial clonus, head nodding, forelimb clonus, clonic rearing and falling (loss of postural control).

Once 2-3 consecutive stage 5 seizures have developed, the animal is considered to be "fully kindled", although additional stimulation can lead to still stronger responses and the appearance of spontaneous seizures (Pinel and Rovner, 1978; Wada et al., 1974). The fully kindled animals exhibit a long-lasting or even permanent state of seizure susceptibility, in which relatively low intensity stimulation trains can trigger epileptiform afterdischarges. In addition, these fully kindled animals typically show sustained enhanced sensitivity to the kindling stimulus. Even after a 12-month stimulus-free period, 1 or 2 stimulations is sufficient for these animals to elicit maximal behavioral and electroencephalographic responses (Racine, 1969; Wada et al., 1974).

A consistent pathological feature of kindling is the mossy fiber sprouting (MFS) of dentate granule cells (Cavazos et al., 1991). Normally, axons of dentate gyrus granule cells, namely mossy fibers, make synapses on the CA3 pyramidal cells, the excitatory mossy cells and inhibitory GABAergic neurons in the hilar regions. The mossy fibers provide very little innervation of targets within the granule cell or molecular layers of the

dentate gyrus (Frotscher et al., 1994; Figure 1.2). Sprouting and reorganization of the mossy fiber pathway has been found to occur reliably in human TLE patients and in many animal models of epilepsy, including kindling, MES, the kainic acid model, and the status epilepticus models. The collaterals of the mossy fibers are induced to sprout into the inner molecular layer (IML) of the dentate gyrus, which is the dendritic layer of the granule cells, and into the stratum oriens of the CA3 region, which contains the basal dendrites of the CA3 pyramidal cells (Sutula et al., 1989).

The Timm method is a histological technique that is used to demonstrate mossy fibers in the dentate gyrus, because of their high concentration of Zn^{2+} (Haung, 1973). Thus, Timm staining serves as a method to identify the trajectory of mossy fiber axons and the location of their synaptic terminals. Using Timm straining, Cavazos et al (1991) have shown that the sprouted collaterals of mossy fibers start to appear in the IML 4 days after the kindling starts. The mossy fiber sprouting (MFS) develops in parallel with the evolution of kindling-induced behavioral seizures, and appears to become permanent.

The mechanisms and the consequences of mossy fiber sprouting remain unclear. However, it has been proposed that the development of mossy fiber sprouting is activity dependent since it is preferentially induced by high-frequency, but not low-frequency, stimulation (Sutula et al., 1988). Moreover, data from several studies (Sutula et al., 1988; Wuarin and Dudek, 2001) suggested that mossy fiber sprouting may lead to the formation of new excitatory recurrent connections between dentate granule cells, which may play an important role in the development and maintenance of epileptogenesis.

It remains controversial whether kindling results in cell damage. Cavazos et al. (1994) have revealed a significant neuronal loss in the hilar region as a consequence of three episodes of kindling-induced generalized tonic-clonic seizures. The neuronal

damage progresses with repeated seizures. After 150 stage 5 seizures, as high as a 50% decrease of neuronal density is observed in the hilus, the CA1 region, piriform cortex, and the entorhinal cortex (Cavazos et al., 1994). In contrast, several other studies (Adams et al., 1997; Goddard et al., 1986; Represa et al., 1989) have not detected any neuronal loss or structural lesions, even in fully kindled animals.

Neuropathological alternations after seizures, such as mossy fiber sprouting and neuronal damage, and their relationship with epileptogenesis will be discussed in more detail in a subsequent section.

2. 2 Chemically Induced Seizures

When applied topically or systemically, certain chemical agents can interfere with normal neuronal excitability and cause seizures in intact animals. Such chemicals can be classified into inhibitory amino acid receptor blockers, excitatory amino acid receptor agonists, hormones, and metals. The behavioral seizures elicited by these convulsants range from subtle and hard-to-detect absence seizures to severe, long-lasting tonic-clonic episodes. Some drugs, when applied in various doses or via different routes, can produce a variety of epileptic responses. For example, penicillin is a common convulsant that can selectively block γ-aminobutyric acid (GABA)-mediated inhibitory postsynaptic currents (Wong and Prince, 1979). When applied topically to the cortex, penicillin elicits focal rhythmical epileptiform spikes that last for hours, serving as an acute model of simple partial seizures (Walker and Johnson, 1945). On the other hand, after systemic administration of high-dose penicillin, animals develop episodes of absence seizures and myoclonic seizures. Eventually, tonic-clonic seizures may occur (Fossieck and Parker,

1974; Prince and Farrell, 1969). Thus, parenteral penicillin can serve as a model for several types of generalized seizures.

Many chemical convulsants, when applied in high doses, can elicit status epilepticus in intact animals. These chemicals include glutamate agonists (e.g. kainic acid) (Lothman and Collines, 1981), acetylcholine agonists (e.g. pilocarpine) (Turski et al., 1983), GABA antagonists (e.g. bicuculline) (Meldrum and Horton, 1971), and adenosine antagonists (e.g. methylxanthines) (Treiman and Heinemann, 1997).

2. 2. 1 Kainic Acid

Kainic acid (KA) is an analog of the excitatory neuronal transmitter, glutamate (GLU), which was first isolated from the seaweed Digenea simplex (Shinozaki and Konishi, 1970). When applied intracerebrally (dose ranges from 10ng to 2μg) or systemically (8-12 mg/kg subcutaneously [s.c.], intraperitoneally [i.p.], or intravenously [i.v.]), KA readily produces seizures, including generalized convulsive seizures (Ben-Ari et al., 1979, 1980 a, b, 1981). The manifestation of behavioral seizures depends in part on the application route and dosage of KA (Speak, 1994). In general, KA treatment can induce acute limbic seizures and status epilepticus, but the long-term effects include spontaneous seizures and neuronal damage similar to that observed in human temporal lobe epilepsy (TLE). KA injection thus serves as a model for TLE (complex partial seizures with secondary generalized seizures), as well as status epilepticus.

Typically, 5 to 10 minutes after the systemic administration of KA, animals assume a catatonic posture with immobility and staring. 15 to 30 min after KA injection, myoclonic twitches of face, head and forelimbs, facial clonus, head nodding, and intermittent forelimb clonus occur. The myoclonic or clonic seizures gradually propagate to rear limbs until

severe intermittent generalized clonic seizures with rearing and loss of postural control take place. Eventually, animals develop status epilepticus, and exhibit continuous seizures for hours. Gradually, the seizures decline, and the animals return to a normal state, but remain exhausted for many hours (Speak, 1994). After the termination of KA-induced acute seizures and SE, spontaneous recurrent seizures (SRS) can develop and last for weeks or even months. Like kindling, KA treatment causes a more seizure-susceptible state, facilitating subsequent electrical amygdala kindling (Feldblum and Ackermann, 1987).

KA treatment induces both acute edema and necrosis in a variety of brain regions. 90 minutes after the KA-induced acute seizures, the volume of cerebral hemispheres, especially the temporal lobes, increases dramatically. Transient diffuse brain edema with swelling of astrocytes occurs (Ben-Ari et al, 1980 a, b). In addition, local or systemic administration of KA elicits massive necrosis in the piriform cortex, the entorhinal cortex, the amygdaloid complex, the lateral septum, the hippocampus, and several thalamic nuclei (Ben-Ari et al., 1979). Within the hippocampus, neuronal degeneration is found in the dentate gyrus, as well as the CA1 and CA3 pyramidal cells (Ben-Ari et al., 1979, 1980 a, b). The epileptogenesis and the cell damage after KA injection have been shown to depend on both the direct neurotoxic action of KA, and the sustained activation of excitatory pathways induced by KA treatment (Sperk, 1994).

KA receptors, the high-affinity receptors for kainic acid, are distributed in a high concentration in the mossy fibers, the hilus and the CA3 pyramidal layer -- three areas that are most sensitive to KA-induced cell damage (Berger and Ben-Ari, 1983). Thus, it is postulated that direct activation of KA receptors by kainic acid, coupled with the evoked glutamate release from the mossy fibers, produces an overactivation of KA receptors and excitotoxic cell damage in these areas (Represa et al., 1987).

In addition to the direct toxic effects, it is suggested that the KA-induced sustained activation of the excitatory glutamate system, and the resulting seizures, also contribute to the cell damage observed after KA treatment. Removal of excitatory glutamatergic and cholinergic afferents to the hippocampus or lesions of the mossy fiber system prior to KA treatment inhibit seizure development and protect neurons from degeneration (Nadler, 1981; Okazaki and Nadler, 1988). In addition, anticonvulsant drugs, such as GABAergic agonist diazepam and Phenobarbital, which dramatically reduce the severity and duration of KA-induced seizures, can rescue neurons in hippocampal regions and amygdala from necrosis (De Bonnel and De Montigny, 1983).

Kainic acid treatment also induces extensive sprouting of mossy fiber collaterals into the inner molecular layer of the dentate gyrus. This sprouting effect progressively increases during the first two to three months after pilocarpine-induced SE, and reaches plateau after three months (Mathern et al., 1993).

The relationship between neuronal loss, axonal growth, and epileptogenesis will be discussed in detail in a subsequent section.

2. 2. 2 Pilocarpine

Inhibition of cholinergic function has been shown to retard or block epileptogenesis in several epilepsy models. For example, application of atropine, a cholinergic antagonist, reverses some of the behavioral effects observed after intraventricular kainic acid (Kleinrok and Turski, 1979), retards the development of electrical kindling (Arnold et al., 1973), and inhibits carbachol-induced chemical kindling (Wasterlain and Jonec, 1983). Such evidence promoted the studies of acetylcholine agonists as convulsants. For example, systemic administration of the muscarinic cholinergic agonist, pilocarpine, at doses of 300

to 400 mg/kg in rats or mice, produces prolonged motor seizures and status epilepticus (Turski et al., 1983a).

The behavioral progression of seizures and the brain damage after pilocarpine treatment are strikingly similar to the symptoms observed after KA injection. Several minutes after pilocarpine injection, animals develop staring and tremor, which gradually evolve into mild-to-severe limbic seizures, and eventually culminate in long-lasting status epilepticus. These behaviors are accompanied by strong salivation and production of foam at the mouth, often mixed with blood. Five to ten days after pilocarpine-induced SE, spontaneous seizures resembling stage 4/5 kindled seizures appear, occurring intermittently for as long as 6 months (Turski et al., 1983a).

Similar to KA treatment, systemic administration of high doses of pilocarpine results in widespread neuronal damage in the hippocampus, thalamus, piriform cortex, amygdala, and entorhinal cortex (Turski et al., 1983b). Other brain regions that are affected by pilocarpine treatment include olfactory cortex, neocortex and substantia nigra (Turski et al., 1983b). At the electron microscopic level, pilocarpine seizures induce massive swelling of dendrites and astroglial cells (Clifford et al., 1987). Extensive mossy fiber sprouting also occurs after pilocarpine treatment (Mello et al., 1993). The mossy fiber sprouting in the inner molecular layer, as visualized by Timm staining, begins 4 days after pilocarpine-induced SE, increases over time, and reaches its maximum after 100 days (Mello et al. , 1993).

In vitro studies have shown that application of acetylcholine (ACh) itself does not produce a neurotoxic effect (Sloviter and Dempster, 1985; Olney et al., 1986). The neuronal damage observed in the pilocarpine model is believed to be elicited by excessive neuronal excitability and seizure afterdischarge. It has been proposed that cholinergic

agonists facilitate burst discharges of hippocampal glutamatergic neurons, triggering and maintaining seizure activities, and therefore lead to cell damage and axonal growth indirectly via the seizure-related excitotoxic effect (Olney et al. , 1986).

2. 3 Genetic Models of Epilepsy

Two major approaches have been taken in the study of the genetic models of epilepsy. The first approach involves the selective inbreeding or isolation of special strains with lowered seizure thresholds. Such strains are now available in a variety of species, including mouse (Suzuki and Nakamoto, 1977), rat (Van Luitelaar and Coenen, 1986; Dailey et al. , 1989; Racine et al. , 1999) and baboon (Naquet et al. , 1995). Because these strains usually display a lowered seizure threshold to a variety of modalities, it is suggested that multiple genes might be involved in their seizure susceptibility. Hence, these strains are referred to as "polygenic models of seizures" (Noebels, 1999). The other approach is to create epileptic phenotypes with mutations in a single locus. The mutation either occurs spontaneously (Noebels, 1999), or is created by inserting or deleting a special gene using recombinant DNA techniques (Rosahl et al., 1995; Tecott et al., 1995).

The photosensitive *papio papio* baboon is one of the most well-known polygenic epilepsy models. When these baboons are exposed to intermittent photic stimulation, bilaterally synchronous spike-and-wave discharges occur, which is associated with clonus of the facial and neck musculatures (Naquet et al., 1995). In the most severe cases, animals may suffer generalized tonic-clonic seizures (Naquet et al., 1995). A significant decrease of GABA and an increase of excitatory amino acids have been detected in the cerebrospinal fluid (CSF) of these baboons (Lloyd et al., 1986).

Several strains of epilepsy-prone rats have been developed independently by various labs. Dailey et al. (1987) selectively inbred two colonies of genetically epilepsy-prone rats (GEPR), the moderate seizure GEPR colony (GEPR-3) and the severe seizure GEPR colony (GEPR-9), based on their seizure predisposition. Auditory stimulation results in running episodes, followed by generalized clonic seizures in the GEPR-3 rats, or by severe generalized tonic-clonic seizures in the GEPR-9 animals. Analysis of neuronal transmission has identified alterations of noradrenergic (NE), serotonergic (5-HT), and GABAergic pathways. A widespread deficit of NE and 5-HT, as well as a decrease of GABAergic activity in the auditory system, have been detected in GEPR colonies (Dailey et al., 1989; Faingold and Naritoku, 1992).

More recently, two special strains, the kindling-prone (FAST), and kindling-resistant (SLOW) strains have been developed and selectively inbred from a cross of the Wistar and the Long-Evans Hooded rats, based on the amygdala kindling rates (Racine et al., 1999). The kindling rate is accelerated in the FAST strain, while it is retarded in the SLOW strain (Racine et al., 1999). Dramatic differences have been found between these two strains in the measurement of inter-hemisphere propagation, paired-pulse facilitation and GABA receptor subunit composition (Racine et al., 1999; McIntyre et al., 1999a). The characteristics of these two strains will be discussed more thoroughly in Chapter 3.

Mutation of one single locus gene is sufficient to produce generalized seizures and epileptiform spike-wave discharge (Mercer et al., 1991; Rosahl et al., 1995; Tecott et al., 1995). These animal models offer a direct opportunity to identify and locate the "epilepsy genes". To date, several single locus mutants have been developed, including the *dilute lethal* mouse (mutation of the dilute coat color gene on chromosome 9), the *tottering* (mutation occurs on chromosome 8), the *stargazer* (mutation on chromosome 15), and the

lethargic mutant (mutation on chromosome 2) (Tecott et al., 1995; Noebels et al., 1995, 1999).

The genetic models described above serve as powerful tools in defining the genetics of epilepsy, identifying the basic mechanisms of seizures, and developing new therapeutic approaches.

3 General Neuropathology of Epilepsy

Several neuropathological changes are consistently detected in the epileptic brain and in animal models of epilepsy. Such changes include neuronal damage, axonal growth, neurogenesis, reactive gliosis, and alterations in protein and receptor expression. It is hypothesized that these neuropathological alterations contribute to the development and maintenance of epilepsy.

3. 1 Normal Hippocampal Anatomy

Human TLE patients and various animal models of epilepsy usually display severe pathological changes in the limbic system, especially the hippocampal formation (Houser, 1999; Mathern et al., 1997), suggesting that the limbic system might play an important role in temporal lobe seizures and epileptogenesis.

The concept of the limbic system was first put forth by Broca (1878), and included structures located at the border of the ventricular system. Subsequently, Pepez (1937) and Maclean (1952) redefined the limbic system as a circuit including the hypothalamus, anterior thalamus, cingulate cortex and hippocampus. Among these structures, the hippocampus has been shown to express a high degree of neuronal plasticity, and contribute to a wide range of psychological and pathological phenomena, such as learning,

memory, Alzheimer's disease and temporal lobe seizures (Schwartzkroin and McIntyre, 1997).

As shown in Figure 1.2, the hippocampus consists of the hippocampus proper (CA1-3) and the dentate gyrus. The dendrites of the dentate gyrus granule cells receive input from the entorhinal cortex via the perforant pathway. The axons of these granule cells, called mossy fibers, project to the apical dendrites of CA3 pyramidal cells. The Schaffer collaterals, which are the axons of CA3 pyramidal cells, synapse onto CA1 pyramidal cells. The axons of CA1 pyramidal cells send output to the subiculum (Schwartzkoin and McIntyre, 1997).

The dentate gyrus consists of three layers, the polymorphic layer (also called the hilus), the granular layer (the stratum granulosum), and the molecular layer (the stratum moleculare). The principle neurons of the dentate gyrus are the granule cells, which are densely packed in the granular layer. Their dendrites reach through the molecular layer. The outer two thirds (the outer molecular layer, OML) of the dendritic field receives input from the perforant pathway, while the inner one third (the inner molecular layer, IML) receives projections from the septal area and cells within the hilus. There are also around 3,500 GABAergic inhibitory basket cells, located at the interface between the granule cell layer and the polymorphic layer, whose axon terminals synapse onto the dendrites of granule cells. In addition, there are roughly 32,500 neurons within the hilus. Among them, around 30% are somatostatin and GAD-labeled (GABAergic interneurons). The remaining two thirds are heterogeneous, including excitatory mossy cells (for review see Amaral et al., 1990). The mossy cells receive input from granule cells via mossy fibers, and send their axons to the dendrites of granule cells and inhibitory basket cells in the IML. Besides the two major excitatory cell types, granule cells and mossy cells, there are many types of

inhibitory basket cells and interneurons located in the dentate gyrus. Most of these inhibitory neurons are GABAergic, and are believed to form synapses on the granule cells or other interneurons (for review see Amaral et al., 1990).

The mossy fibers, which constitute the axons of DG granule cells, synapse onto the dendrites of CA3 pyramidal cells, the mossy cells, and the GABAergic interneurons within the hilar area. The synaptic connection (terminals) between mossy fibers and CA3 pyramidal cells are sparse, large, powerful, and terminate close to the soma of CA3 neurons (Claiborne et al., 1986; O'Relly et al., 1994). In contrast, the mossy fibers form a large number of small, weak synapses on the GABAergic hilar interneurons, which may exert extensive feedback inhibition on DG granule cells, resulting in a low activation level for the dentate gyrus (Ascady et al. , 2000). Such a high level of inhibition might keep the dentate gyrus resistant to seizure activitiy and serve as a gate for seizure propagation (Heinemann et al. , 1992)

The principle neurons of the hippocampal gyrus are the pyramidal neurons, located in a layer called the stratum pyramidale. Each pyramidal cell has two types of dendrite, a thick apical dendrite that passes through the stratum lucidum, the stratum radiatum and the stratum lacunosum-moleculare, and several basal dendrites located in the stratum oriens. The mossy fiber projections run along the stratum lucidum, making contact with the apical dendrites of CA3 pyramidal cells.

3. 2 Neuronal Loss

Neuronal loss is by far one of the most frequently observed pathological alterations in human TLE patients (Houser, 1999). Early autopsy studies by Bouchet and Cazauvielh (1825) showed that the hippocampal region of TLE patients was shrunken, hypocellular,

Figure 1.2 Structure of the limbic system and the hippocampus. (A) An illustration of the limbic system in the human brain. The structures of the limbic system include the hypothalamus, anterior thalamus, cingulate cortex, and hippocampus. **(B)** The structure of the rat hippocampus. The hippocampus comprises the dentate gyrus (DG) and the hippocampus proper (CA1, CA2 and CA3 regions). The DG can be divided into three layers: the molecular layer, the granule cell layer, and the polymorphic layer or hilus, (gray region). The molecular layer contains dendrites of the DG granule cells (open circles), and can be divided into two subregions. The outer molecular layer receives inputs from the entorhinal cortex via the perforant pathway, while the inner molecular layer receives associative input from hilar mossy cells and inhibitory basket cells. The major cell type of the CA3 region is the pyramidal cell (black triangle), which is located in stratum pyramidale. The apical dendrites of the pyramidal cells extend through stratum lucidum, stratum radiatum and stratum lacunosum-moleculare. The axons of granule cells (mossy fibers) synapse onto the apical dendrites in the stratum lucidum and the neurons located in the hilar area (the darkly shaded area represents the regions to which the mossy fibers project) (Adapted from Houser, 1999a).

A

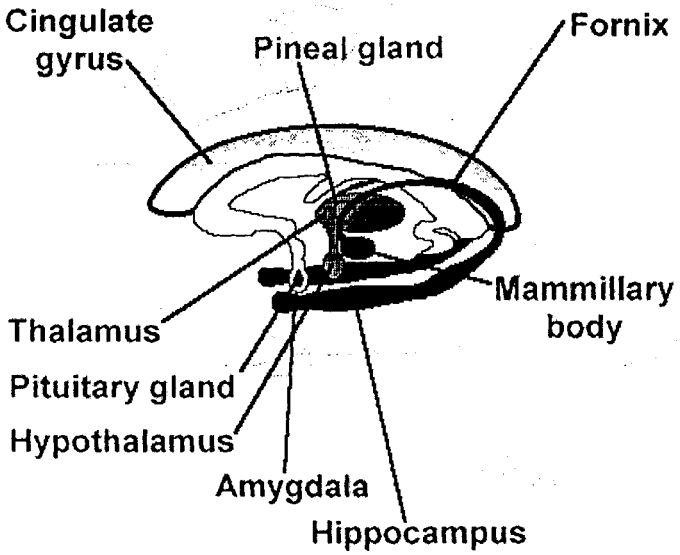

The Limbic System

B

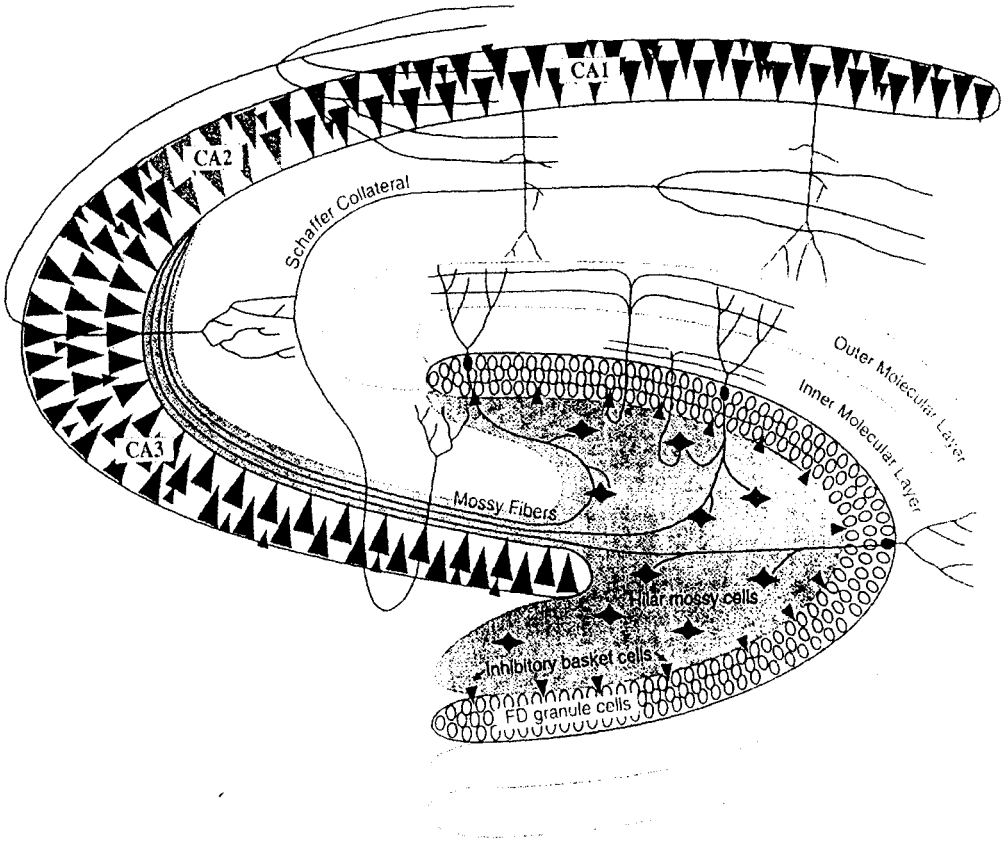

A

Figure 1.3 Neuronal damage in the hilar region. **(A)** The hilus of a naïve animal, showing the normal distribution of neurons within the hilus. **(B)** The hilus after KA-induced SE, a severe decrease of neuronal density is detected in the hilus region. H: hilus.

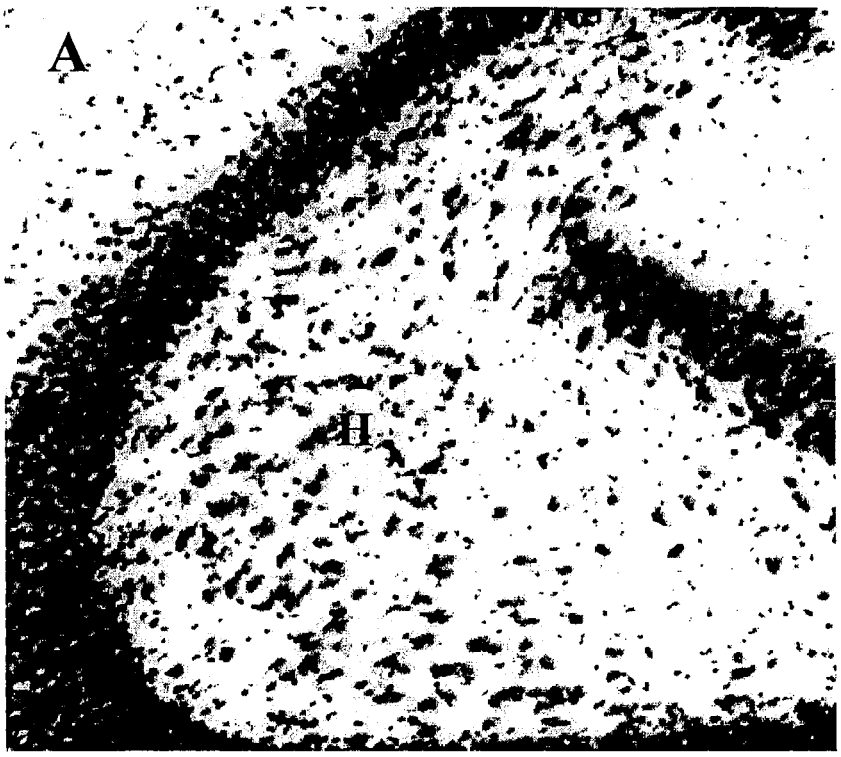
A
H

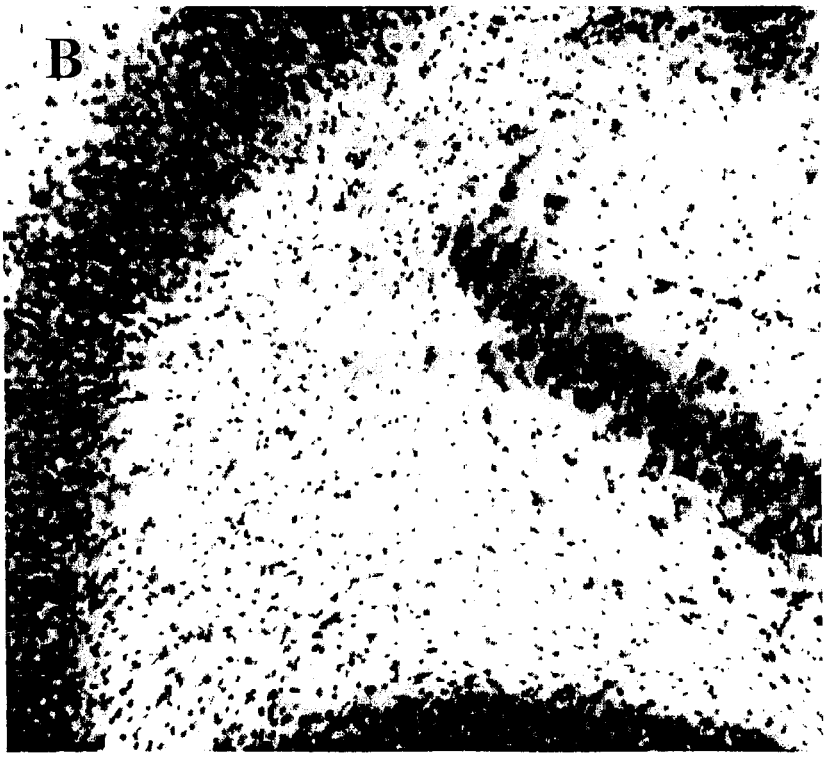
B

and gliotic. They named this pathological change hippocampal sclerosis. Since then, hippocampal sclerosis has been considered an anatomical hallmark of TLE.

Detailed microscopic observation has detected severe cell loss in the dentate gyrus and CA fields in hippocampal sclerosis (Sommer, 1880; Bratz, 1899). The pattern of neuronal loss varies dramatically among patients. The areas that are profoundly damaged include (1) the CA1 region and the prosubiculum (also called Sommer's section), and (2) the hilus and part of the CA3 regions (also called end folium). The remaining regions of the hippocampus, including the DG granule cells, the CA2 pyramidal cells, and the subicular neurons, are are resistant to seizures and remain reasonably well preserved.

Margerison and Corsellis (1966) have found that the existence of hippocampal sclerosis is strongly correlated with the occurrence of temporal lobe epilepsy. Around 85% of patients who suffered TLE symptoms developed neuronal loss in either the CA1 region or the hilus, while hippocampal sclerosis occurred in only 30-40% of patients who showed no signs of TLE.

Studies on animal models of epilepsy suggest that the pattern and extent of neuronal loss in hippocampal regions are partially determined by the modes of seizure induction, as well the severity and the duration of the seizure episodes (Houser, 1999). For example, pilocarpine treatment usually induces only end-folium sclerosis. However, with an increase in dosage, and the severity of SE, pilocarpine can elicit substantial neuronal loss in the Sommer's section (Liu et al. , 1994).

Despite the considerable variation of the pattern of cell loss observed, neuronal loss in the hilus is detected consistently in around 80% of human TLE patients and various animal models of epilepsy, including KA or pilocarpine-induced seizures, MES, and kindling models (Houser, 1999; Figure 1.3). The hilus contains many types of non-

pyramidal neurons, which are functionally connected to the DG granule cells. These neurons include the excitatory mossy cells and a wide variety of inhibitory interneurons. It has been suggested the susceptibility to seizure activities is dramatically different among different types of neurons. After pilocarpine-induced seizures, neurons expressing the glutamic acid decarboxylase (GAD) messenger RNA (mRNA), a special marker of GABAergic cells, decrease by 40% in the hilar area (Obenaus et al., 1993). In contrast, immunohistochemistry and in situ hybridization studies of GAD protein or mRNA have shown that the GABAergic basket cells located along the inner border of the DG granule cell layers and the GABAergic neurons in the CA1 regions are resistant to excitotoxic damage and well preserved in human TLE patients or after KA or pilocarpine induced seizures (Obenaus et al., 1993; Franck et al., 1988; Babb et al., 1989). Since most of the GABAergic interneurons within the hilus form functional connection with the dendrites of the DG granule cells, it has been suggested that severe loss of these neurons may result in a decrease of inhibition and contribute to the hyperexcitation of epileptic brain (Houser, 1999).

Neuronal loss in the polymorphic layer of the DG is not restricted to GABAergic neurons. Physiologic and pathological studies have shown that the excitatory mossy cells are quite sensitive to excitotoxic neuronal damage. Mossy cells are believed to send their excitatory inputs to the inhibitory DG basket cells. Removal of excitatory inputs to the basket cells after mossy cell loss, therefore, might cause a malfunction or suppression of these basket cells and an increase on granule cell excitability (Houser, 1999).

The pathological origins of hippocampal sclerosis remain unclear, but it has been suggested that the occurrence of hippocampal sclerosis is related to transient ischemia during seizure onset, trauma or brain damage early in life, repeated seizures, and/or a

prolonged seizure episode involving loss of consciousness for more than 30 minutes (for review see Mathern et al. , 1997). Such evidence suggests that brain trauma, ischemia and prolonged hyperexcitability contribute to the development of hippocampal sclerosis.

Studies on animal models show that hours after a severe episode of SE induced by KA or pilocarpine treatment, massive necrosis starts to appear within the hilar area (Turski et al., 1983b; Ben-Ari et al., 1979, 1980 a,b). In addition, the extent of neuronal loss is correlated with the occurrence of spontaneous seizures in the KA and pilocarpine models, and with repeated electrical stimulations in the kindling model (Turski et al., 1983b; Ben-Ari et al., 1979, 1980 a,b; Cavazos et al., 1994). These results provide further evidence that prolonged or repeated episodes of seizures may result in neuronal damage in the hippocampal formation, especially the hilar area.

The relationship between hippocampal sclerosis and epileptogenesis remains controversial. The fact that temporal lobe resections including hippocampus cure 80% TLE patients (Tailairach and Bancaud, 1974) strongly implies the association of hippocampal neuropathology and epileptogenesis. One of the prevalent hypotheses, "the dormant basket cell hypothesis" (Figure 1.5), proposed that hilar cell loss removes the main excitatory inputs to the GABAergic basket cells in the dentate gyrus, compromising the balance between excitation and inhibition, and resulting in epilepsy (Houser, 1999 a,b; Mathern et al., 1997, Figure 1.5). However, previous studies in Racine's lab (Adams et al., 1997; Adams et al., 1998) have shown that generalized seizures can be readily induced in the kindling model without any indication of gross cell damage in the hilar area, arguing against a causal relationship between epilepsy and neuronal loss.

In addition to hippocampal sclerosis, neuronal loss is also observed in other areas including the amygdaloid complex, entorhinal cortex and piriform cortex in human TLE

patients and animal models (Houser, 1999a,b). The cause and contribution of neuronal loss in these areas remain poorly understood.

3. 3 Axonal Growth

3. 3. 1 Mossy Fiber Sprouting

3. 3. 1. 1 The Basic Phenomenon

Another neuropathological alteration that is frequently observed in TLE patients is axonal sprouting and reorganization. Seizure-related mossy fiber sprouting is the most well-documented axonal growth observed in human epilepsy (Houser, 1999a,b; Cavazos et al., 1991; Sutula et al., 1989; Mathern et al., 1993; Mello et al., 1993). Consistent with the pathological findings from human TLE patients, many animal models, including maximal electrical shock, kindling, KA, and pilocarpine treatment, readily induce axonal growth in the mossy fiber pathway (Houser, 1999a,b; Cavazos et al. , 1991; Sutula et al. , 1989; Mathern et al. , 1993; Mello et al. , 1993). Intracellular labeling of granule cells has shown that the sprouted collaterals of the mossy fibers project to the IML of the dentate gyrus and the stratum oriens of the CA3 region (Figure 1.4), forming synaptic contacts with other granule cells, CA3 pyramidal cells, and possibly inhibitory neurons (Sutula et al., 1989; Sloviter, 1992; Franck et al., 1995).

3. 3. 1. 2 What Triggers Mossy Fiber Sprouting?

The trigger for sprouting of mossy fibers remains controversial. A common assumption is that the sprouting of mossy fibers is a consequence of neuronal loss. Several types of hilar neurons, especially the mossy cells, normally project onto the dendrite layer (IML) of DG granule cells. Selective damage of these neurons creates vacant synaptic

Figure 1.4 Mossy fiber sprouting. **(A)** An illustration of mossy fiber sprouting. Normally, the axons of DG granule cells project to the apical dendrites of the CA3 pyramidal cells (left). After seizures, the sprouted mossy fiber collaterals project to the stratum oriens of the CA3 region and the IML of dentate gyrus (right), forming synapses on the basal dendrites of CA3 pyramidal cells and the dendrites of DG granule cells, respectively. **(B)** Mossy fiber sprouting in IML as shown by Timm labeling. Left panel is taken from a naïve rat, where little or no Timm granules are observed in the IML. Right panel is taken from a KA-treated Wistar rat, where extensive sprouting of mossy fibers is detected. **(C)** Mossy fiber sprouting in stratum oriens. Left panel is taken from a naïve Wistar rat, while the right panel is a section from KA-treated Wistar rat. KA-treatment induces sprouting in the stratum oriens of the CA3 region. Arrows indicate Timm granules. MFS: mossy fiber sprouting; IML: inner molecular layer; Oriens: stratum oriens; Luc. : stratum Lucidum; Rad. : stratum radium.

A Normal **MFS**

B IML

C CA3 region

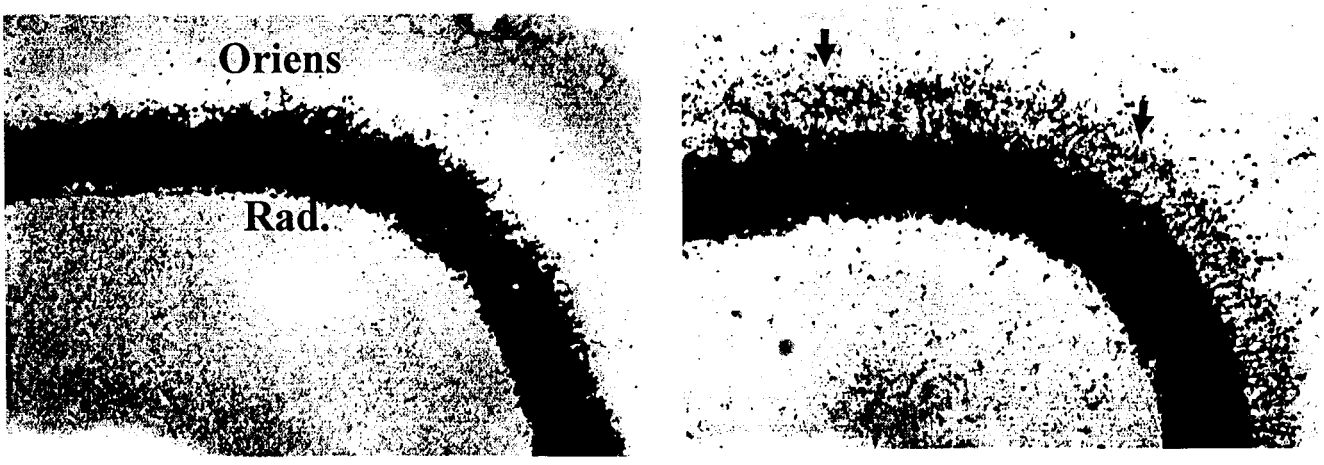

sites in the IML, allowing mossy fiber collaterals to sprout into and occupy these vacant sites. Indeed, an extensive literature on human TLE patients and animal models suggests a close correlation between the extent of hilar cell loss and mossy fiber sprouting (for review see Houser, 1999). Mossy fiber sprouting is consistently detected among TLE patients with hippocampal sclerosis (Houser et al. , 1990; Babb et al. , 1991; Mathern et al. , 1995; Masukawa et al. , 1995), while tissue specimens from patients without sclerosis show almost no mossy fiber sprouting (Proper et al. , 2001). A negative correlation between the density of MFS in the inner molecular layer and hilar cell density has been detected in human TLE patients (Masukawa et al., 1995) and KA-treated rats (Buckmaster and Dudek, 1997). In addition, both the mossy fiber sprouting and the hilar cell loss are more prominent in the anterior hippocampus when compared with the posterior hippocampus (Masukawa et al., 1995).

However, several other studies have detected no correlation or even a negative correlation between neuronal loss in the hilus and the extent of mossy fiber sprouting (Babb et al., 1991; Mathern et al., 1995). Previous studies in Racine's lab using the kindling model have consistently shown the development of the seizure-prone state, and axonal growth in the mossy fiber pathway, with little or no sign of hilar neuronal loss (Racine, 1986; McIntyre and Racine, 1986; Spiller and Racine, 1994; Adams, et al., 1997; Adams, et al., 1998). Although a decreased density in hilar neurons is detected after kindling, this has been attributed to an increase in the volume of the hilar area. Overall, there is no gross neuronal loss in the hilar region.

Based on these observations, an alternative hypothesis has been proposed, suggesting that mossy fiber sprouting in the hilus can be *activity-dependent*, rather than solely *lesion-dependent*. It has been shown, in fact, that mossy fiber sprouting can be

induced by even milder treatments, such as long-term potentiation and Morris water maze training, in which no neuronal loss is involved (Adams et al, 1997; Ramirez-Amaya et al. , 2000). These studies indicate that axonal growth in the mossy fiber pathway can be triggered by normal, or mildly stimulating, neuronal activities.

3. 3. 1. 3 The Consequences of Mossy Fiber Sprouting

A common hypothesis about the consequences of mossy fiber sprouting is that the mossy fiber collaterals form recurrent excitatory circuits with the dendrites of granule cells, and contribute to the development and maintenance of epileptogenesis (Sutula et al. , 1988; Houser, 1999, Babb, 1999, Figure 1.5).

As suggested by the electron-microscopic studies, the sprouted collaterals form functional excitatory synapses with the dendritic spines of granule cells and the basal dendrites of CA3 pyramidal cells (Babb et al., 1991, 1992; Represa et al., 1993). The newly-formed terminals express several common ultrastructural features of mossy fiber terminals, such as a high concentration of synaptic vehicles and dense core vesicles, distinct synaptic connections with postsynaptic targets, and several mitochondrial profiles, suggesting that they are functional excitatory glutamate-secreting synapses (Houser, 1999a; Babb, 1999). The sprouted mossy fiber collaterals may exert powerful influences on granule cells and pyramidal cells via these functional synapses.

Physiological studies have shown that the dentate granule cells of TLE patients exhibit abnormal hyperexcitable responses to electrical stimulation. The amplitude and frequency of spontaneous excitatory postsynaptic current in granule cells (Wuarin and Dudek, 2001) and the action potential burst (Babb et al. , 1991; Lynch & Sutula, 2000)

Figure 1.5 Dormant basket cell and mossy fiber sprouting hypotheses. (A) Dormant basket cell hypothesis. Normally, the mossy cells in the hilar region (M) provide excitatory inputs to both the inhibitory basket cells (B) and the DG granule cells (G). Seizures result in a selective loss of mossy cells. Basket cells become dormant after the removal of the excitatory inputs from the mossy cells, leading to hyperexcitability of granule cells. (B) Mossy fiber sprouting hypothesis. In epilepsy, the sprouted axonal collaterals form recurrent synapses with the dendrites of the GCs, which is postulated to contribute to the increased granule cell excitation in epilepsy (Adapted from McNamara, 1999).

A Dormant basket cell hypothesis

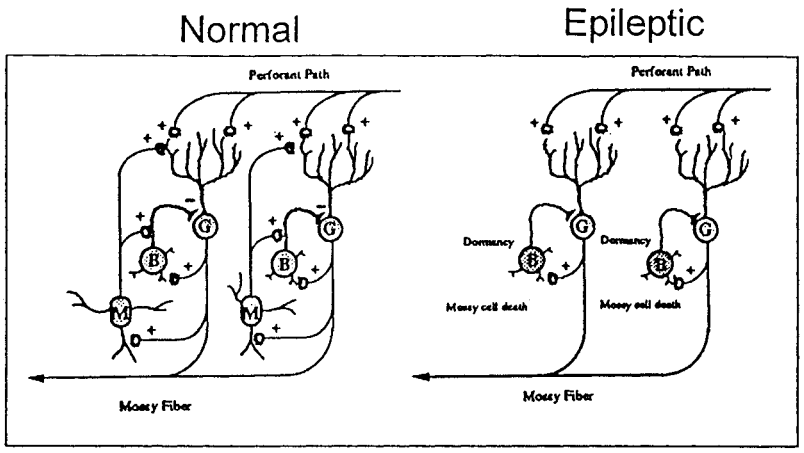

B Mossy fiber sprouting hypothesis

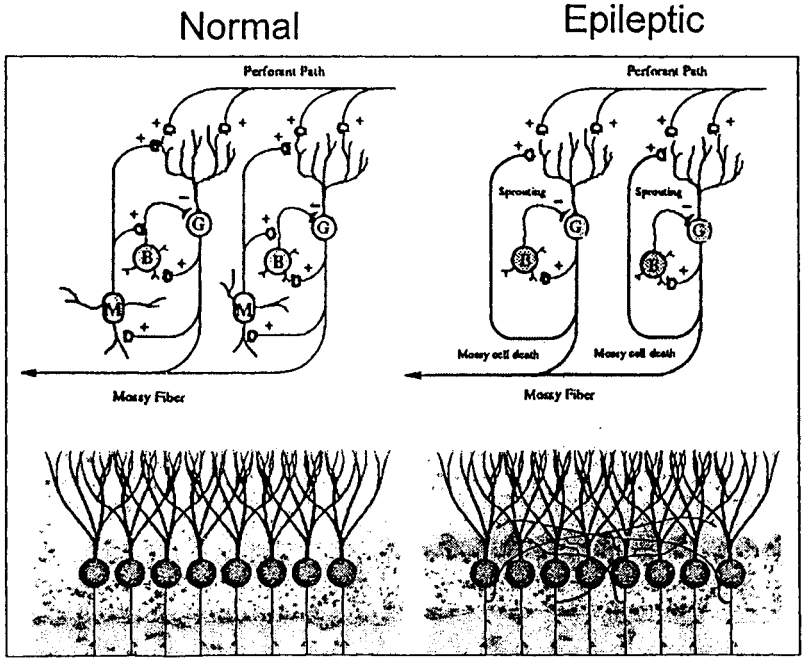

increased in parallel with the intensity of MFS in the IML. The sprouted mossy fiber system exhibits a more frequent occurrence of multiple firing, or even prolonged seizure-like bursts of action potentials (Franck et al., 1995; Wuarin and Dudek, 1996). The incidence of multiple firing is also correlated with the extent of mossy fiber sprouting (Franck et al., 1995). All of these studies provide evidence for a strong relationship between the mossy fiber sprouting result and the hyperexcitability observed in the epileptic brain, implying that the MFS might contribute to epileptogenesis (Babb, 1999; Houser 1999b).

Although mossy fiber sprouting might contribute to epileptogenesis, it is clear that the development and maintenance of epilepsy can occur independently of MFS. Several studies have shown that recurrent seizures can develop in both patients and seized animals showing no sign of mossy fiber sprouting (Spencer and Spencer, 1994; Wu and Leung, 1997). In other reports, the recurrent seizures developed days before mossy fiber sprouting started to appear (Stafstrom et al., 1992). Blocking of mossy fiber sprouting by the protein synthesis inhibitor, cycloheximide, does not affect the development of spontaneous recurrent seizures after KA or pilocarpine injection (Longo and Mello, 1997, 1998, 1999; Covolan, 2000). In addition, generalized seizures and an increase of seizure sensitivity can be induced within hours by repeated short-interval electrical stimulations, while mossy fiber sprouting usually takes days or even weeks (Lothman and Williamson, 1993). Thus, it is clear that MFS is not critical for epileptogenesis.

3. 3. 1. 4 Modulation of Mossy Fiber Sprouting

The molecular basis of MFS remains poorly understood. However, it has been

suggested that MFS can be modulated by many factors that affect protein synthesis (Longo and Mello, 1997, 1998, 1999; Covolan, 2000), neuronal growth (Adams et al., 1997; Jankowsky and Patterson, 2001; van der Zee et al. , 1995), and cellular excitability (Chen et al., 2001; Ikegaya et al., 2000).

The trophic factors, including the neurotrophins, are a class of proteins that affect neuronal growth and cell survival. In vivo and in vitro studies have shown that these factors act on distinct subsets of neurons, promoting cell survival, causing neurite outgrowth, and regulating neuronal excitability (Debeir et al., 1989; Knusel, 1992). More recently, it has been shown that neurotrophins modulate epileptogenesis and the development of mossy fiber sprouting. Continuous infusion of exogenous nerve growth factor (NGF) into the brain enhances mossy fiber sprouting (Adams et al., 1997), while an NGF antibody inhibits mossy fiber sprouting (van der Zee et al., 1995). In addition, infusion of glial cell line-derived neurotrophic factor (GDNF), a member of the TGF- β family of neurotrophic factors, significantly decreases kindling rate and mossy fiber sprouting (Li et al., Submitted).

Several chemicals that affect neuronal excitability can also alter the extent of MFS. For example, repetitive administration of nicardipine, an L-type Ca^{2+} channel blocker, attenuates the aberrant sprouting of the mossy fibers without affecting epileptogenesis in pilocarpine-treated mice (Ikegaya et al., 2000). Pre-treatment with Ketamine, an antagonist of N-methyl-D-aspartate (NMDA) receptors, decreases MES-induced mossy fiber sprouting in IML (Chen et al., 2001).

In summary, mossy fiber sprouting is one of the most frequently observed pathological alterations found in human epilepsy patients and animal models. It is postulated that neuronal loss and/or repetitive seizure activity contributes to the

development of MFS. The sprouted collaterals form recurrent synapses on DG granule cells, and are believed to contribute to the hyperexcitability of epileptic patients and animal models. Although the exact molecular mechanisms of MFS remains poorly understood, it has been shown that neurotrophic factors and chemicals affecting neuronal excitability can modulate the development of MFS *in vitro* and *in vivo*.

3. 3. 2 Sprouting in Other Systems

Current evidence suggests that, in addition to the sprouting of the mossy fiber system, the axons of GABAergic and CA1 pyramidal cells also sprout in response to seizure activity. The axons of spared GABAergic neurons within the dentate gyrus sprout into the IML of the dentate gyrus in human TLE patients and KA-treated rats (Babb et al. 1989; Davenport et al. , 1990). It is postulated that such a sprouting might alter the extent of inhibition in epileptic hippocampus.

Using fluorescent dextran amines as labels, Lehmann et al. (2001) have shown that the axon collaterals of CA1 pyramidal cells are increased in human TLE and in pilocarpine-treated rats. These sprouted collaterals project to the adjacent CA1 pyramidal cells and form synapses in the stratum pyramidale and the stratum radiatum of area CA1. As with mossy fiber sprouting, it has been proposed that the aberrant sprouting of CA1 pyramidal cells forms recurrent excitatory feedback networks and contributes to hyperexcitability.

In addition, an increase of synaptophysin, a synaptic vesicle protein, has been detected in the CA3 region, the CA1 region and the piriform cortex after kindling, implying that axonal growth and formation of new synapses occur in these areas.

3. 4 Other Pathological Alterations

3. 4. 1 Neurogenesis and Cell Proliferation

Bromodeoxyuridine (BrdU) immunohistochemistry selectively identifies newly generated cells. Studies using BrdU labeling have shown that seizures can cause a dramatic increase in neurogenesis and cell proliferation in the dentate subgranular proliferative zone (SGZ), an area known to contain neuronal precursor cells. The cell proliferation is observed in epileptic patients and in a variety of epilepsy models, including KA or pilocarpine-induced SE, electrical shock, and kindling (Parent et al., 1997, 1998, 1999; Covolan et al. , 2000; Bengzon et al. , 1997; Scott et al. , 2000). Recent studies have shown that these newborn granule cells project axons to both the CA3 pyramidal cell region and the dentate inner molecular layer, and may contribute to epileptogenesis as well as the aberrant network reorganization observed in epileptic brain (Parent et al. , 1997). However, completely blocking neurogenesis by low-dose, whole-brain x-irradiation does not affect the development of pilocarpine-induced SE or the extent of mossy fiber sprouting, suggesting that neurogenesis is not the only cause of epilepsy and axonal growth.

3. 4. 2 Reactive Gliosis

A constant feature detected in the epileptic foci of human patients and animal models is reactive gliosis of astrocytes. Seizure activity results in an increase of astrocyte proliferation and a prominent hypertrophy of astrocytes. It also leads to a reorganization of astrocytic cytoskeletal proteins, such as glial fibrillary acidic protein (GFAP) and vimentin, in the hippocampal formation, amygdala, and piriform cortex (Khurgel et al, 1992; Khurgel and Ivy, 1996). The transient increase of GFAP immunoactivity is correlated

closely with the temporary enlargement of the hilar area, indicating that kindling-induced glial cell changes are the major contributor to hilar expansion (Adams et al. , 1998).

3. 4. 3 Alteration of gene and protein expression

Neuronal excitation by chemically and electrically induced seizures modulates the expression of a variety of genes and proteins. For example, seizure activity elicits a rapid transcriptional activation of immediate early genes (IEGs), including c-fos, c-jun and Krox, which serve as transcription factors and cytokines (for review see Kiessling and Gass, 1993; Morgan and Curran, 1991). In addition, epileptiform discharges induce alterations of several classes of proteins, including the glutamate and GABA receptor subtypes (Sperk et al. , 1998; Coulter et al. , 2001), the neurotrophins and their receptors (Kokaia et al., 1996; Bengzon et al., 1993; Ballarin et al., 1991), tubulin and microtubule-associated proteins (Represa and Ben-Ari, 1997), and the protein kinases (McNamara and Lenox, 2000). It has been suggested that the alteration of gene expression and the regulation of protein levels in epileptic brain contribute to epileptogenesis and epilepsy-related morphological changes.

3. 4. 3. 1 Regulation of neurotrophic factors and their receptors

Neurotrophins comprise a family of target-derived polypeptides that promote the differentiation, growth, and survival of certain peripheral and central nervous system neurons (Fernette et al. 1993). Nerve growth factor (NGF), brain-derived neurotrophic factor (BDNF), neurotrophin-3 (NT-3), neurotrophin-4 (NT-4), and neurotrophin-5 (NT-5) all belong to this family. These neurotrophic factors not only are responsible for neuronal survival and target innervation during development, but also exert a modulatory role on

neuronal plasticity and activity during adulthood. The high-affinity receptors of neurotrophins are Trk A, B, and C, which preferentially bind to NGF, BDNF and NT-3, respectively (Kaplan et. al., 1989).

Recent research has shown that seizure activity induces robust changes in the expression of both neurotrophins and their high-affinity receptors. The level of mRNA for NGF and BDNF are transiently increased following seizures in many animal models, including kindling, KA or pilocarpine-induced SE, and hilus lesion-induced seizures (Kokaia et al., 1996; Bengzon et al., 1993; Ballarin et al., 1991). Even a single afterdischarge triggered by a kindling stimulus is sufficient to elicit a rapid and transient increase of NGF and BDNF mRNA. Such increases can be detected in regions that are highly associated with epileptogenesis, such as the dentate gyrus, the piriform and entorhinal cortics, and the amygdaliod complex. NT-3 mRNA, by contrast, is reported to show either no change (Ballarin et al., 1991) or a decrease (Bengzon et al. , 1992) in the hippocampus, especially in the granule cell layer, following seizure activity.

Since previous studies in Racine's lab have demonstrated that infusion of exogenous neurotrophic factors into brain can alter the development of EEG and behavioral seizures and modulate the extent of MFS, it is possible that the regulation of neurotrophic factors after seizures serves as a molecular mechanism for axonal growth and seizure development.

3. 4. 3. 2 Alteration of $GABA_A$ Subunit Composition

The $GABA_A$ receptor is a ligand-operated chloride channel. It has a pentameric structure. Different subunits are recruited from five gene subfamilies, designated α, β, γ, δ, and ε. Several subtypes of α, β, and γ subunits exist in the mammalian CNS, including 6 α, 3 β, and 4 γ subunits (Sperk et al., 1997). Different combinations of subunits give $GABA_A$

receptors diverse kinetic and pharmacological properties (Pritchett et al. , 1989; Pritchett and Seeburg, 1990; Verdoorn, 1994; Ducic et al. , 1995; Gingrich et al. , 1995; McKernan and Whiting, 1996; Tia et al., 1996).

Dramatic changes in the expression of these subunits and the composition of the $GABA_A$ receptors have been detected following kindling or status epilepticus (Clark et al., 1994; Kamphuis et al., 1994, 1995; Tsunashima et al., 1997; Schwarzer et al., 1997; Sperk et al., 1998; Brooks-Kayal et al., 1998). Shortly after kindling or SE, an upregulation of the α3, α4, and α5 subunit mRNAs (embryonic phenotype of GABA receptors) and downregulation of the α1 mRNA (adult phenotype) are detected in the dentate gyrus (Tsunashima et al., 1997; Schwarzer et al., 1997; Sperk et al., 1998; Brooks-Kayal et al., 1998). As a consequence, GABAergic pharmacology is reversed to mimic that seen in the embryonic state. It is suggested that such a re-configuration of embryonic subunits might lead to a failure in inhibitory neurotransmission and increased seizure susceptibility (Brooks-Kayal et al. , 1998).

Another piece of evidence suggesting the relationship between epileptogenesis and the subunit composition of $GABA_A$ receptors comes from a particular genetic model of epilepsy, the kindling-prone/resistant rat strains (Michael et al. , 1999; see chapter 3 for details of this model). The composition of $GABA_A$ receptors in the kindling-prone strain is similar to that found in the late embryonic state (Laurie et al. , 1992; Poulter et al. , 1992), in which the α2, α3, and α5 subunits are overexpressed and α1 subunits are underexpressed. In contrast, the kindling-resistant strain contains fewer α2, α3, and α5 subunits and more α1 subunit when compared with wild-type animals. Such alterations of

expression profiles in genetic models are consistent with GABAergic mechanisms of epilepsy.

3. 5 Summary

Many neuropathological alterations, including neuronal loss, axonal sprouting, neurogenesis, gliosis, and alteration of gene and protein expression, are repeatedly detected in human epileptic patients and animal models of epilepsy. Virtually all of these changes have been proposed to serve as the underlying mechanism for epileptogenesis. However, it remains controversial whether any single change is either necessary or sufficient to fully account for the development and maintenance of epilepsy.

4. Rationale for the Current Study

The main objectives of the current studies are (1) to explore the relationship between epileptogenesis, neuronal damage and axonal reorganization; and (2) to investigate the modulation of MFS and epileptogenesis by neurotrophins and axonal growth factors.

As stated above, the neuron loss in the hilus of the dentate gyrus (hippocampal sclerosis) and sprouting in the mossy fiber pathway are two of the most reliable consequences of KA or pilocarpine induced status epilepticus (Sloviter, 1999). Some researchers have detected neuronal loss and substantial MFS in the kindling model as well (Cavazos, and Sutula, 1990). However, studies in Racine' lab have not supported any indication of gross cell loss in the kindling model (Adams et al., 1997, 1998). More surprisingly, pilot studies in our lab using Long-Evans hooded rats have shown a less-extensive MFS and no reliable neuronal damage following status epilepticus. Such a

controversy between the results of our lab and previous research using Wistar or Sprague-Dawley rat strain raises the possibility that the rat strain might determine the severity of neuronal damage and the extent of MFS. Indeed, several studies have suggested a substantial difference among outbred or inbred mouse or rat strains in their behavioral and/or EEG responses to electrical or chemical convulsants (Golden et al., 1991; 2001). Therefore, it is likely that different genotypes could affect the extent of seizure activity and seizure-related morphological changes. In an effort to solve the apparent controversy, and to understand the relationship between epileptogenesis, neuronal damage and MFS, we compared the development of acute and spontaneous recurrent seizures, as well as the extent of MFS and hilar neuronal loss between Wistar and Long-Evans rats. We also manipulated the extent and severity of status epilepticus by controlling the duration of SE and examined the effects of SE on mossy fiber sprouting and neuronal loss.

Another genetic model of epilepsy, the kindling-prone or kindling-resistant rat strains, were also used in the present research. These two strains were initially developed at McMaster University and show virtually no overlap in amygdala kindling rates (Racine, et al., 1999). Keeping the severity and duration of SE compatible between strains, we examined the development of spontaneous seizures, MFS and neuronal damage. The goals of this study were (1) to test the responses of these two kindling-prone/resistant strains to the induction of SE and spontaneous seizures, and (2) more importantly, to compare the potential differences between these two strains in epileptogenesis, axonal growth, and neuronal loss, in order to explore the underlying connections between these three phenomena.

What we found is that short-duration SE resulted in spontaneous seizures and moderate MFS without any reliable sign of gross hilar neuronal loss. Consistent with

previous studies from our lab, the Long-Evans rats did not develop any measurable hilar cell loss, even after prolonged SE. Thus, we proposed that neuronal loss is neither the necessary consequence nor a prerequisite of epileptogenesis and axonal growth, although it might contribute to them. Therefore, we have switched our attention to the modulation of mossy fiber sprouting.

Using osmotic minipumps, we have continuously infused bioactive agents, such as NT-3 and axonal guidance molecules, into the adult CNS. These factors have been proven to play an important role in axonal targeting and growth during neuronal development. Based on the effects of NGF and BDNF on kindling and/or kindling-induced axonal growth, we postulated that such factors might modulate activity-induced axonal growth and contribute to the development of epilepsy in adult CNS as well. Introducing antagonists or agonists of these factors into the brain, therefore, might alter the development of kindling, and the extent of axonal reorganization. These experiments also advanced our understanding of axonal growth processes in adult brain tissue.

CHAPTER 2: BEHAVIORAL AND ANATOMICAL CHANGES ASSOCIATED WITH STATUS EPILEPTICUS: A COMPARISON OF LONG-EVANS HOODED AND WISTAR RAT STRAINS

2. 1 Introduction

Significant heterogeneity exists in the rodent population in response to electrical or chemical convulsants. Previous studies have shown that different mouse or rat strains react differently to a wide range of epilepsy models, including kindling (Loscher et al., 1998), KA-induced status (Golden et al., 1992, 1995; Cantallops and Routtenberg, 2000), electrical shock seizures (Frankel et al., 2001), pentylenetetrazol (PTZ)-induced seizures (Kosobud et al., 1992; Becker et al., 1997; Kliioueva et al., 2001), cocaine-related seizures (Golden et al., 2001), and bicuculline seizures (Freund et al., 1987). These studies indicate that both the threshold for epileptiform events and the behavioural responses triggered by the epileptogenic treatment differ dramatically among inbred and outbred rodent strains. Such strain differences suggest that genetic factors play an important role in epileptogenesis.

The strain differences, however, are not always consistent across models. For example, the kindling rate of Sprague-Dawley rats is significantly faster than that of Wistar rats (Racine et al., 1975; Loscher et al., 1998), while Wistar rats show greater sensitivity and more reliable convulsant responses to KA than Sprague-Dawley rats (Golden et al., 1992, 1995). The effects of genetic heterogeneity on epileptogenesis depend partly on the type of seizure being studied.

More recently, it has been shown that the neurological alterations induced by epileptogenic treatments, including MFS and neuronal loss, also differ between strains

(Cantallops and Routtenberg, 2000). The ICR mouse strain shows no MFS or hilar neuronal loss after KA-treatment, while KA induces both axonal growth and neuronal loss in the 129/SvEMS mouse strain.

Strain differences may also account for discrepant results in kindling experiments on rats. Racine and co-workers detected no reliable gross neuronal loss in the hilar region after kindling (Adams et al., 1997 a, b) or status epilepticus (unpublished observation) in Long-Evans hooded rats. In contrast, many studies from other groups demonstrated severe hilar neuronal damage after SE, or even after kindling, in Sprague-Dawley or Wistar rat strains (Mello et al., 1993; Cavazos, and Sutula, 1990; Sloviter, 1999). Pilot studies in the Racine lab detected much weaker MFS after SE in Long-Evans rats when compared to the multiple reports of extensive MFS in the IML in Wistar rats. It is possible that Long-Evans hooded rats are more resistant to seizure-related neuronal damage and axonal growth than Wistar or Sprague-Dawley rats.

In the present study, we examined the occurrence of SE, spontaneous seizures, hilar cell loss and mossy fiber sprouting in Wistar and Long-Evans hooded rats using either KA- or pilocarpine-induced SE. In an effort to manipulate the duration of epilepsy, and the subsequent pathological damage, we attempted to control the amount of SE by delivering an anticonvulsant at different time points after SE (1 hour or 3 hours). The aims of the present study were (1) to determine whether there exist strain differences between Wistar and Long-Evans hooded rats in their behavioural responses to KA or pilocarpine-treatment; (2) to systematically compare the extent of neuronal loss and axonal growth between strains; and (3) to explore the relationship between behavioural seizures and histological changes. We also studied the effects of manipulating

histological and measurement variables on the assessment of MFS and neuronal damage. We compared different counting techniques and staining durations for Timm labelling.

2. 2 Materials and Methods

2. 2. 1 Experiment 1: Long Duration (3 hour) Status Epilepticus

2. 2. 1. 1 Animals

27 male Long-Evans hooded rats and 27 male Wistar rats (weight between 250 to 400 g) were randomly divided into 4 groups: Long-Evans KA-treated group (n=16), Long-Evans control group (n=11), Wistar KA-treated group (n=16), and Wistar control group (n=11). The animals were housed individually, maintained on an *ad lib* feeding schedule, and kept on a 12 hr on/12 hr off light cycle.

2. 2. 1. 2 Induction of Status Epilepticus and Monitoring of Spontaneous Seizures

Twenty minutes after pretreatment with atropine methyl nitrate (5 mg/kg, i.p.), the two KA-treated groups were injected with kainic acid (12 mg/kg; i.p.), while the control animals were injected with an equal amount of 0. 9% NaCl solution. Previous studies have shown that the behavioral seizures observed in KA or pilocarpine-induced SE are similar to those in the kindling model (Speak, 1994; Turski et al., 1983a). Therefore, the development of behavioral seizures was evaluated using Racine's classification (Racine, 1972) for kindling. The animals were continuously monitored and rated every 30 seconds. The typical development of behavioral seizures and SE were defined in detail in Chapter 1. In the present study, status epilepticus was defined as continuous seizures lasting for 3 hours. 3 hours after the SE started, 2 mg diazepam was administered i.p. to

the animals in order to bring them out of status epilepticus. Behavioral seizures were continuously monitored after the diazepam injection until the animals showed no sign of seizure activities for at least 5 minutes. Experimental animals that failed to develop status epilepticus and control animals were observed for 2 hours after the KA or saline injection and then injected with 2 mg diazepam i.p. The lethality and the failure rate (the number of animals failing to develop SE divided by the total number of animals in each group) were calculated and evaluated with the chi-square test. Animals that received KA treatment but failed to develop SE were excluded from subsequent tests for spontaneous seizures, MFS, and neuronal loss. The severity of SE was evaluated by the percentage of time the animals spent in stage IV or higher seizures during status epilepticus. The latency, duration and severity of SE were measured for each animal and subjected to a Student's *t* test for statistical analysis.

All animals that developed SE were observed for one hour daily for 8 weeks after the induction of status epilepticus, to monitor the development of spontaneous recurrent seizures (SRS). Stage I and II seizures were often difficult to distinguish from normal behaviors, so only stage III or higher seizures (seizures involving forelimb clonus) were recorded. Consistent with previous studies (for review see Cavalheiro et al. , 1995), a period characterized by apparently normal behaviors lasted for 1 - 4 weeks following SE induction. After this period, spontaneous recurrent seizures began to develop. The weekly frequency of SRS was calculated and a two-way ANOVA with one between variable (groups) and one within variable (weeks) was conducted for statistical comparisons.

2. 2. 1. 3 Comparison of Cell Counting Techniques: Unbiased Versus Biased Techniques

2. 2. 1. 3. 1 The Principles of Stereology

The issue of whether or not hilar neurons die in epilepsy is of fundamental importance for understanding the development and the consequences of epilepsy. Unfortunately, studies over the last century have presented conflicting results (see Chapter 1 for details). It has been proposed that these discrepancies might arise from inconsistent or inadequate cell counting techniques (West, 1993; 1999).

The traditional unbiased cell counting procedure treats brain sections as two-dimensional images from which the numbers of three-dimensional objects, the cells, are counted. Such counting procedures explicitly or implicitly make assumptions about three-dimensional factors, such as the shape, orientation and size of the cells, and are therefore referred to as assumption-based counting or biased counting techniques (West, 1993,1999). It is clear that changes in these three dimensional factors could potentially alter the estimates obtained from biased counting procedures. For example, larger cells have a greater chance to appear in a given section, or in multiple sections, than smaller cells. Thus, if a treatment increases or decreases cell size, it will result in incorrect estimates of cell number (Figure 2.2).

Unbiased counting techniques (stereology) have been developed over the past two decades, allowing researchers to estimate neuronal numbers more accurately and consistently (Coggeshall and Lekan, 1996; Saper, 1996; West, 1993,1999; Guillery and Herrup, 1997). By definition, stereology is a collection of general principles based on integral geometry, probability theory, and sampling theory, designed especially to

estimate numbers of three-dimensional (3-D) structures from measurements made in random two-dimensional plane sections or projections (Cruz-Orive, 1993; Jensen and Gundersen, 1985). Stereology treats histological sections, no matter how thin, as three dimensional regions and makes no underlying assumption about the specimen prior to the measurement. Such procedures are referred to as design-based or unbiased counting techniques. With the principles introduced below, stereological methods are capable of removing the effects of many potentially confounding variables, such as the alteration of cell size or shape, or changes in structure volume (Figure 2.2).

The typical stereological technique usually involves the following principles:

1. Sampling: In order to produce an unbiased estimate of the parameter from a sample of the structure, the fraction being measured has to be a representative sample of the structure. Therefore, the sampling procedure used in stereology must meet the following two criteria: (1) it must have access to the entire structure; and (2) all parts of the structure must have the same chance of being included in the sampling procedure. The systematic random uniform sampling method used in this study is one example of such sampling procedure. The procedure requires a randomly-determined start location and subsequent uniform sampling. For example, the start section to be analyzed in the current studies is randomly selected, and all the following sections are 300 μm apart from the start section and from each other. As described below, the selection of disectors within the same section also follows the systematic random uniform sampling rule.

2. Disector counting rule: Disector counting is one of the most commonly used stereological counting procedures. The measurements taken during this procedure are the number of objects that appear in one section but not in the sections immediately adjacent

(Figure 2.2). The estimates obtained using the disector counting rule have been shown to be independent of the shape, size, or orientation of the objects (Figure 2.2, Coggeshall and Lekan, 1996; Saper, 1996; West, 1993,1999; Guillery and Herrup, 1997).

More recently, Gundersen et al. (1986) has suggested using *optical* sections within thick histological sections by utilizing high magnification microscope objectives that produce images with a shallow depth of focus. The focal plane (or optical section) could be moved a known distance through the thickness of the section, creating a series of superimposed sections. The disector counting rule can be applied to these superimposed optical sections and unbiased estimates obtained by counting the number of objects that come into (or out of) focus through the tissue section. This optical disector counting procedure is widely used in many stereological studies (West, 1993,1999).

2. 2. 1. 3. 2 Tissue Preparation

Eight weeks after the induction of status epilepticus, a total of 20 rats (5 rats from each group) were randomly selected and were administered an overdose of pentobarbital (100mg/kg i.p.). They were perfused transcardially with PBS solution, followed by 10% formol-saline solution. The brains were removed and placed in formol-saline for 2 weeks. Frozen 60-micron horizontal sections were taken, using a cryostat, through the brain region containing hippocampus (4.3 - 7.6 mm ventral to Bregma). The sections were mounted on chromium potassium sulfate-coated slides, and cresyl violet was used to visualize neurons in the hilar area. The first section to be analyzed was randomly chosen from the sections that were located between 4.3 and 4.6 mm below Bregma. An additional 9 serial sections were taken at 360 μm increments from the first section and

used to complete the imaging analysis. The same set of 10 sections was used for measurement of hilar area, unbiased cell counting, and biased cell counting.

2. 2. 1. 3. 3 Hilar Area Measurement and Estimate of Hilar Volume

The slides were examined at 100X magnification by creating a digitized image with a BIOQUANT true color imaging system for windows 98 (BioQuant-R&M Biometrics, Inc., Tonawanda, New York) attached to a light microscope (Zeiss Axioskop, Oberkochen, Germany). The hilar area was defined by the inner edge of the granule cell layer and the lines connecting the tips of the two granule cell blades to the beginning of the pyramidal cell layer of Ammon's Horn (Figure 2. 1).

The estimated volume of the hippocampus was calculated as the sum of the hilar area from all the measured sections, multiplied by the distance between sections (360 μm).

2. 2. 1. 3. 4 Biased Cell Counting and Biased Estimates of Hilar Cell Number

All the cells within the defined hilar area with visible nuclei (neurons) were counted manually at 100X magnification. Both the left and the right hilar area were counted for each section. Since one out of every six sections was analyzed in the current experiment, the biased estimate number of neurons per hippocampus was calculated as the sum of the number of neurons for all the sections counted, multiplied by 6.

Figure 2.1 Digital images of Cresyl Violet and Timm-stained sections. **(A)** A digitized image of a Cresyl violet-stained rat hippocampal section. The hilar area was defined by the inner edge of the granule cell layer and the lines connecting the tips of the two granule cell blades to the beginning of the pyramidal cell layer of Ammon's Horn. **(B)** Digitized image of a Timm-stained hippocampal section. Density readings were taken by placing an open circle cursor with a diameter of 0.12 mm at 16 adjacent positions along the stratum oriens of the CA3 region, 9 adjacent positions along the inner molecular layer (IML) of the dentate gyrus,and 8 adjacent positions along the stratum radiatum.

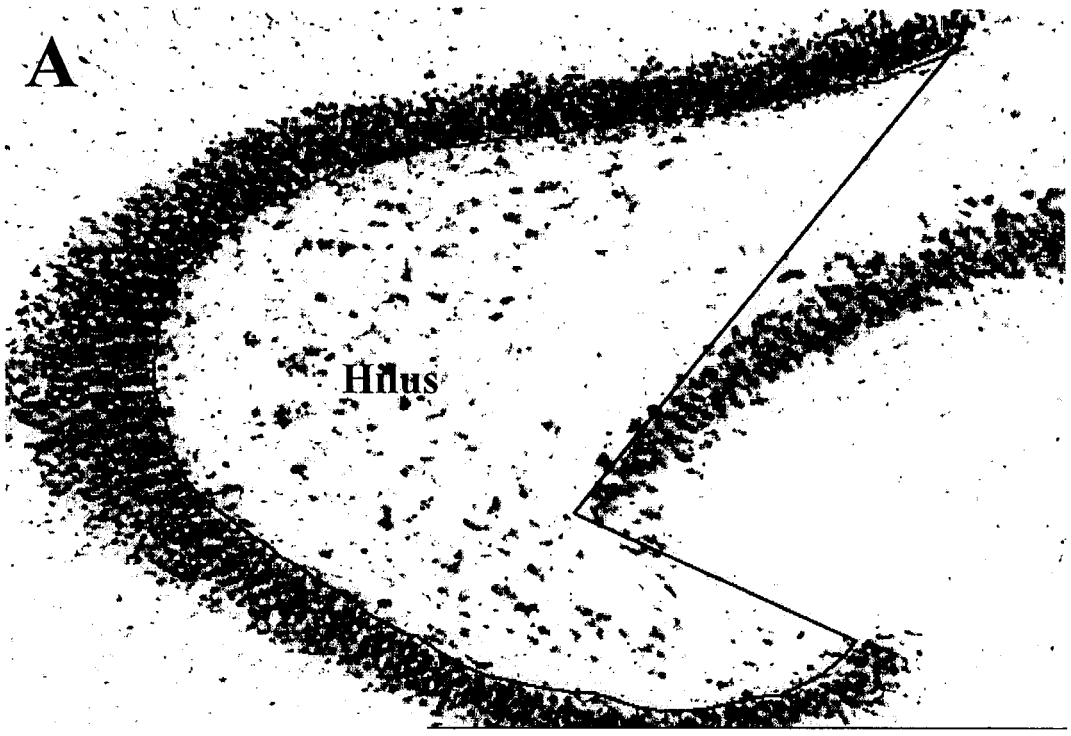
A
Hilus

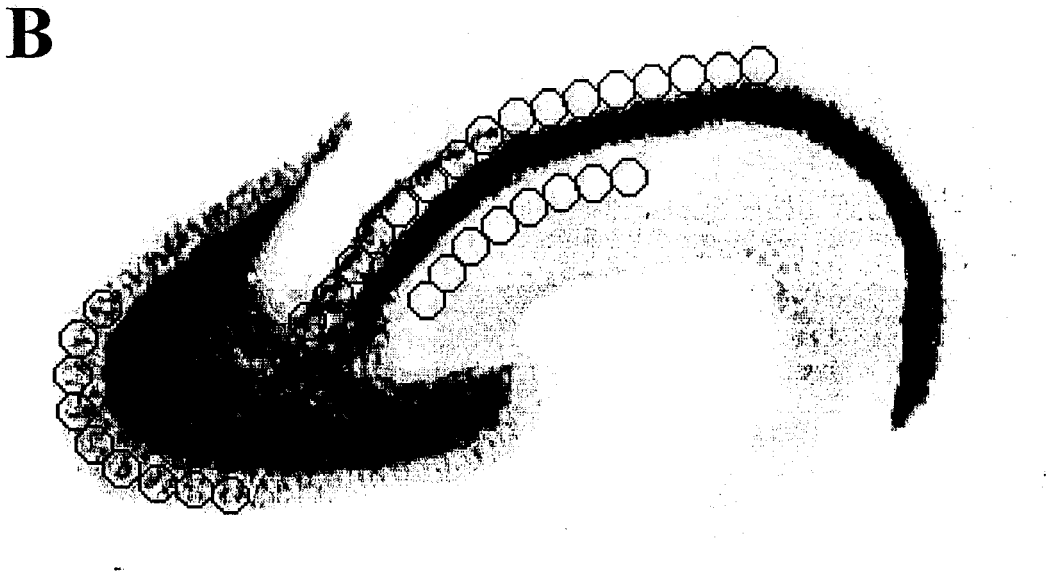
B

Figure 2.2 The effects of object size on biased and unbiased estimates. (A) and **(B)** represent two specimens that contain 10 objects located in similar positions. The only difference between (A) and (B) is the size of the objects. A total of 6 sections (1-6) are indicated in each specimen. The biased estimate of object number is the sum of the objects counted in each section. Therefore, the biased estimates for specimens A and B are 19 (2 + 3 + 3 + 3 + 5 + 3) and 14 (1 + 3 + 2+ 3+ 2+ 3), respectively. Apparently, three-dimensional parameters such as object size significantly affect the biased estimates. On the other hand, the disector counting rule of stereology only counts objects that appear in the subsequent sections once. For example, in the second section of specimen A, only the 2 objects marked with * are counted because they were the only two objects that appear in Section 2. The unbiased estimates are calculated as number of new objects in sections 2 to 6, divided by the volume measured and then multiplied by the volume of the specimen. The unbiased estimates of specimen A and B are 9.6 and 10.8, respectively, providing a close estimate of the real values, unaffected by the object size.

A

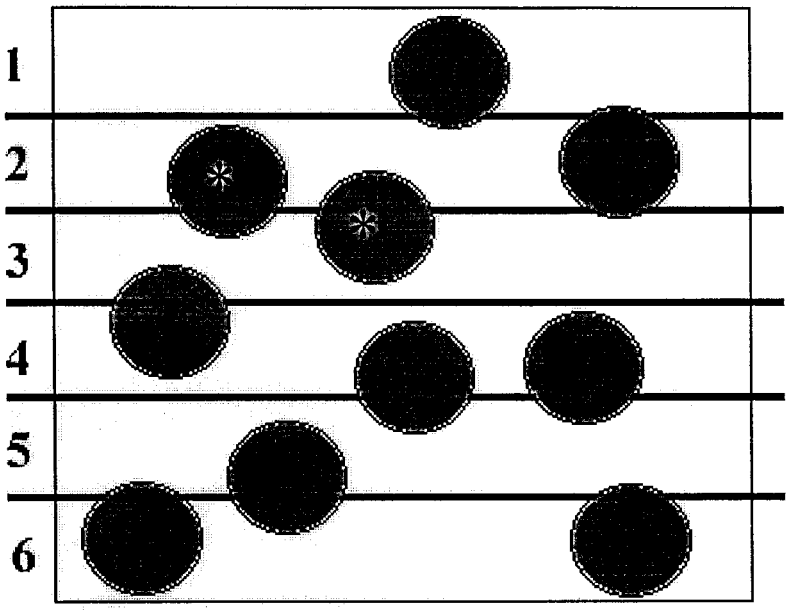

B

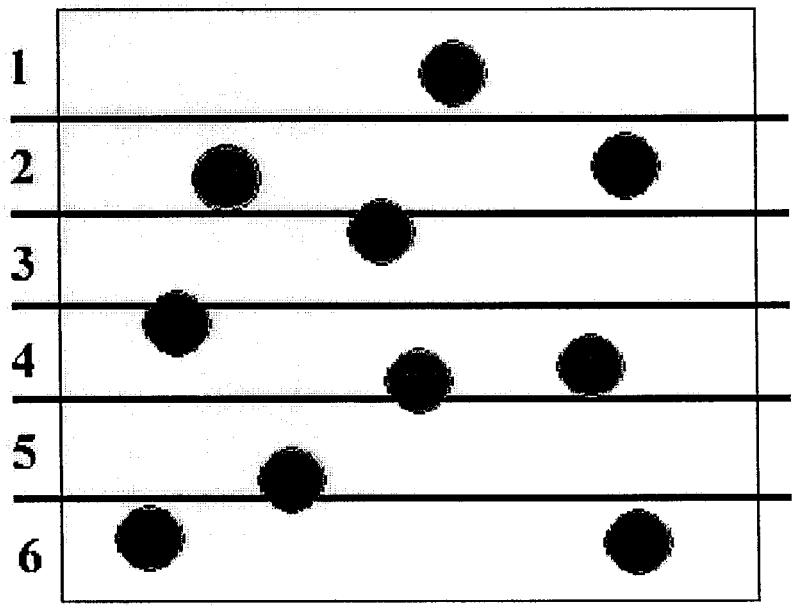

2. 2. 1. 3. 5 Unbiased Cell Counting and Unbiased Estimates of Hilar Cell Number

The slides were examined at 1000× magnification. A 150 × 150 μm grid was randomly positioned on the defined hilar area. All the intersections within the defined hilar area were counted by placing an optical disector on each intersection. The total number of intersections counted for each side of the section ranged from 7 to 17. At least 100 intersections were counted for each hilus. The counting frame of the optical disector was 30 X 30 μm square. Cells that intersect with the left or bottom boundaries of the frames were excluded, while cells lying on the right or top boundaries were included in the cell counting procedure. The height of the optical disector was 10 μm. Cells with morphological characteristics of neurons (either with distinct dendrites or irregular cell bodies with large nucleus) within the disector (30 X 30 X 10 μm) were counted according to the optical disector principles. Neurons that intersected the uppermost focal plane were excluded from counting, only those neurons that came into focus within the 10 μm height were counted. The cell numbers in the optical disectors ranged from 0 to 3. The unbiased estimate of the total neuronal number per hippocampus (N) was calculated using the equation below:

$$N = \frac{\text{Number of neurons counted}}{\text{Total volume of all the disectors counted}} \times \text{estimated hippocampal volume}$$

The regression between the unbiased and biased estimates of the total neuronal number per hippocampus was established and the correlation coefficient was calculated. In addition, two-tailed *t* tests were used to compare groups.

2. 2. 1. 4 Histology

8 weeks after the KA treatment, all the remaining animals were perfused transcardially with 50 ml sodium sulfide solution (8. 9 g $Na_2S{\cdot}9H_20$, 10. 9 g sucrose, 1. 19 g $Na_2HPO_4{\cdot}H_2O$ per 100ml dH_2O). The brains were removed, immediately frozen in isopentane cooled to -40°C, and stored at -70°C until sectioning. Horizontal, serial, 40-micron sections were taken through the brain region containing hippocampus. Alternate sections were stained using either a modified Timm method (van der Zee et al. , 1995) for the analysis of Timm granule density or cresyl violet to determine the neuronal density of the hilar area.

2. 2. 1. 4. 1 Qualification of Timm Staining and Measurement of MFS

The Timm staining procedure selectively labelled mossy fibers in the dentate gyrus due to their high concentration of Zn^{2+}. A typical Timm protocol included 3 steps: hydration, "development" (slices were kept in citrate buffer-hydroquinone-gum arabic-$AgNO_3$ solution, in which the $AgNO_3$ selectively labels the heavy metal within the slice), and dehydration. A pilot study in our lab suggested that the density of Timm labeling could be affected by the development time of the Timm stain, but it was not clear to what extent variations in absolute density affected measures of relative density (e.g., the mossy fiber pathway compared to adjacent regions). In order to quantify the effect of development time on Timm density, adjacent brain sections were divided into three groups, each receiving a different development time (35 min, 50 min or 65 min). Sections from different animals were stained simultaneously to minimize staining variability. Adjacent sections with different development times taken from five

horizontal levels, which were roughly 4.6, 5.2, 5.8, 6.4 and 7mm ventral to the Bregma, were chosen for further analysis.

The slides were examined at 50X magnification by creating a digitized image with a Micro Computer Imagining Device (MCID) image analysis system (Brock University, St Catharine's, Ontario, Canada) attached to a light microscope (Zeiss Axioskop, Oberkochen, Germany) with a high-resolution charge-coupled device (CCD) camera (MTI CCD 72). The density of Timm granules in the CA3 region and dentate gyrus was measured, as illustrated in Figure 2. 1. The optical densities of the CA3 region and the dentate gyrus were measured by placing an open circle cursor with a diameter of 0.12 mm at 16 adjacent positions along the stratum oriens of the CA3 region, and 9 adjacent positions along the inner molecular layer (IML) of the dentate gyrus. To control for variations in background Timm staining across sections, an additional 8 density readings were obtained from 8 adjacent open cursors placed in the stratum radiatum, which normally contains few Timm granules. Both the right and left sides of the brains were measured for all five sections. The relative optical density (ROD), defined as follows, was used for the statistical tests:

$$\text{ROD} = \frac{\text{Density reading in stratum oriens or IML}}{\text{Average of the background density reading in stratum radiatum}}$$

A five-way ANOVA [4 × (3 × 5 × 2 ×16/9)] with one between variable (group) and four within variables [development time (35, 50 and 65 mins), section (1-5 ventral to

dorsal), brain hemisphere (left or right) and cursor position (1–16 in CA3, 1–9 in IML)] was conducted for the analysis of Timm granule density in the CA3 or IML regions.

The ANOVA tests reported in this thesis were always followed by *post hoc* Tukey comparisons. A probability of < 0.05 was considered significant. All measures reported in the following experiments, Figures, and tables are expressed as mean ± standard error of the mean (SEM).

2. 2. 1. 4. 2 Hilar Area Measurement and Hilar Cell Counting

Cresyl violet was used to visualize neurons in the hilar area. Both the area of the hilus and the hilar cell density were evaluated with the BIOQUANT system. As stated in the Results section, the estimates of cell numbers obtained from unbiased optical disector techniques were highly correlated with the estimates from traditional biased cell counting techniques used in our lab. Since the biased cell counting procedure we have used is capable of providing accurate estimates of neuronal numbers and is simpler and less time-consuming than the optical disector method, only the biased cell counting technique was employed in subsequent studies.

Five sections from approximately the same vertical coordinates as those used in Timm density measurements were analyzed. The hilar area was defined as described in section 2. 2. 1. 3. 3. All the cells within the defined hilar area with visible nuclei were counted manually. A three-way ANOVA [4 × (2 × 5)] with one between variable (group) and two within variables [brain hemisphere (left or right) and brain section depth (1-5, ventral to dorsal)] was conducted for statistical analysis of hilar area and hilar cell number.

2. 2. 2 Experiment 2: Short Duration Status Epilepticus

2. 2. 2. 1 Background and Rationale

The SE induced by pilocarpine or KA injection can last for hours if no intervention, such as anticonvulsants is applied. The durations of SE most frequently used in rodent studies range from 2 to 8 hours (Speak, 1994; Ben-Ari et al., 1980 a, b; Olney et al., 1986). Severe neuronal damage has been reported following such long-duration SE (Speak, 1994; Ben-Ari et al., 1980 a, b; Olney et al., 1986). Several studies have proposed that the sustained activation of neurons during SE results in neuronal damage in certain sensitive brain regions, and contributes to the subsequent MFS (Speak, 1994; Olney et al., 1986). Manipulations that inhibit the development of epilepsy usually protect neurons from SE-induced neuronal degeneration and/or axonal sprouting (Speak, 1994; Nadler, 1981; Okazaki and Nadler, 1988; De Bonnel and De Montigny, 1983).

Preliminary results indicated that status epilepticus as short as 5 minutes might be sufficient to produce subsequent spontaneous seizures as manifested by EEG discharge. It is unclear whether SE lasting for only minutes could induce pathological changes such as those seen following prolonged SE. The main purpose of the following short-term SE, therefore, was to examine the effects of short-duration seizures in two different rat strains.

2. 2. 2. 2 Animals and Measurement of Behavioral Seizures

13 male Long-Evans hooded rats and 14 male Wistar rats (weight between 250 to 350 g) were divided into 4 groups: Long-Evans experimental group (n=7), Wistar experimental group (n=8), Long-Evans control group (n=6), and Wistar control group

(n=6). Twenty minutes after atropine sulfate (5mg/kg i.p.) pretreatment, the two experimental groups received injections of 350 mg/kg pilocarpine i.p., while the control groups received equal amounts of saline. The development of behavioral seizures was monitored as described in Experiment 1. Five minutes after the onset of status epilepticus, animals were injected with 1 mg diazepam i.p. to stop seizures. Most of the rats remained in status epilepticus for another 5 to 25 minutes before status was terminated. Observation ended when the animals remained seizure-free for at least 1 minute. About half of the animals spent little or no time in stage 4 and 5 seizures. The severity of SE in these cases was defined as the percentage of time animals spent in stage 3 and higher seizures during SE. The latency, duration and severity of SE was recorded and subjected to two-tailed Student's *t* test. Both animals failing to develop SE and control animals were injected with diazepam after 2 hours of observation.

Over the following 8 weeks, animals were observed for one hour daily to monitor the development of spontaneous seizures.

2. 2. 2. 3 Histology

8 weeks after the KA treatment, animals were perfused transcardially with 50 ml sodium sulfide solution (8. 9 g $Na_2S{\cdot}9H_20$, 10. 9 g sucrose, 1. 19 g $Na_2HPO_4{\cdot}H_2O$ per 100ml dH_2O). Horizontal, serial, 40-micron sections were taken through the brain region containing the hippocampus. Alternate sections were stained using either a modified Timm method (van der Zee et al., 1995) for the analysis of Timm granule density or cresyl violet to determine the neuronal density of the hilar area.

To minimize variability of Timm staining, sections from different animals were stained simultaneously, and the development time was controlled at 50 min. Five

horizontal sections were taken at 4. 6, 5. 2, 5. 8, 6. 4 and 7mm ventral to the Bregma and examined with a BIOQUANT true color imaging system for windows 98 (BioQuant-R&M Biometrics, Inc. , Tonawanda, New York) attached to a light microscope (Zeiss Axioskop, Oberkochen, Germany). The relative optical density (ROD) of IML and stratum oriens was calculated as stated in Experiment 1.

Cresyl violet staining was used to visualize neurons in the hilar area. Five sections taken from approximately the same vertical coordinates as those used in Timm density measurements were analyzed. The biased cell counting technique was used in this experiment. In brief, the hilar area was defined by the inner edge of the granule cell layer and the lines connecting the tips of the two granule cell blades to the beginning of the pyramidal cell layer of Ammon's Horn. All the cells within the defined hilar area with visible nuclei were counted manually. A three-way ANOVA [4 × (2 × 5)] with one between variable (group) and two within variables [brain hemisphere (left or right) and brain section depth (1-5, ventral to dorsal)] was conducted for statistical analysis of hilar area and hilar cell number.

2. 3 Results

2. 3. 1 Experiment 1: Long Duration Status Epilepticus

2. 3. 1. 1 Status Epilepticus and Spontaneous Seizures

An example of the development of status epilepticus after kainic acid is shown in Figure 2.3. Typically, 10 minutes after the KA injection, animals started to show signs of epileptic activity such as immobility and facial clonus. Intermittent forelimb clonus developed at around 20 min after the KA injection, and lasted for about 30 min. Status

epilepticus, which is defined as continuous seizures, started at roughly 1 hour after the injection of KA, and continued until the anticonvulsant was administered. In the first hour of status epilepticus, the pattern of seizure activity was phasic. Animals remained for much of the time in stage 2 or 3 seizures, while jumping to stage 4 or 5 seizures every 3 to 6 minutes. Eventually, such cycles of seizure activities disappeared, and the animals remained in stage 4 for another 1 to 2 hours. 3 hours after status epilepticus started, the rats were injected with diazepam and the behavioral seizures gradually ceased.

The outcome of kainic acid treatment is shown in Table 2. 1. The only difference between the two strains was that Long-Evans hooded rats required significantly longer duration to develop status epilepticus (52.2 ± 8.1 minutes) than Wistar rats (32.7 ± 5.3 minutes) (two-tailed *t* test, $p<0.01$). All the other measurements, including the lethality and the failure rate, the duration and severity of status epilepticus, and the average frequency of spontaneous seizures, revealed no significant differences between Long-Evans and Wistar animals. Overall, similar amounts of behavioral seizure activity were observed in the two strains.

2. 3. 1. 2 Methodology: Comparison of Cell Counting Techniques

The unbiased estimates of the total cell number in the hilus were highly correlated with the biased estimates (correlation coefficient r = 0.93, Figure 2.4 A). A two-tailed *t* test revealed a decrease in total hilar cell numbers after KA treatment in the Wistar strain, using either cell counting technique (two-tailed *t* test, $p<0.05$, Figure 2.4 B). No obvious hilar cell loss was observed in Long-Evans rats (two-tailed *t* test, $p>0.05$, Figure 2.4B).

Figure 2.3 A representative example of KA-induced acute seizures. The animal received a KA injection at time 0. The square represents the time period during which the rat stayed in SE. The starting point of status epilepticus (56.5 minutes after KA injection) was judged as the time point from which continuous seizures began. The animal received diazepam (DZ) 2mg i.p. 3 hours after SE started. SE stopped 17 minutes after the diazepam injection.

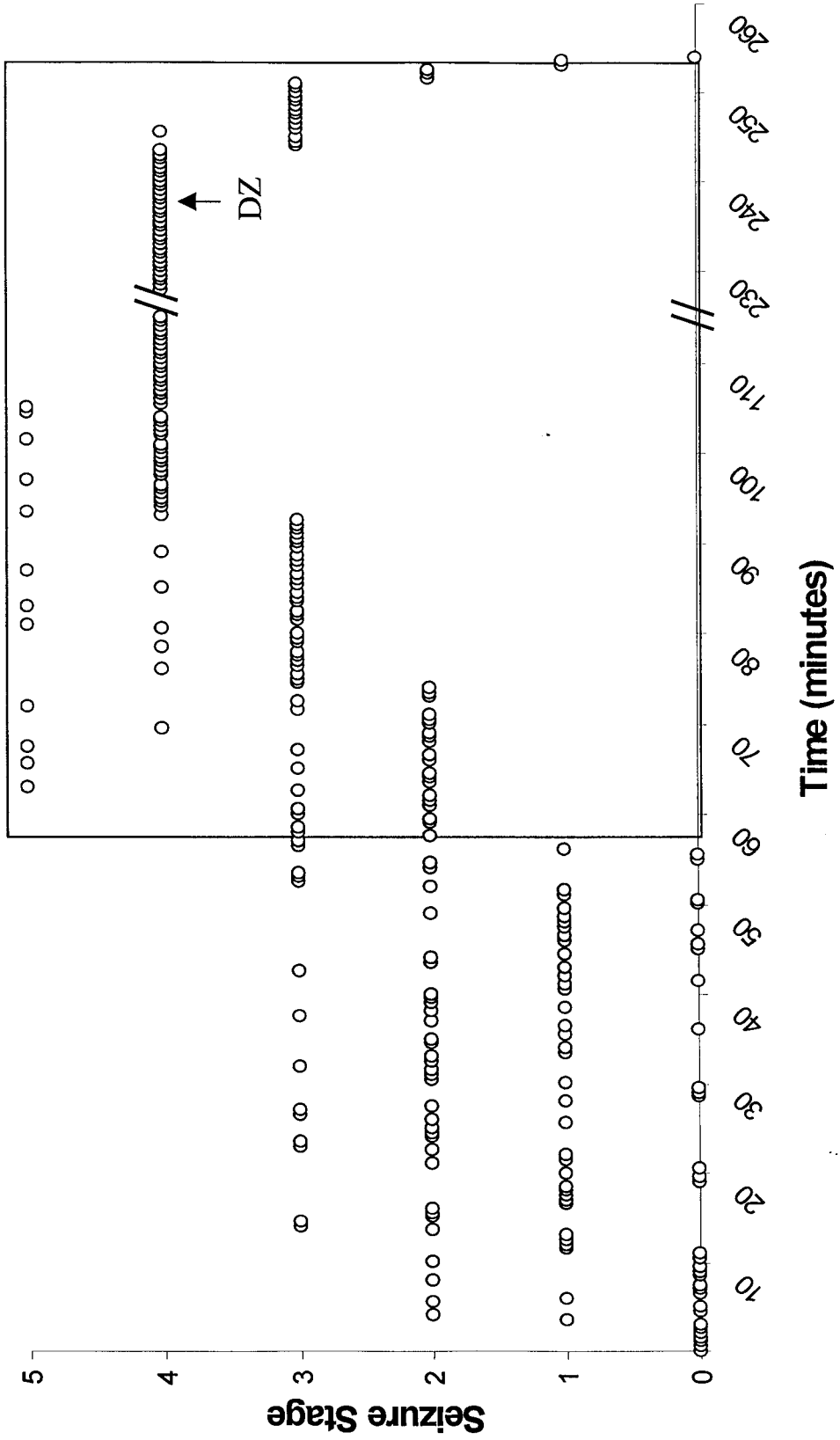
Seizure Stage
0
1
2
3
4
5
DZ
10
20
30
40
50
60
70
80
90
100
110
230
240
250
260
Time (minutes)

Table 2.1 Characteristics of long-duration status epilepticus and spontaneous recurrent seizures (SRS) elicited by kainic acid treatment

Animals	Outcome of KA treatment			Status epilepticus			SRS frequency
	SE	Fail[a]	Death[b]	Latency (min)	Duration (min)	Severity[c]	(times/week)[d]
Wistar	11	3	2	32.7±5.3	233.2±18.9	45.9%±9.5%	2.83±0.42
Long-Evans	12	2	2	52.2±8.1*	245.4±26.4	41.6%±8.8%	2.41±0.37

[a]Fail: animals failed to develop status epilepticus after KA injection.

[b]Death: animals died during or after the induction of status epilepticus.

[c]Severity: percentage of time animals spent in stage 4 and higher during status epilepticus.

[d]One episode of SRS was defined as spontaneous seizures involving stage 3 and higher seizures.

*Two-tailed Student's *t* test revealed a significant difference between Long-Evans hooded rats and Wistar rats in the measurement of SE latency.

The results indicated that the estimates generated by the biased cell counting technique were highly correlated with those from the unbiased cell counting procedure. Thus, in these experiments, the biased cell counting procedure could serve as a simpler, reliable method to estimate the hilar cell number. Therefore, only the biased cell counting technique was used in subsequent experiments of this thesis. There is, however, an undercounting in the biased procedure due to the lower magnifications used. Many cells that did not contain visible nuclei at 100X magnification (biased cell counting procedure) were judged as neurons by their morphology at 1000X magnification. However, our results indicated that the biased cell counting procedure was a valid method for evaluating relative group differences since the biased counting produced estimates that were closely correlated with unbiased estimates, yielding results that were very similar to those obtained using the optical disector method.

2. 3. 1. 3 Methodology: Control of Development Time During Timm Staining

A *post hoc* Tukey test showed that there was an overall tendency for the relative optical density to increase with the prolongation of development time (Figure 2.5A). The highest Timm density was observed in slides stained for 65 minutes. A significant difference in Timm labeling was found between sections with 65-min and 35-min development time (*post hoc* Tukey test, $p<0.05$ for CA3 region, $p<0.01$ for dentate gyrus, Figure 2.5 A). In addition, Timm labeling in the IML of the dentate gyrus in the 65-min group was significantly higher than that in the 50-min group (*post hoc* Tukey test, $p < 0.05$, Figure 2.5A). However, it was shown that such an increase in relative optical density with development time did not significantly affect the observed relative group

differences. No significant group-development time interaction was detected by five-way ANOVA (p=0.15, Figure 2.5 B). These results are reassuring in that they rule out the most likely source of bias from tissue preparation – small differences in development from stain to stain.

2. 3. 1. 4 Comparison of Mossy Fiber Sprouting Between Strains

No significant difference was detected between naïve Wistar and naïve Long-Evans hooded rats on Timm density measurement, suggesting that the baseline structure of the mossy fiber system is similar between these two strains (*post hoc* Tukey test, p>0.05, Figure 2.6).

As suggested by previous studies (Mathern et al., 1993), kainic acid treatment results in extensive mossy fiber sprouting in Wistar rats in both the IML and the stratum oriens (*post hoc* Tukey comparison between Wistar KA-treated rats and Wistar control rats, $p < 0.0005$, and $p < 0.001$, respectively, Figure 2.6). In contrast, KA-induced SE and spontaneous seizures only elicit a moderate mossy fiber sprouting in the inner molecular layer of the dentate gyrus in Long-Evans hooded rats (*post hoc* Tukey test, $p <$ 0.05, Figure 2.6). No obvious axonal sprouting was observed in the CA3 region in the Long-Evans strain (*post hoc* Tukey test, $p > 0.05$). Kainic acid treatment resulted in significantly more prominent mossy fiber sprouting in Wistar rats, when compared with Long-Evans hooded rats (*post hoc* Tukey test, $p < 0.001$ for the CA3 region, $p < 0.05$ for the dentate gyrus).

Figure 2.4 Comparison of unbiased counting technique and biased counting technique. **(A)** The unbiased estimates of total cell number per hilus were closely correlated with the biased estimates. The correlation coefficient r = 0. 93. **(B)** Both the unbiased and biased technique revealed a decrease in total hilar cell number after KA treatment in the Wistar strain (two-tailed *t* test, $p<0.05$). No obvious hilar cell loss was observed in Long-Evans rats using either cell counting technique.

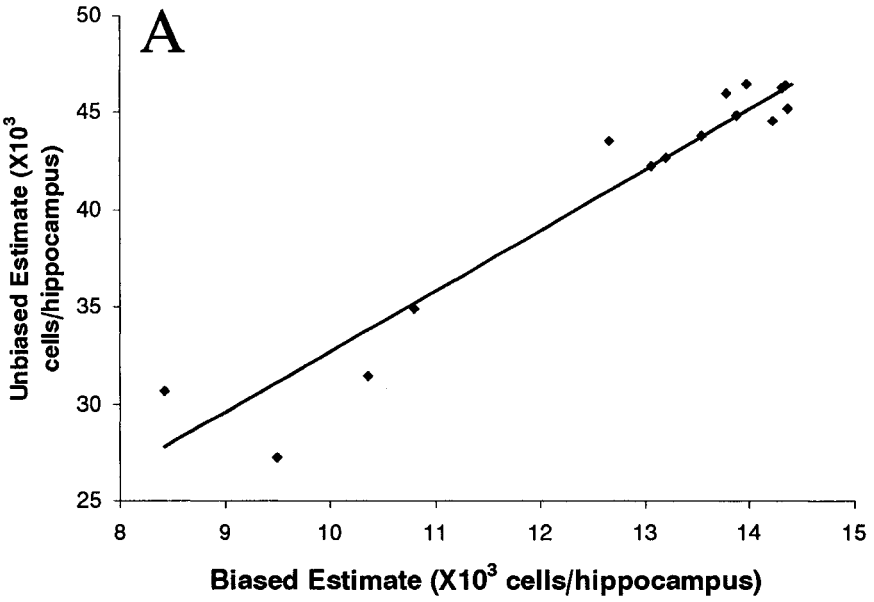
A
Unbiased Estimate (X10³ cells/hippocampus)
Biased Estimate (X10³ cells/hippocampus)
50
45
40
35
30
25
8
9
10
11
12
13
14
15


Wistar KA
Long-Evans KA
Wistar Control
Long-Evans Control

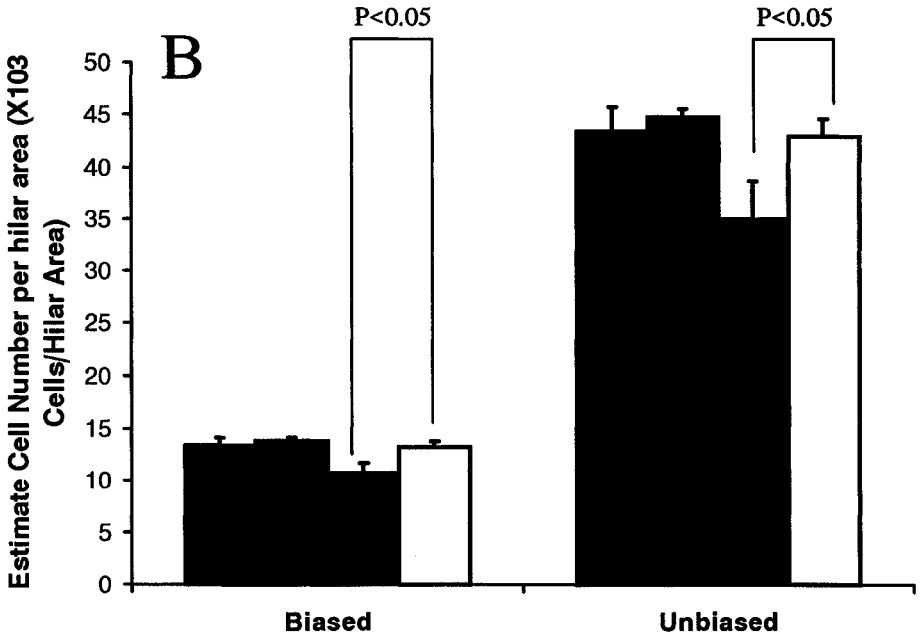
B
P<0.05
P<0.05
Estimate Cell Number per hilar area (X103 Cells/Hilar Area)
50
45
40
35
30
25
20
15
10
5
0
Biased
Unbiased

2. 3. 1. 5 Hilar Area Measurement and Biased Hilar Cell Counting

A *post hoc* Tukey test indicated that SE and spontaneous seizures did not alter the hilar area (Figure 2.7A, $p > 0.05$). In addition, no significant difference in hilar area was found between strains, whether KA-treated or not (*post hoc* Tukey test, $p > 0.05$).

The status epilepticus and the spontaneous seizures resulted in severe hilar cell loss in the Wistar strain (*post hoc* Tukey test, $p < 0.001$, Figure 2.7 B). The total number of hilar cells per section decreased by roughly 50% in Wistar KA-treated animals when compared with Wistar control rats. The decrease in hilar cell number was only observed in Wistar rats; there was no significant cell damage detected in Long-Evans hooded rats (*post hoc* Tukey test, $p > 0.05$, Figure 2.7 B).

Regression analysis suggested that the extent of hilar cell loss was significantly negatively correlated with the amount of Timm labeling in both the stratum oriens of CA3 region (correlation coefficient r = - 0.71, Figure 2.8A), and the inner molecular layer of the dentate gyrus (r = -0. 56, Figure 2.8B).

2. 3. 2 Experiment 2: Short Duration Status Epilepticus

2. 3. 2. 1 Development of Behavioral Seizures

The outcomes of the pilocarpine treatment are outlined in Table 2.2. No significant difference was detected in any of the SE measurements between the Wistar rats and the Long-Evans hooded rats. Short duration SE appeared to result in a lower lethality (0%) when compared with the long duration SE (12.9%), although the difference was not significant (chi-square test, p=0.15).

Figure 2.5 Effects of development time on Timm labeling. **(A)** The relative optical density increased with prolongation of development time. *Post hoc* Tukey test revealed a significant difference in Timm labeling between sections with 65-min and 35-min development times (* $p < 0.05$ for CA3 region, $p<0.01$ for dentate gyrus). Timm labeling in the IML of the dentate gyrus in the 65-min group was significantly higher than that in the 50-min group (** *post hoc* Tukey test, $p < 0.05$). **(B)** The overall relative group differences were not affected by the development time. No significant group-development time interaction was detected by five-way ANOVA (p=0.15).

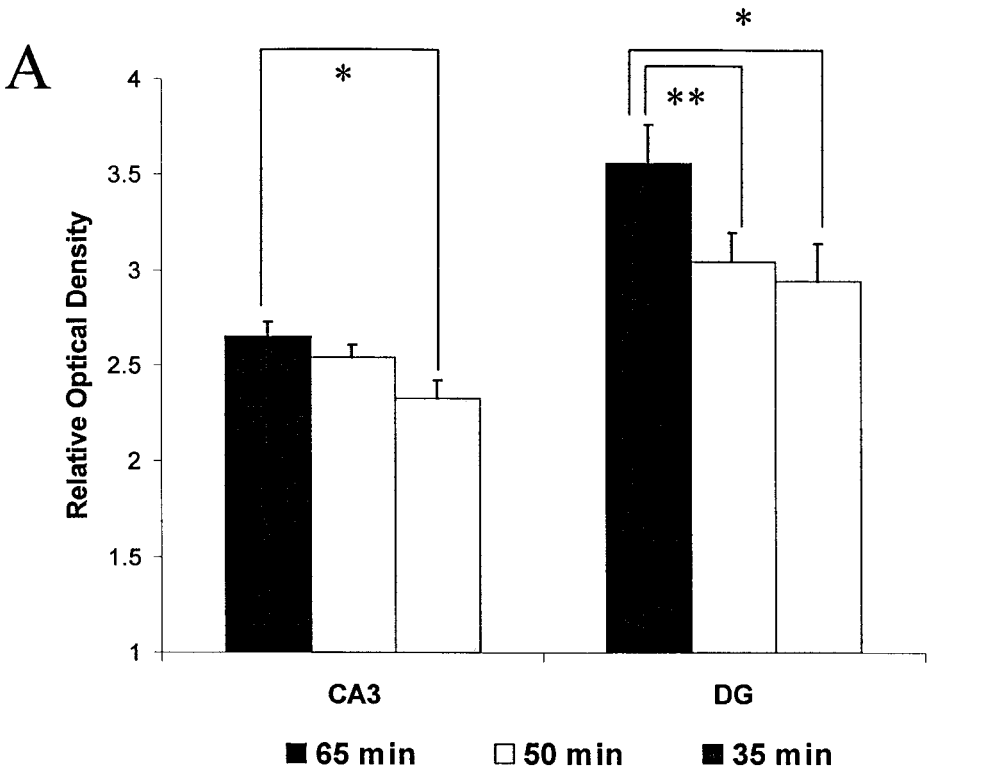
A
*
*
**
4
3.5
3
2.5
2
1.5
1
Relative Optical Density
CA3
DG
65 min
50 min
35 min

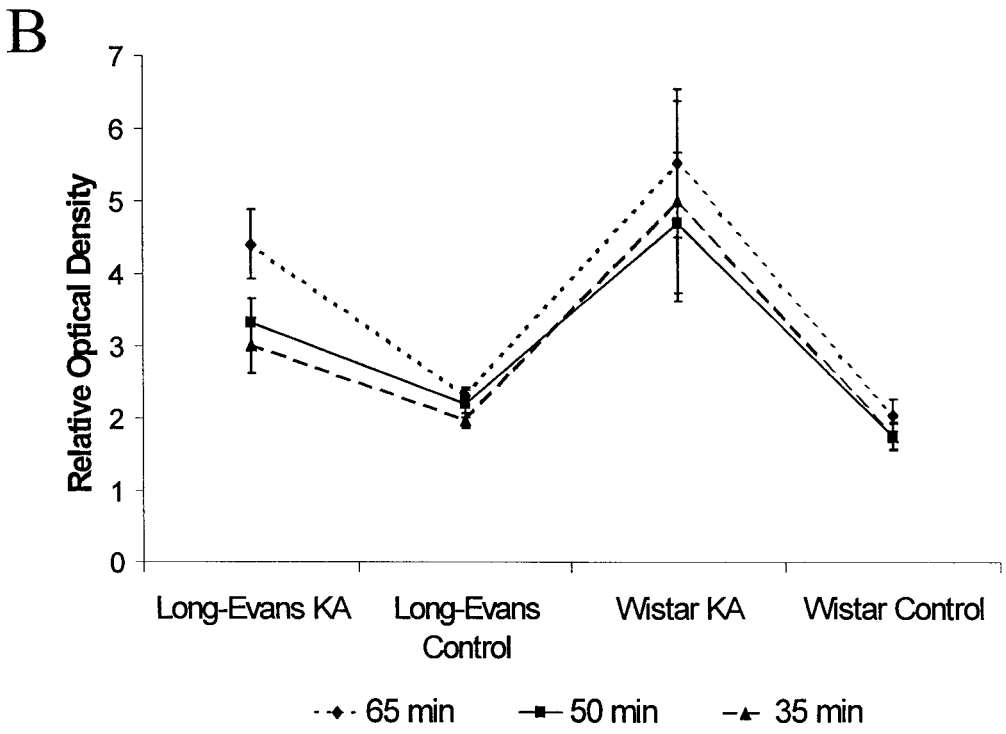
B
7
6
5
4
3
2
1
0
Relative Optical Density
Long-Evans KA
Long-Evans Control
Wistar KA
Wistar Control
65 min
50 min
35 min

Figure 2.6 Effects of kainic acid treatment on Timm labeling. Kainic acid treatment resulted in significantly more prominent mossy fiber sprouting in Wistar rats when compared with Long-Evans hooded rats (* *post hoc* Tukey test, $p < 0.001$ for CA3 region, $p < 0.05$ for dentate gyrus). KA-related status epilepticus and spontaneous seizures induced significant axonal growth in both the IML of the dentate gyrus (** *post hoc* Tukey test, $p < 0.0005$) and the stratum oriens of the CA3 region (** *post hoc* Tukey test, $p < 0.001$). Mossy fiber sprouting was only observed in the inner molecular layer in Long-Evans hooded rats after KA treatment (+ *post hoc* Tukey test, $p < 0.05$). No significant increase in Timm labeling was detected in the CA3 region in Long-Evans KA-treated rats compared to controls.

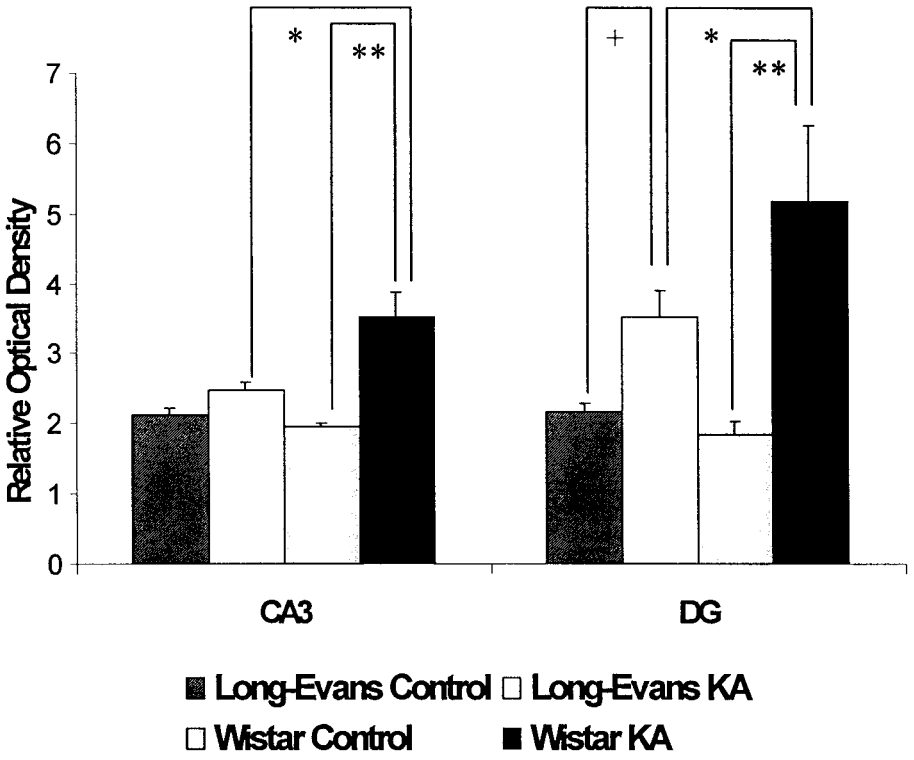
Relative Optical Density
0
1
2
3
4
5
6
7
*
**
+
*
**
CA3
DG
Long-Evans Control
Long-Evans KA
Wistar Control
Wistar KA

Figure 2.7 KA status produces severe neuronal loss in the Wistar strain, but not in the Long-Evans hooded strain. **(A)** The average size of the hilus did not differ between groups (*post hoc* Tukey test, $p > 0.05$ for the comparison of any of the two groups). **(B)** KA treatment significantly reduced the average number of hilar cells per section in Wistar rats (*post hoc* Tukey test, $p < 0.001$). No detectable difference in hilar cell number was observed in Long-Evans hooded rats between KA-treated rats and controls (*post hoc* Tukey test, $p > 0.05$).

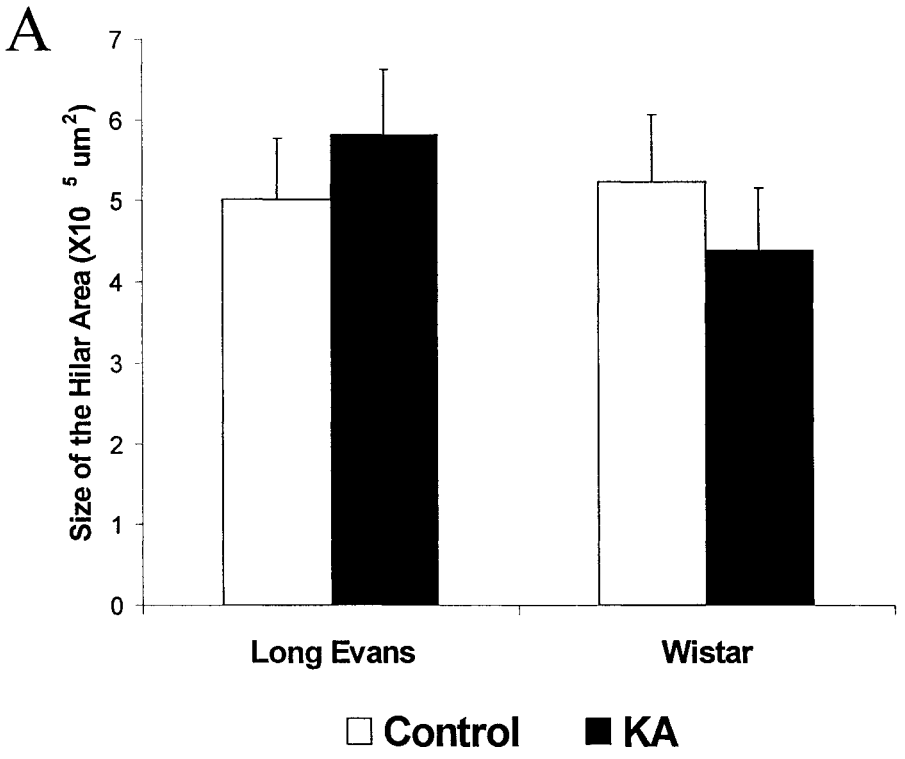
A
Size of the Hilar Area (X10 5 um2)
0
1
2
3
4
5
6
7
Long Evans
Wistar
Control
KA

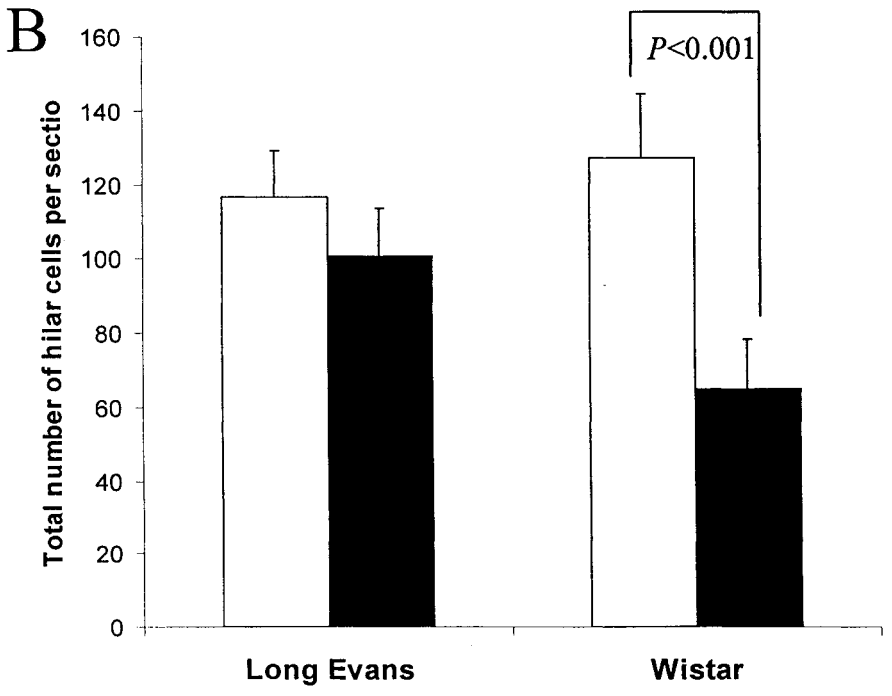
B
Total number of hilar cells per sectio
0
20
40
60
80
100
120
140
160
P<0.001
Long Evans
Wistar

Figure 2.8 Correlations between hilar cell number and mossy fiber sprouting. (A) The total hilar cell number per section was negatively correlated with Timm labeling in the CA3 region (r = -0. 71). **(B)** There was a negative correlation (r = -0. 56) between the Timm labeling in the IML and total hilar cell number per section. Both correlations were significant.

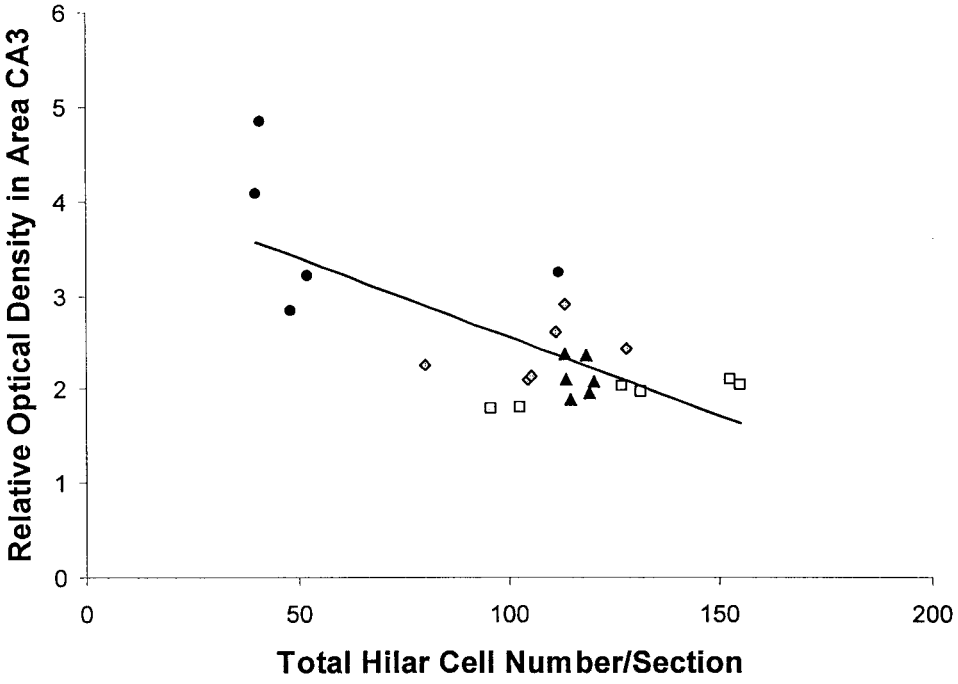
Relative Optical Density in Area CA3
0
1
2
3
4
5
6
0
50
100
150
200
Total Hilar Cell Number/Section


Wistar KA
Wistar Control
Long-Evans KA
Long-Evans Control

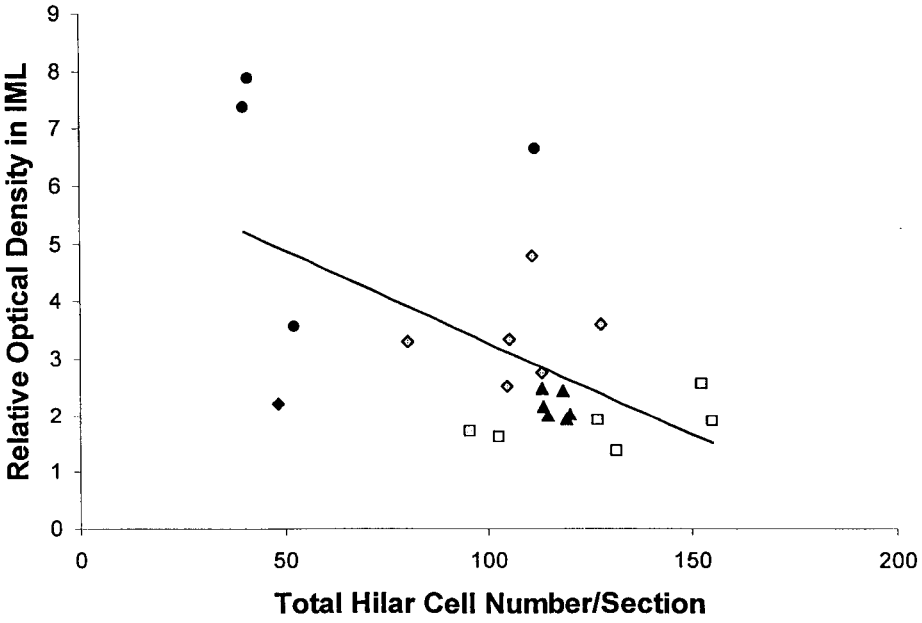
Relative Optical Density in IML
0
1
2
3
4
5
6
7
8
9
0
50
100
150
200
Total Hilar Cell Number/Section

Out of the 12 animals which developed SE after pilocarpine treatment (6 Long-Evans hooded rats and 6 Wistar rats), spontaneous behavioral seizures were only observed in 2 Long-Evans rats and 2 Wistar rats. However, since the rats were only observed for 1 hour daily, we could not rule out the possibility that the remaining animals developed SRS during these two months. The frequency of recorded spontaneous seizures also did not differ between the two strains (two-way ANOVA, $p > 0.05$, data not shown).

2. 3. 2. 2 Histology

Although the SE and spontaneous seizures elicited in this experiment were much shorter or weaker than those in Experiment 1, short duration status epilepticus appeared to be sufficient to trigger mossy fiber sprouting in the dentate gyrus (Figure 2.9). The short-duration SE elicited an increase of Timm labeling in the inner molecular layer in both the Long-Evans hooded rats ($p < 0.05$) and the Wistar rats ($p < 0.005$). In addition, a more severe mossy fiber sprouting was found in the Wistar strain after pilocarpine treatment when compared with the Long-Evans hooded rats (*post hoc* Tukey test, $p < 0.05$). No significant mossy fiber sprouting was observed in the CA3 region in either strain (*post hoc* Tukey test, $p > 0.05$, data not shown).

Because two different imaging programs were used in Experiments 1 and 2 (MCID imaging analysis system for Experiment 1, and BIOQUANT imaging system for Experiment 2), the density measures from these two experiments were not compatible with each other. Therefore, no direct comparison of Timm labeling was made between

Table 2.2 Characteristics of short duration status epilepticus evoked by pilocarpine treatment

Animals	Outcome of KA treatment			Status epilepticus		
	SE	Fail[a]	Death[b]	Latency (min)	Duration (min)	Severity[c] (%)
Wistar	6	2	0	35.3±6. 9	23.8±5.5	30.3±4.5
Long-Evans	6	1	0	39.1±10.1	18.9±9.9	25.4±6.9

[a]Fail: animals failed to develop status epilepticus after pilocarpine injection.

[b]Death: animals died during or after the induction of status epilepticus.

[c]Severity: percentage of time animals spent in stage 3 and higher seizures during status epilepticus.

the long-duration and the short-duration SE experiment. However, as expected and shown in Figure 2.10, short-duration SE resulted in only a mild to moderate sprouting in the inner molecular layer, while the Timm granule density observed following long-duration SE appeared to be much greater.

Short-duration SE did not elicit any detectable changes in the hilar area or hilar cell number in either strain (*post hoc* Tukey test, $p > 0.05$, data not shown). There was also no difference between the two strains in hilar area or hilar cell number (*post hoc* Tukey test, $p > 0.05$, data not shown).

2. 4 Discussion

The major findings of the current experiment are as follows: (1) although the development of SE and spontaneous seizures is similar between Wistar and Long-Evans hooded strains, the Wistar rats consistently show more severe mossy fiber sprouting and/or neuronal loss than the Long-Evans hooded rats; (2) short-duration status epilepticus is sufficient to trigger spontaneous seizures and subsequent mossy fiber sprouting, although it does not induce measurable neuronal loss; (3) the extent of mossy fiber sprouting and neuronal loss are correlated in the long-duration SE model. However, it is clear that MFS can be induced independently of neuronal loss in the Long-Evans strain; (4) the biased cell counting technique used in the current study provides a measure that is reliably proportional to the real neuronal numbers.

Figure 2.9 Mossy fiber reorganization after short-duration SE. Short-duration SE elicited an increase in Timm labelling in the inner molecular layer in both Long-Evans hooded rats (*post hoc* Tukey test, $p < 0.05$) and Wistar rats (*post hoc* Tukey test, $p < 0.005$). In addition, a more severe mossy fiber sprouting was found in the Wistar strain after the pilocarpine treatment when compared with Long-Evans hooded rats (*post hoc* Tukey test, $p < 0.05$).

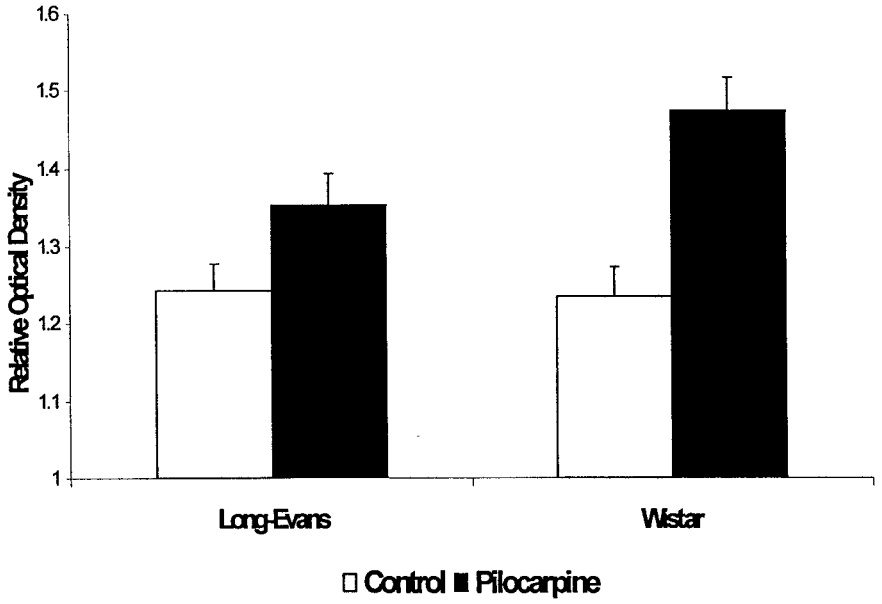
1.6
1.5
1.4
1.3
1.2
1.1
1
Relative Optical Density
Long-Evans
Wistar
□ Control ■ Pilocarpine

Figure 2.10 Representative examples of Timm labelling from different groups. Both long-duration SE (bottom) and short-duration SE (middle) resulted in MFS in the IML of the dentate gyrus when compared with control animals (top). The extent of mossy fiber sprouting was stronger in the long-duration SE groups when compared with short-duration SE. In addition, strain differences were detected after KA or pilocarpine-induced SE. The Wistar SE rats showed significantly more extensive axonal growth in the IML when compared with Long-Evans hooded rats.

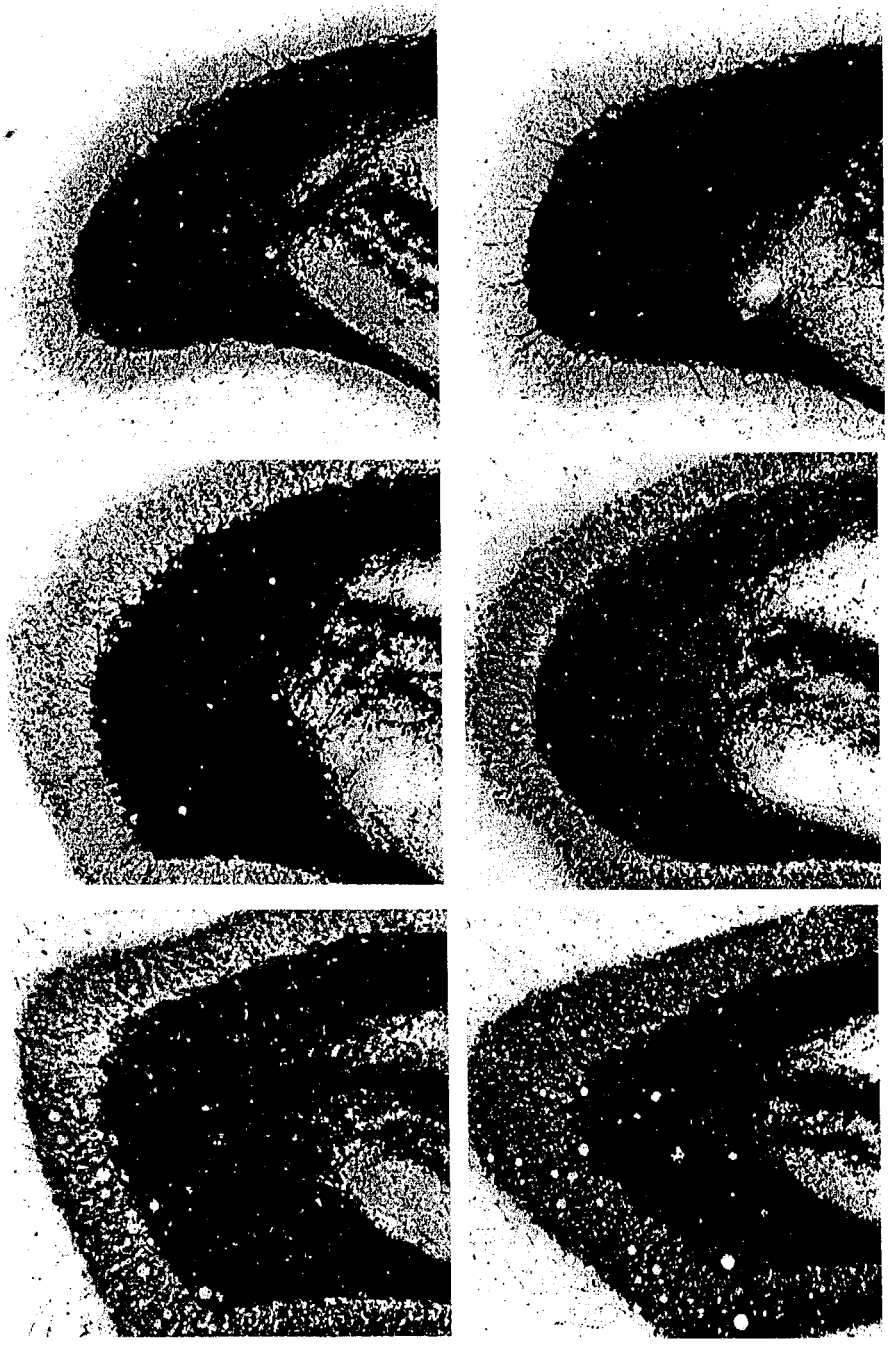

2. 4. 1 Strain Differences in the Development of Behavioral Seizures and Morphological Changes After KA Treatment

Golden et al. (1992,1995) have shown that Wistar strains are more sensitive to KA treatment and exhibit more reliable convulsant responses to kainic acid than Sprague-Dawley and Long-Evans hooded rats when tested for latency, duration and severity of seizure activity. However, we failed to detect any strain difference in their behavioural responses to KA treatment, except that the latency to develop SE was shorter in Wistar rats than in Long-Evans hooded rats. Consistent with Golden's results, however, we found that the variance of most of the behavioural measures was smaller in Wistar rats than in Long-Evans hooded rats. The underlying mechanisms for such strain differences remain unclear. Overall, similar amounts of acute and spontaneous recurrent seizures were observed in Wistar and Long-Evans hooded animals after KA and pilocarpine treatment.

Although the observed seizure activities were similar between strains, the Wistar rats showed significantly more mossy fiber sprouting after short-duration SE when compared with Long-Evans hooded rats. In addition, prolonged SE resulted in more severe neuronal loss and axonal growth in the Wistar strain. Thus, it is clear that the Wistar strain is more prone to developing epilepsy-related cell damage and axonal reorganization than the Long-Evans strain.

2. 4. 2 Relationship between Epileptogenesis, Axonal Growth and Neuronal loss

We detected a positive correlation between MFS and hilar cell loss in the long-duration SE model. In addition, Wistar animals, which develop severe neuronal damage

after prolonged SE, also demonstrate more axonal growth in both the dentate gyrus and the CA3 region than Long-Evans rats. Such results show that the extent of mossy fiber sprouting is to some extent related to the neuronal loss, suggesting that synaptic reorganization is partially a consequence of cell loss.

On the other hand, it is clear that neuronal damage is not crucial for either the development of seizures or axonal growth. No apparent neuronal loss was detected in the Long-Evans strain after short-duration or even after prolonged SE. However, these rats did develop spontaneous seizures and showed a prominent axonal reorganization. In addition, spontaneous seizures and axonal reorganization were induced despite the lack of neuronal damage in the short-duration SE model, further indicating that neuronal loss is not an essential prerequisite for the induction of axonal growth. Thus, we have dissociated both the axonal sprouting and the development of spontaneous seizures from hilar cell loss.

The extent of mossy fiber sprouting is clearly related to the amount of seizure activity. Prolonged SE results in more frequent spontaneous seizures and more severe axonal growth than short-duration SE. As suggested by previous studies, it is likely that excessive neuronal activity can induce axonal growth (Adams et al, 1997; Ramirez-Amaya et al. , 2000; Sutula et al. , 1988), and the sprouted collaterals contribute to the abnormal excitability observed in the epileptic brain (Babb et al. , 1991; Lynch & Sutula, 2000).

However, it has been shown that blocking axonal sprouting using a protein synthesis inhibitor does not affect the induction of spontaneous seizures (Longo and Mello, 1997, 1998, 1999; Covolan, 2000). In agreement with these results, we found no

correlation between the frequency of spontaneous seizures and the degree of mossy fiber sprouting. Therefore, it is clear that axonal growth is not a primary mechanism for this form of epilepsy.

2. 5 Conclusions

Although the Wistar and the Long-Evans hooded strains respond similarly to KA and pilocarpine-induced SE, we found that the Wistar rat strain showed reliable neuronal loss in the hilar region, while the Long-Evans strain showed no detectable neuron damage. In addition, the Wistar animals developed more severe neuronal growth than the Long-Evans hooded animals after status epilepticus, suggesting that genetic factors might be important for the induction of seizure-related morphological changes. We also found that spontaneous seizures and mossy fiber sprouting can be induced independently of cell damage, at least in the Long-Evans hooded animals. This evidence argues against the "dormant basket cell hypothesis" (for details of this theory see Chapter 1) and suggests that neuronal loss is neither the primary cause nor a necessary consequence of epilepsy.

CHAPTER 3: BEHAVIORAL AND ANATOMICAL CHANGES ASSOCIATED WITH PILOCARPINE-INDUCED STATUS EPILEPTICUS: A COMPARISON OF KINDLING-PRONE (FAST) AND KINDLING-RESISTANT (SLOW) STRAINS

3. 1 Introduction

The comparison between Wistar and Long-Evans hooded rats confirms that genetic predisposition is a crucial factor for seizure-related axonal growth and cell damage. In the experiments reported in this Chapter, we monitored status-induced behavioural responses and morphological changes in two additional rat strains, selectively bred in our lab.

3. 1. 1 The Kindling-Prone (FAST) and the Kindling-Resistant (SLOW) Strains

The original parent population of these two strains was a cross between two outbred rat strains, the Wistar and the Long-Evans Hooded rats. From the first to the eleventh generation (F1 - F11), kindling-prone (FAST) and kindling-resistant (SLOW) strains were selected and bred based on their susceptibility to electrical kindling stimulation. By the sixth generation (F6) and thereafter, there was little or no overlap between these strains in the distribution of amygdala kindling rate, defined as the number of electrical stimulations required to reach the first stage V seizure. On average, the SLOW rats required five times or more stimuli to develop generalized seizures than the FAST rats (Racine et al., 1999).

In addition to kindling rapidly, the FAST rats often advance directly from stage II to stage V convulsive seizures (Racine et al., 1999). Indeed, electrophysiological studies have shown that the FAST strain is characterized by a faster inter-hemispheric propagation of seizure discharges and weaker paired-pulse inhibition, raising the possibility that the two strains differ in inhibitory mechanisms (Racine et al., 1999).

More recently, it has been shown that the GABAergic system, which plays an important role in epileptogenesis (for review see Burnham, 1989), differs dramatically between the FAST and SLOW strains (Steingert, 1983; Poulter et al., 1999; MyIntyre et al., 1999a). The FAST strain is more sensitive to GABA antagonist-induced seizures (Steingert, 1983), while the SLOW animals require lower doses of sodium pentobarbital for anaesthesia (MyIntyre et al., 1999a). In addition, *in situ* hybridization studies have shown that the $GABA_A$ receptor α subunits are differentially expressed in FAST and SLOW rats (Poulter et al., 1999). Over-expression of the embryonic α subunits ($\alpha 2$, $\alpha 3$ and $\alpha 5$) and under-expression of adult α subunits ($\alpha 1$) have been found in FAST rats, which may account for their increased seizure susceptibility.

Also playing an inhibitory role in epileptogenesis is the noradrenergic system (McIntyre and Edson, 1989). Although the baseline concentration and utilization of noradrenaline (NA) appears to be similar between FAST and SLOW animals (McIntyre et al. , 1999b), it has been shown that the SLOW rats exhibit a much higher and more sustained NA release in response to stressors (Merali et al., 1997). Thus, it is possible that a stress-linked deficiency in the NA system contributes to epileptogenesis.

The functions of the glutamatergic system, which is the major excitatory pathway in the hippocampus, appear to be similar between the FAST and SLOW strains. Such

functions include the induction of LTP and LTD within the hippocampus (Racine et al., 1999), and baseline NMDA and AMPA receptor binding (McIntyre, personal communication). However, Elmer et al. (1998) have found that the structure of the glutamatergic mossy fiber pathway differs significantly between the FAST and the SLOW strains. They detected a significantly darker Timm labelling in the IML of the SLOW strain than in the FAST strain, indicating either a relatively denser mossy fiber distribution in the IML, or a higher concentration of zinc within the axons, of the SLOW animals. These differences in baseline mossy fiber structure raise the possibility that this system might also respond differently to seizure activity in the two strains.

3. 1. 2 Rationale of the Current Study

The kindling-prone and kindling-resistant strains were selectively bred based on their amygdala kindling rate (Racine et al., 1999). Subsequent studies have shown that kindling rates are also different between these two strains when the kindling stimulation is delivered to other brain regions, including the hippocampus, piriform cortex, and perirhinal cortex (McIntyre et al., 1999a). However, the proportional difference in kindling rate between FAST and SLOW strains varies with the focus of kindling stimulation. The greatest difference is found in amygdala kindling, where the SLOW rats reached their first stage V seizures five times slower than the FAST rats. During hippocampal kindling, by contrast, the SLOW strain required only twice as many stimulations to achieve criterion (McIntyre et al., 1999a). There have been few experiments that have tested the response of these strains to other epileptogenic treatments. In the present study, we explore the response of the FAST and SLOW strains

to pilocarpine-induced SE. In addition to the immediate behavioral responses to pilocarpine treatment, we monitored the structure of the mossy fiber system as well as the size and cell density of the hilus. The average duration of status epilepticus was controlled at roughly 1 hour in an effort to produce a moderate level of axonal sprouting and cell damage while minimizing loss of animals.

3. 2 Materials and Methods

3. 2. 1 Animals

Two strains of genetically kindling-prone (FAST) and kindling-resistant (SLOW) rats, characterized by their different kindling rate (Racine et al., 1999), were used in the current study. 20 FAST and 20 SLOW male rats (weight between 250 to 300 g) were randomly divided into four groups: the FAST experimental group (n=12), the FAST control group (n=8), the SLOW experimental group (n=13), and the SLOW control group (n=7). The animals were housed individually, maintained on an *ad lib* feeding schedule, and kept on a 12 hr on/12 hr off light cycle.

3. 2. 2 Induction of Status Epilepticus and Observation of Spontaneous Seizures

Twenty minutes before the pilocarpine treatment, animals received atropine methyl nitrate (5 mg/kg, i.p.) to prevent the peripheral side effects of pilocarpine. Pilot experiments suggested that both strains were more sensitive to pilocarpine treatment than either parent strain. Pilocarpine treatment at a dose of 300mg/kg i.p. resulted in severe generalized seizures, jumping, and eventually, death. Therefore, the pilocarpine doses for the experimental groups were lowered to 200-250 mg/kg pilocarpine i.p., while the two

control groups were injected with an equal volume of 0. 9% NaCl. The development of behavioral seizures was continuously monitored by an experimenter blind to the experimental conditions. The behavioral progression of pilocarpine-induced seizures was rated and recorded every 30 seconds using Racine's classification (Racine, 1972). Status epilepticus was defined as continuous seizure activity lasting for at least 15 minutes. Fifteen minutes after status epilepticus started, animals received an injection of 2mg diazepam i.p. in order to stop the seizure activity. An additional dose of diazepam (1 mg, i.p.) was administered 30 minutes after the first injection if animals remained in status epilepticus at that time point. Behavioral seizures were continuously monitored after the diazepam injection until the animals showed no sign of seizure activity for at least 5 minutes. Experimental animals that failed to develop status epilepticus and control animals were observed for 2 hours after pilocarpine or saline injection and then injected with 2mg diazepam i.p. The lethality and the failure rate were calculated and evaluated with a chi-square test. Experimental animals that failed to develop SE were excluded from histological analyses. The severity of SE was evaluated by the percentage of time the animals spent in stage IV and higher seizures during status epilepticus. The latency, duration and severity of SE were measured for each animal and subjected to a Student's *t* test for statistical analysis.

All animals were observed for one hour daily for 8 weeks to monitor the development of spontaneous recurrent seizures (SRS). Only stage 3 and higher seizures (seizures involving forelimb clonus) were recorded. The weekly frequency of SRS was calculated, and a two-way ANOVA with one between variable (groups) and one within variable (weeks) was conducted for statistical purposes.

3. 2. 3 Timm Staining and Mossy Fiber Sprouting Measurement

Two months after the induction of status epilepticus, animals were perfused and the brains removed and sectioned for Timm and cresyl violet staining (for details see Chapter 2). To minimize variability, sections from different animals were stained simultaneously and the development time was maintained at 60 min.

Five horizontal sections roughly 4. 6, 5. 2, 5. 8, 6. 4 and 7mm ventral to Bregma were examined at 50× magnification with a BIOQUANT true color imaging system. The relative optical density of the stratum oriens and inner molecular layer were measured and calculated as stated in Chapter 1. A four-way ANOVA [4 × (2 × 5 × 16/9)] with one between variable (group) and three within variables [section (1-5 ventral to dorsal), brain hemisphere (left or right) and cursor position (1–16, in CA3; 1–9, in IML)] was conducted for the analysis of Timm density in the CA3 or IML regions.

3. 2. 4 Hilar Area Measurement and Hilar Cell counting

Cresyl violet was used to visualize neurons in the hilar area. Both the area of the hilus and the hilar cell density were evaluated with the BIOQUANT imaging system as stated in Chapter one. Five sections taken from approximately the same vertical coordinates as those used in the Timm density measurements were analyzed. All the cells within the defined hilar area with visible nuclei were counted manually. A three-way ANOVA [4 × (2 × 5)] with one between variable (group) and two within variables [brain hemisphere (left or right) and brain section depth (1-5, ventral to dorsal)] was conducted for statistical analysis.

3. 3 Results

3. 3. 1 Status Epilepticus and Spontaneous Recurrent Seizures

The outcome of the pilocarpine treatment and the measurement of SE and SRS are described in Table 3.1. Higher lethality (46%) was observed in the SLOW strain, after pilocarpine treatment, compared to the FAST strain (25%), but the difference was not significant (Chi-square test, χ^2=1.60, p=0.21). Two FAST rats and one SLOW rat failed to develop status epilepticus, and the data from these three animals were excluded from the following analysis. The FAST rats required significantly less time to develop SE (14.8±4.6 mins) than SLOW rats (28.3±5.5 mins) (two tailed t test, p<0.05). The FAST strain also showed a tendency to develop more severe seizures during status epilepticus as measured by the percentage of time animals spent in stage IV and V seizures when compared with the SLOW strain (40.2%±9.1% for the FAST strain, 23.6±11.2% for the SLOW strain). However, such a tendency was not significant (two-tailed t test, p=0. 23 for SE severity measurement). There was also no significant difference found between these two strains on measurements of total SE duration (two-tailed t test, p=0. 93), or the frequency of spontaneous seizures (two-way ANOVA, p=0. 25), although the frequency of spontaneous recurrent seizures did increase over time (two-way ANOVA, week main effect, p<0.00001) (Figure 3.1). A seizure-free period (~2 weeks) was observed after the induction of acute seizures, in which no spontaneous seizures were observed.

In summary, the development of status epilepticus and spontaneous seizures did not differ between the kindling-prone and kindling-resistant strains, although there was a

Table 3.1 Characteristics of status epilepticus and spontaneous recurrent seizures (SRS) evoked by pilocarpine treatment

Animals	Outcome of pilocarpine treatment			Status epilepticus			SRS frequency
	SE	Fail[a]	Death[b]	Latency (min)	Duration (min)	Severity[c]	(times/week)[d]
FAST	7	2	3	14.8±4. 6	70.2±27. 5	40.2%±9.1%	1.68±0.48
SLOW	6	1	6	28.3±5.5	67.3±15. 1	23.6±11.2%	1.58±0.51

[a]Fail: animals failed to develop status epilepticus after pilocarpine injection.

[b]Death: animals died during or after the induction of status epilepticus.

[c]Severity: percentage of time animals spent in stage 4 and higher during status epilepticus.

[d] One episode of SRS was defined as spontaneous seizures involving stage 3 or higher seizures.

Figure 3.1 Development of spontaneous recurrent seizures after pilocarpine-induced status epilepticus in FAST and SLOW rats. The average frequency of SRS increased with time (two-way ANOVA, $p<0.00001$), but an ANOVA revealed no significant strain difference in the development of spontaneous seizures ($p>0.05$). Error bars represent standard errors of means.

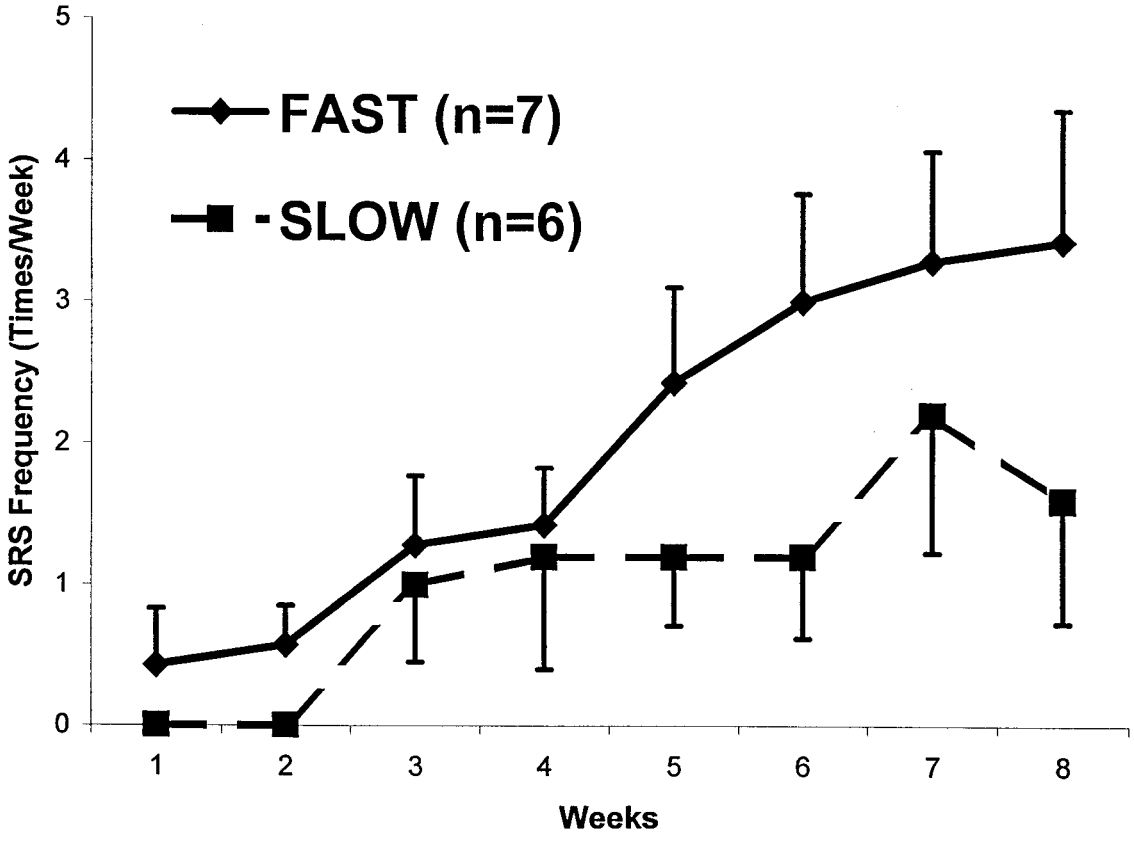
FAST (n=7)
SLOW (n=6)
SRS Frequency (Times/Week)
0
1
2
3
4
5
1
2
3
4
5
6
7
8
Weeks

tendency for the FAST strain to require less time to develop status epilepticus and to remain in the generalized seizure stages (stages 4 and 5) for longer periods of time.

3. 3. 2 Mossy Fiber Sprouting Measurement

A *post hoc* Tukey test revealed a significant difference in baseline Timm labelling between the two strains. The zinc-laden mossy fibers were significantly more heavily labelled in the inner molecular layer of the dentate gyrus (*post hoc* Tukey test, $p<0.01$) and the striatum oriens of CA3 region (*post hoc* Tukey test, $p<0.05$) in the naïve FAST animals than in SLOW animals (Figure 3.2).

Although pilocarpine treatment elicited a similar level of status epilepticus and spontaneous recurrent seizures between the two strains, only SLOW animals developed significant mossy fiber sprouting in the IML (*post hoc* Tukey test, $p<0.005$, Figure 3.3 A) and stratum oriens (*post hoc* Tukey test, $p<0.001$, Figure 3.3 B). No significant change in the Timm granule density was found in these regions after pilocarpine treatment in FAST animals (*post hoc* Tukey test, $p>0.05$, Figure 3.3).

3. 3. 3 Hilar Area Measurement and Hilar Cell Density

Pilocarpine-induced status epilepticus led to a significant enlargement of the hilar area (*post hoc* Tukey test, $p<0.0005$, Figure 3.4 A) in the FAST strain, but not in the SLOW strain (*post hoc* Tukey test, $p>0.05$, Figure 3. 4A). Although there was no significant difference in baseline hilar area measurements between the naïve FAST and SLOW animals (*post hoc* Tukey test, $p>0.05$), hilar area was significantly larger in the

Figure 3.2 Timm labelling in the inner molecular layer of the dentate gyrus and the stratum oriens of the CA3 region. The zinc-laden mossy fibers showed a significantly greater density of Timm labelling in the dentate gyrus (*post hoc* Tukey test, $p<0.01$) and CA3 region (*post hoc* Tukey test, $p<0.05$) in the FAST strain compared to the SLOW strain.

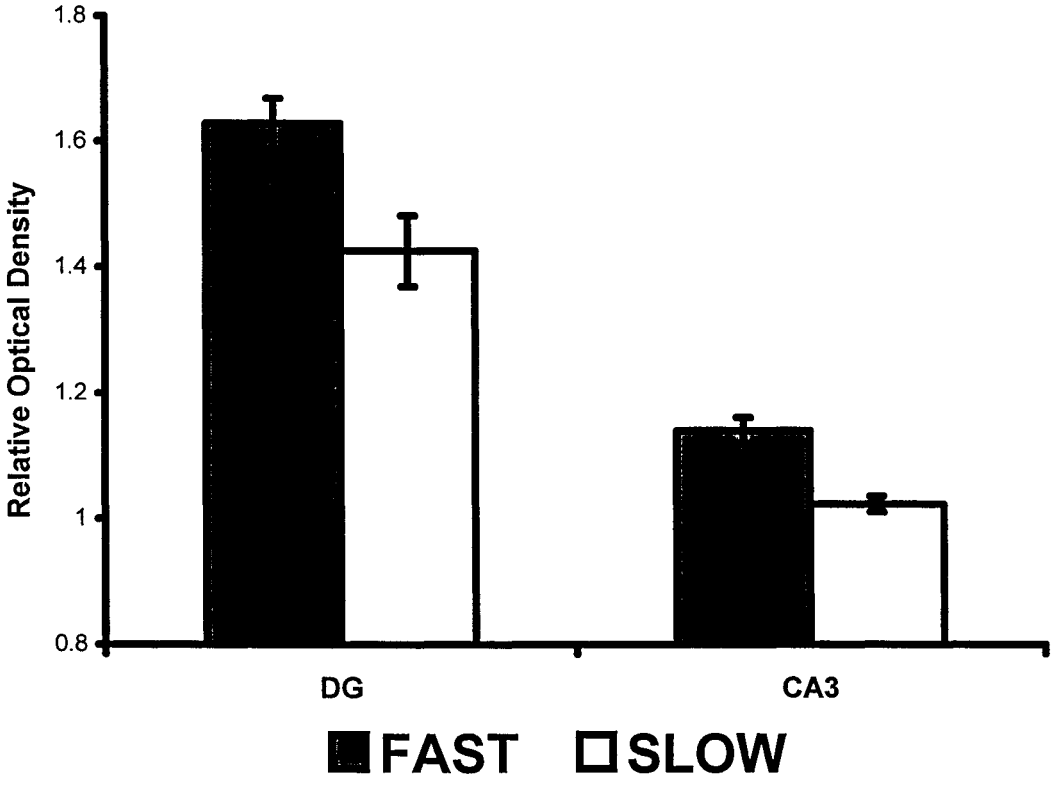
1.8
1.6
1.4
1.2
1
0.8
Relative Optical Density
DG
CA3
FAST
SLOW

Figure 3. 3 Effects of seizure activity on Timm labelling. The SLOW strain showed significant mossy fiber sprouting in both the IML of dentate gyrus (*post hoc* Tukey test, $p<0.005$) (upper panel, A) and the stratum oriens of the CA3 region (*post hoc* Tukey test, $p<0.001$) (lower panel, B) after pilocarpine-induced SE and SRS. No evident mossy fiber sprouting was detected in FAST rats after pilocarpine treatment.

A. DG

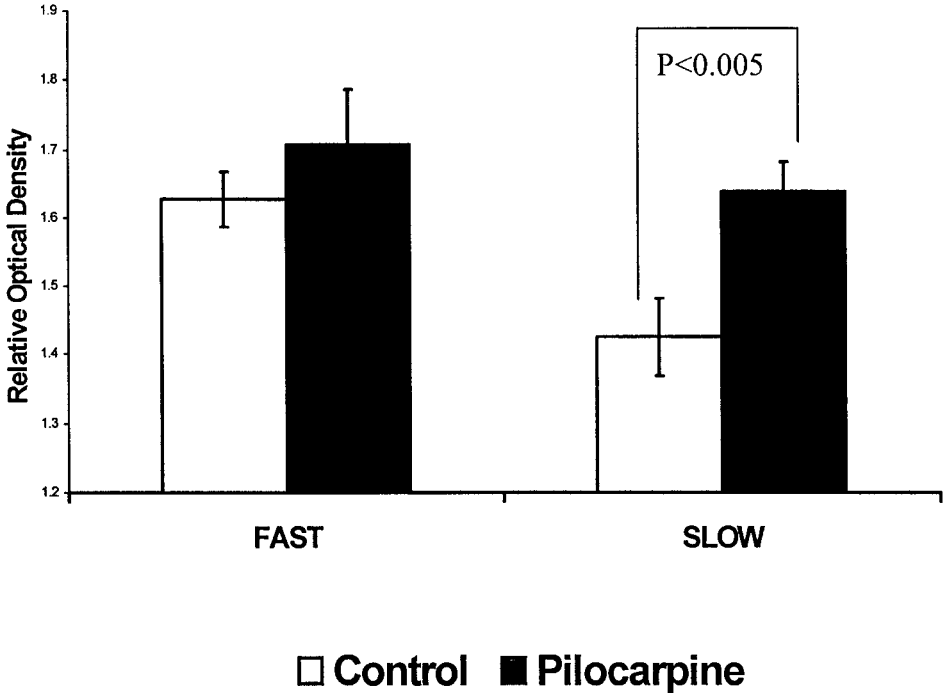
Relative Optical Density
1.9
1.8
1.7
1.6
1.5
1.4
1.3
1.2
P<0.005
FAST
SLOW
Control
Pilocarpine

B. CA3

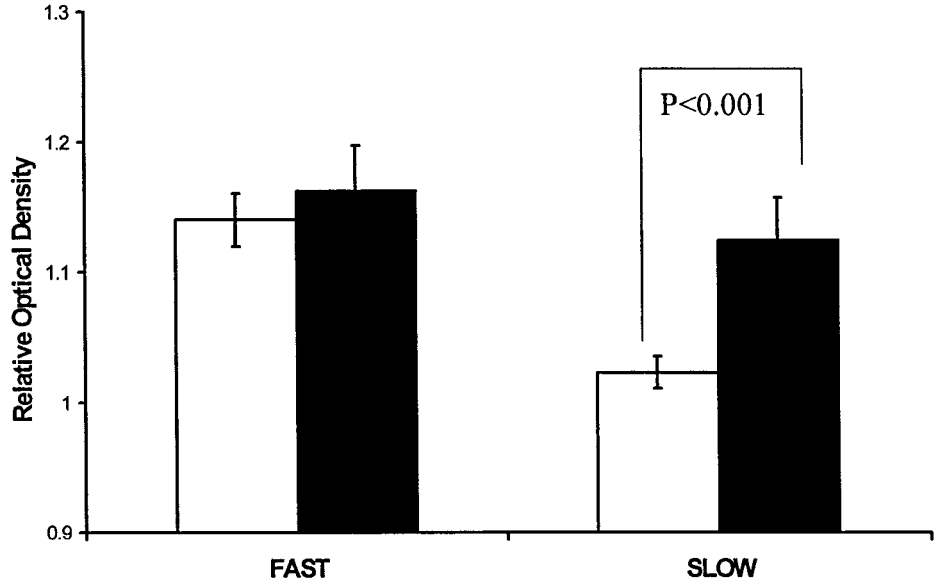
Relative Optical Density
1.3
1.2
1.1
1
0.9
P<0.001
FAST
SLOW

Figure 3.4 Group differences in hilar area and hilar cell density measurements (upper panel, **A**, and lower panel, **B**, respectively). Seizure activity resulted in an enlargement of hilar area (*post hoc* Tukey test, $p<0.0005$) and a decrease in hilar cell density (*post hoc* Tukey test, $p=0.05$) in the FAST strain. The SLOW strain was resistant to seizure-related changes in hilar area. In addition, the hilar cell density in naïve FAST animals was significantly higher than that in SLOW animals (*post hoc* Tukey test, $p<0.05$).

A. Hilar Area

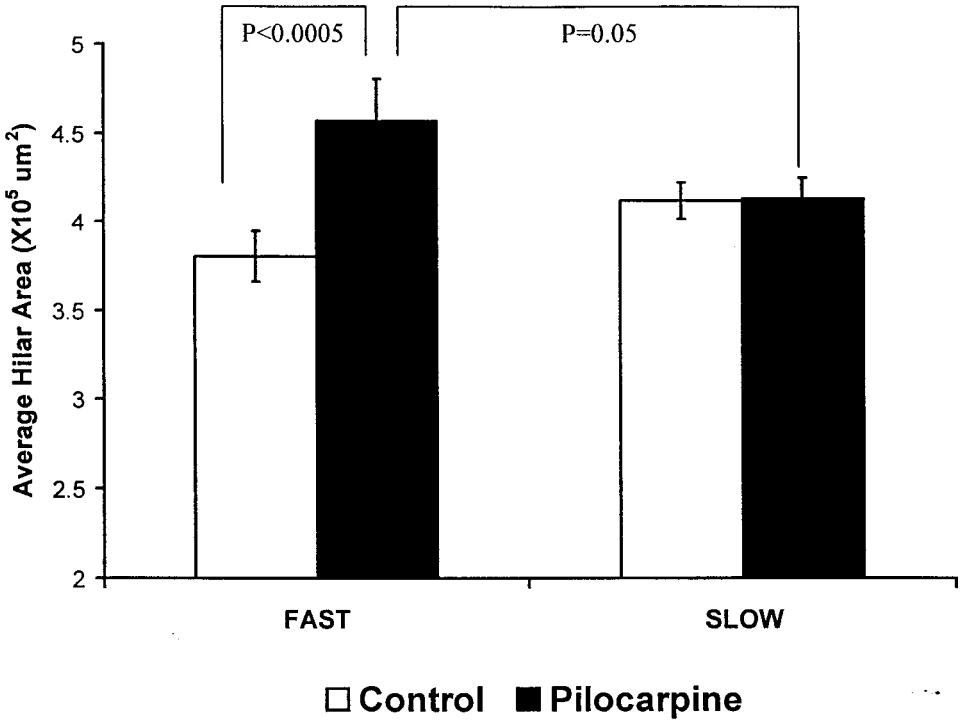

B. Hilar Cell Density

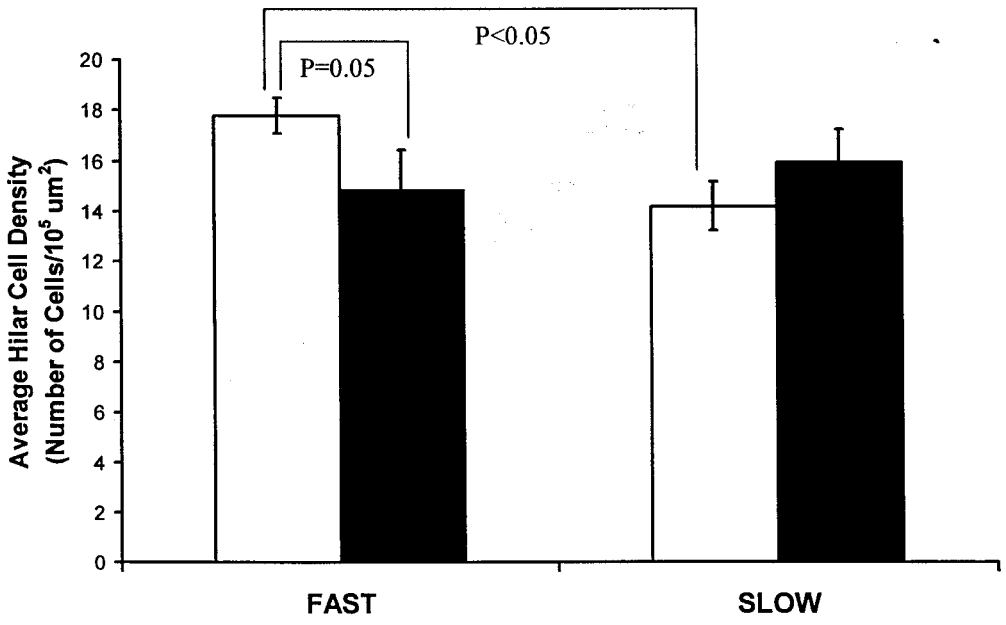

Figure 3.5 Correlation between SRS, MFS and neuronal damage. (A) There exists a positive correlation between the average frequency of spontaneous seizures and mossy fiber sprouting (r = 0. 66), indicating that the extent of mossy fiber sprouting may be partially determined by the frequency of SRS. (B) A negative correlation was found between the average area of the hilus and the average hilar cell density (r=-0. 69). Overall, no clear cell loss was detected after seizures, so the observed decrease in hilar cell density is likely a consequence of hilar area expansion.

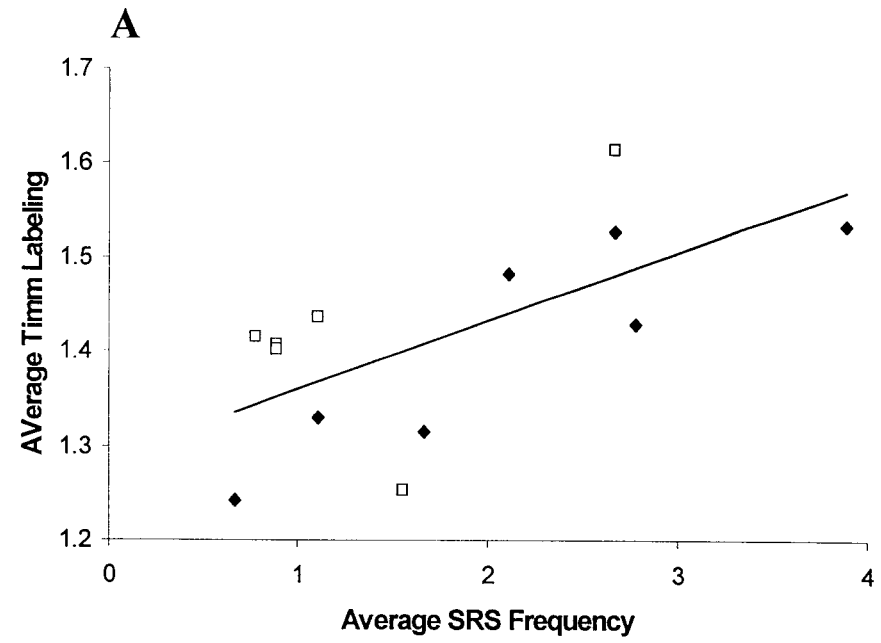
A
AVerage Timm Labeling
1.7
1.6
1.5
1.4
1.3
1.2
0
1
2
3
4
Average SRS Frequency

◆ FAST □ SLOW

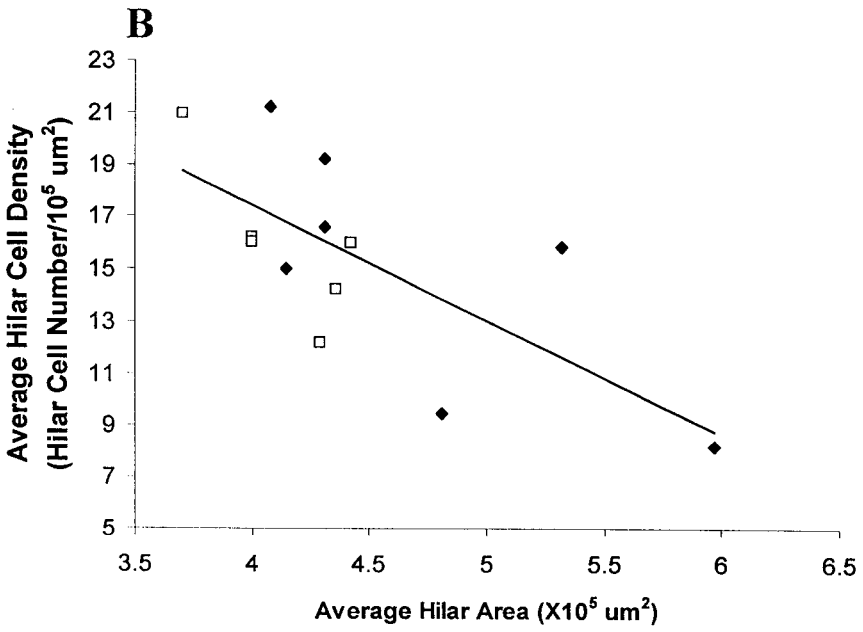
B
Average Hilar Cell Density
(Hilar Cell Number/10^5 um^2)
23
21
19
17
15
13
11
9
7
5
3.5
4
4.5
5
5.5
6
6.5
Average Hilar Area (X10^5 um^2)

FAST compared to the SLOW strain following pilocarpine-induced SE and SRS (*post hoc* Tukey test, p=0. 05).

The total hilar cell number within each section did not differ between groups (*post hoc* Tukey test, p>0. 05, data not shown). The cell density for each section was calculated as the total cell number within the hilus divided by the area of the entire hilus. The cell density within the hilus was significantly higher in naïve FAST animals when compared with naïve SLOW animals (*post hoc* Tukey test, p<0. 05). As shown in Figure 4B, seizure activity significantly reduced the hilar cell density in the FAST animals (*post hoc* Tukey test, p=0. 05) but not in the SLOW animals (*post hoc* Tukey test, p>0. 05).

3. 3. 4 Correlation Analysis

A total of 8 variables were selected for correlation analysis, including: SE latency, SE duration, SE severity, week of onset for SRS, average frequency of SRS, average Timm labeling, average size of hilar area, and average hilar cell density. A positive correlation (r = 0.66, Figure 3.5A) was found between the average frequency of SRS and the average Timm labeling, suggesting that the extent of mossy fiber sprouting was correlated with the frequency of spontaneous seizures. The average hilar cell density was shown to be negatively correlated with the average hilar area (r = -0. 69, Figure 3. 5B). Such a negative correlation between hilar area and hilar cell density was consistent with our previous findings (Adams et al., 1996; Li et al., in preparation), suggesting that the observed decrease in hilar neuronal density might be a consequence of hilar area expansion.

No correlation was found between any of the status epilepticus measurements and the measurements of SRS, nor was there a correlation between the SE measurements and any of the histological measurements.

3. 4 Discussion

Although the kindling-prone (FAST) and kindling-resistant (SLOW) strains respond differently to amygdala kindling, we demonstrate in this study that pilocarpine treatment elicits similar levels of status epilepticus and numbers of spontaneous recurrent seizures in these two strains.

The FAST animals required significantly less time to develop status epilepticus than the SLOW animals. It has been suggested that status epilepticus is primarily due to a failure of seizure-terminating mechanisms, such as a failure of GABAergic inhibition (DeLorenzo, 1990). There is also some indication that the major difference between the FAST and the SLOW animals lies in the GABA system. Electrophysiological and molecular biological studies have shown a decrease of GABAergic inhibition and an alteration of the composition of the $GABA_A$ receptor in the FAST animals (Steingert, 1983; Poulter et al., 1999; McIntyre et al., 1999a). Thus, we propose that the shorter latency to status observed in the FAST strain might be a consequence of a more rapid failure of GABAergic inhibition under challenge.

In the present study, we found that the Timm density in both the inner molecular layer of the dentate gyrus and the stratum oriens of the CA3 region was significantly higher in naïve FAST compared to naïve SLOW animals, suggesting that the baseline organization of mossy fiber systems is different between these two strains. Normally, the

mossy fibers project to CA3 pyramidal cells, hilar mossy cells, and hilar inhibitory interneurons. The greater Timm granule density in the FAST strain suggests that the mossy fibers have made abnormal synaptic contact with the basal dendrites of CA3 pyramidal cells and the dendrites of DG granule cells. Such aberrant connections might result in an increase of feed-forward and recurrent excitability, contributing to the faster kindling rates in the FAST animals.

Surprisingly, pilocarpine treatment elicited mossy fiber sprouting in the SLOW strain but not in the FAST strain. One possibility is that the Timm density changes in the FAST and SLOW strains proceed at different rates. Previous studies indicated that mossy fiber sprouting reaches its maximal level 3 months after the induction of SE in wild-type animals (Mathern et al., 1993). In the present studies, the animals were sacrificed two months after SE. Another possibility is that the dense baseline Timm granule density in the FAST rats is already near maximal levels.

Status epilepticus and subsequent spontaneous seizures elicit an expansion of hilar area and a decrease in hilar cell density in the FAST strain but not in the SLOW strain. Again, no gross hilar neuronal loss is observed in either strain, suggesting that neuronal loss is neither the cause nor a necessary consequence of seizure activity. Several potential mechanisms might explain the difference between FAST animals and SLOW animals. It is possible that the SLOW rats are resistant to seizure-related reactive gliosis, or that the gliosis lasts for a shorter period of time in the SLOW strain.

We have also found that the extent of mossy fiber sprouting is not well correlated with any measurement of status epilepticus but is positively correlated with the frequency

of spontaneous recurrent seizures. Such results suggest an important role for spontaneous seizures in the development of axonal sprouting.

Consistent with previous studies (Adams et al., 1997), we found that the hilar cell density is negatively correlated with the hilar area, indicating that the decrease in hilar cell density might be a consequence of seizure-induced hilar area enlargement. Although no overall hilar cell loss was observed in either strain, they both developed spontaneous seizures, arguing against a casual relationship between gross cell damage and epilepsy.

3.5 Conclusions

In the present study, we tested the responses of kindling-prone (FAST) and kindling-resistant (SLOW) strains on pilocarpine-induced seizures. We found that the FAST animals required less time to develop SE, probably due to a failure of inhibitory mechanisms. No detectable neuronal loss was observed in either strain after SE, arguing against a casual relationship between neuronal damage and epilepsy. The mossy fiber system was significantly different between these two strains and responded differently to seizure activity, raising the possibility that these circuit differences might contribute to the strain differences in epileptogenesis.

CHAPTER 4: INTRAVENTRICULAR ADMINISTRATION OF NT-3 RETARDS KINDLING AND INHIBITS KINDING-INDUCED MOSSY FIBER SPROUTING IN ADULT RATS

4.1 Introduction

The neurotrophins, including NGF, BDNF, NT-3 and NT-4/5, play an important role in the survival, differentiation, and neurite outgrowth of many types of neurons (for reviews see Lindsay et al., 1994; Davies, 1994). In adult CNS, the most prominent expression of BDNF and NT-3 and their cognate receptors, TrkB and TrkC, is found in structures associated with epilepsy and synaptic plasticity such as hippocampus, olfactory cortex, amygdala, cerebellum, and neocortex (Ebendal, 1992; Ernfors et al., 1990; Katoh-Semba et al., 1996; Kokaia et al., 1993; Zhou and Rush, 1994), suggesting that these factors may modify neuronal plasticity in adult animals. Indeed, accumulating evidence indicates that neurotrophins, especially BDNF and NT-3, are involved in synaptic transmission, the development and maintenance of neuronal plasticity such as LTP, and epileptogenesis in adult CNS (for review see Gall, 1993; McAllister et al., 1999). Seizure activity induces dramatic changes in the mRNA and/or protein levels of neurotrophins and their high-affinity Trk receptors in a variety of experimental models of epilepsy such as kindling, pilocarpine-, pentylenetetrazol- or quinolinic acid-induced seizures, kainic acid-induced status epilepticus, or even a single epileptiform afterdischarge (Bengzon et al., 1993; Binder et al., 1998; Elmer et al., 1998; Ernfors et al., 1991; Gall and Isackson, 1989; Hughes et al., 1998; Humpel et al., 1993; Inoue et al., 1998; Katoh-Semba et al.,

1999; Kokaia et al., 1996; Merlio et al, 1993; Morimote et al., 1998; Mudo et al., 1996; Rocamora et al., 1992, 1994; Rudge et al., 1998; Schmidt-Kaster & Olson, 1995).

Furthermore, kindling procedures have been shown to regulate the expression of neurotrophins and Trk receptors differently in the kindling-prone and kindling-resistant strains (Kokaia et al., 1996). The seizure-induced increase in NGF, BDNF, TrkB and TrkC messenger RNAs and decrease in neurotrophin-3 messenger RNA levels in the DG granule cell layer are only observed in the FAST, but not in the SLOW strain. It is postulated that the differential regulation of neurotrophins and Trk receptors might contribute to the strain differences in epileptogenesis and kindling rates.

Previous studies in Racine's lab have shown that continuous infusion of NGF into the brain enhanced the development of kindling and kindling-induced axonal growth (Adams et al., 1997). In contrast, infusion of BDNF (Larmet et al., 1995; Osehobo et al., 1999), high-affinity TrkB receptor immunoadhesins (Binder et al., 1999), or reagents that block NGF activity (van der Zee et al., 1995; Rashid et al., 1995) inhibited the development of kindling-induced seizures and/or kindling-related axonal growth. However, the development of kindling-induced behavioral seizures was significantly retarded in both BDNF and NT-3 heterozygous mice (+/-) (Kokaia et al., 1995; Elmer et al., 1997). The effects of the deficits in the mutant mice are difficult to interpret because the knockout of NT-3 during development influenced seizure-induced regulation of BDNF and TrkB in these mice (Elmer et al., 1997). Continuous infusion of NT-3 into the normal adult animal might be a way of determining the influence of NT-3 on kindling development and kindling-induced axonal growth in the absence of developmental effects on BDNF regulation. In the present study, we test whether continuous infusion of NT-3

has any effect on kindling and kindling-induced mossy fiber sprouting. The effects of continuous infusion of NT-3 on Trk expression and phosphorylation are also addressed using Western-blotting techniques. Our primary interest is in activation-induced rather than damage-induced neural growth, so we used the Long-Evans rat strain.

4.2 Materials and Methods

4.2.1. Production and Purification of Recombinant NT-3

Human NT-3 cDNA was a generous gift from Dr. L. F. Reichardt (University of California, San Francisco). NT-3-expressing baculoviruses were constructed and used to prepare baculovirus-infected insect cell supernatants as previously described (Fahnestock and Zhu, 1999). NT-3 was purified from the supernatants by affinity chromatography. Purity of the NT-3 (>95%) was determined by sodium dodecyl sulfate-polyacrylamide gel electrophoresis (SDS-PAGE). Protein concentration was determined by Bradford assay (Bio-Rad Laboratories, Hercules, CA), and biological activity was analyzed by neurite outgrowth assay (Rashid et al., 1995). The biological activity of our purified NT-3 was equivalent to that of a commercially-available NT-3 (Alomone Labs, Israel) in the neurite outgrowth assay. The NT-3 was suspended in phosphate-buffered saline (PBS) at a concentration of 1 mg/ml for infusions. For some experiments, human recombinant NT-3 was obtained from Regeneron Pharmaceuticals (Tarrytown, N.Y.). It was suspended in histidine buffer [4.5% (w/v) mannitol, 0.5% (w/v) sucrose, 10mM histidine, pH 5.0].

4.2.2 Animals and Surgery

Adult male Long-Evans hooded rats (n=67) weighing between 300 and 450 gm were divided into 6 groups as shown in Table 1. They were housed individually, maintained on an *ad lib* feeding schedule, and kept on a 12 hr on/12 hr off light cycle. The rats were anesthetized with sodium pentobarbital (65 mg/kg) and placed in a stereotaxic frame. A teflon-coated, stainless steel bipolar electrode (diameter, 190 μm) was implanted into the right perforant pathway. The stereotaxic coordinates (Paxinos and Watson, 1985) were 7.6 mm posterior and 4.8 mm lateral to Bregma, and 3.3 mm ventral from the brain surface. A cannula was implanted into the right lateral ventricle at 0.6 mm posterior and 1.3 mm lateral to Bregma and 5.0 mm below the skull surface. Both the electrode and the cannula were firmly attached to the skull with dental cement and three stainless steel screws anchored into the skull. A flow-regulated osmotic minipump (Alzet model 2000, flow rate 0.5μl/hr, maximally effective for 18 days) was connected to the cannula via polyethylene tubing and placed subcutaneously in the dorsal neck/back region. A total of 27 rats received continuous NT-3 infusions (12 μg/day) via the minipumps. Vehicle control for NT-3 was either PBS or histidine buffer, depending on whether the NT-3 was produced in our lab or obtained from Regeneron Pharmaceuticals. In order to control for the effects of protein infusion alone, an additional group of animals received cytochrome C (12 μg/day), which has a similar molecular weight and charge as NT-3. Animals were given 7 d recovery after surgery before the kindling protocol started.

Table 4.1 Groups involved in this experiment

Groups	Number of animals
NT-3 kindled	16
NT-3 non-kindled	11
Cytochrome C kindled	11
Cytochrome C non-kindled	11
Vehicle kindled	12
Vehicle non-kindled	6
Total	67

4.2.3 Kindling Procedure

Each kindling stimulation comprised a one-second train of 1 msec biphasic rectangular pulses at a frequency of 60 Hz with a pulse intensity ranging from 500 to 700 μA. This was sufficient to trigger an epileptiform afterdischarge (AD) after each stimulation. Animals were stimulated twice daily for a total of 11 days, and the duration of the ADs was recorded. An observer blind to the experimental conditions monitored the behavioral progression of kindling-induced seizures and rated the seizures according to Racine's classification (Racine, 1972): class 0, no behavioral change; class 1, facial clonus; class 2, head nodding; class 3, unilateral forelimb clonus; class 4, rearing with bilateral forelimb clonus; and class 5, rearing and falling (loss of postural control). Animals that failed to reach stage 5 after 22 stimulations were assigned a value of 22 for the purpose of calculating kindling rate.

4.2.4 Immunoprecipitation and Western Blotting

Two hours after the last kindling stimulation, five animals were randomly chosen from the NT-3-infused kindled, NT-3-infused non-kindled, cytochrome C-infused kindled, and cytochrome C-infused non-kindled groups. They were anesthetized with sodium pentobarbital (65 mg/kg) and decapitated. The brains were removed and the hippocampi from both hemispheres were isolated. The tissues were immediately frozen in liquid nitrogen and stored at -80°C until homogenization.

Primary antibodies. Rabbit polyclonal TrkC antibody (C-14; Santa Cruz Biotechnology, Santa Cruz, CA) was raised against a peptide at the carboxy terminus of TrkC and broadly reacted with TrkA, TrkB, and TrkC. This was used as a pan-Trk

antibody. Rabbit polyclonal TrkA antibody (Chemicon International, Temecula, CA) was raised against the extracellular domain of TrkA and is specific for TrkA. Mouse monoclonal TrkB antibody (BD Transduction Laboratories, Franklin Lakes, NJ) was raised against amino acids 156-322 of human TrkB, corresponding to the extracellular domain. This antibody detects both full-length (145kDa) and truncated (95kDa) forms of TrkB. The rabbit polyclonal TrkC(out) antibody, raised against amino acids 88-108 of rat TrkC, detects all isoforms of TrkC and was kindly provided by Dr. David Kaplan (Montreal Neurological Institute, Montreal, Quebec, Canada). Rabbit polyclonal phospho-TrkA (Tyr490) antibody (Cell Signaling Technology, New England Biolabs, Mississauga, ON, Canada) detects all Trks phosphorylated at Tyr490. Mouse monoclonal anti-β-actin was obtained from Sigma-Aldrich (Mississauga, ON, Canada).

Secondary antibodies: Horseradish peroxidase (HRP)-conjugated donkey anti-rabbit and sheep anti-mouse antibodies were obtained from Amersham Pharmacia Biotech (Oakville, ON, Canada). HRP-dextran-labeled goat anti-rabbit secondary was purchased from DAKO (Mississauga, ON, Canada).

Sample preparation. The right hippocampus from each animal was homogenized in 10 ml/g tissue of lysis buffer (20 mM Tris pH 8, 137 mM NaCl, 1% NP-40, 10% glycerol, 1 mM phenylmethylsulfonyl fluoride [PMSF], 10 μg/ml aprotinin, 10 μg/ml leupeptin, 2 mM sodium orthovanadate, 50 mM sodium fluoride, 1 μM okadaic acid, 2mM ethylene glycol-bis [β-aminoethyl ether] N,N,N',N'-tetraacetic acid [EGTA]). The homogenates were incubated 30 min on ice and centrifuged at 12,000 rpm for 15 min at 4°C in an Eppendorf microcentrifuge. Some supernatants required an additional 5-min centrifugation to completely clarify. Supernatants containing solubilized protein were

aliquoted and stored at -80°C. Protein concentrations were determined using a DC protein assay kit (Bio-Rad, Hercules, CA). For Western blotting of homogenates, 60 μg protein was loaded per lane for TrkA analysis, and 10-30 μg for TrkB.

Immunoprecipitation. All incubations were performed at 4°C with gentle rotation. 12 mg of proteinA-Sepharose (Amersham Pharmacia Biotech) in 60 μl lysis buffer was added to 2 mg protein and incubated for 1 hour to reduce nonspecific binding. Supernatants were collected by centrifugation for 15 s at 12,000 rpm in an Eppendorf microcentrifuge, and 16 μl pan-Trk antibody (C-14) was added. Incubation was performed for 2.5 hours and was followed by a 2.5-hour incubation with 24 mg proteinA-Sepharose in 220 μl lysis buffer. Supernatants were collected by centrifugation as above and saved. The beads were washed 5 times with 1 ml ice-cold washing buffer (20 mM Tris pH 8, 137 mM NaCl, 1% NP-40, 10% glycerol, 1 mM PMSF, 2 mM sodium orthovanadate) and then boiled in 110 μl of 2 X SDS-PAGE sample buffer (0.125 M Tris-HCl pH 6.8, 4 % sodium dodecyl sulfate, 20 % glycerol, 10 % mercaptoethanol, 0.002 % bromophenol blue) for 5 min. Supernatants were collected by a brief centrifugation as above, and divided into aliquots for immunoblotting. 15% of each immunoprecipitate was loaded per lane for TrkA detection, 10% for TrkB, 25-30% for TrkC, and 25-35% for phosphoTrk.

Western Blot Analysis. The immunoprecipitates were resolved on 6% or 8% SDS polyacrylamide gels and homogenates were resolved on 4-20 % acrylamide Ready Gels™ (Bio-Rad) by electrophoresis at 130V for about 1 hr. Proteins were transferred to PVDF membrane (Amersham Pharmacia Biotech) in transfer buffer (25mM Tris, 192 mM glycine, 20% (v/v) methanol) for 1.5 hour at 350 mA at 4°C and blocked for 1hour at

room temperature in TBS-T (10 mM Tris pH 7.5, 100 mM NaCl, 0.1% Tween 20) with 5% (w/v) Carnation nonfat milk powder. Incubations with primary antibodies were performed overnight at 4°C in TBS-T at dilutions of 1:1,000 for TrkC(out), 1:2,000 for TrkA, 1:2,000 in 5% nonfat milk powder for TrkB and 1:2,000 in 5% BSA for phosphoTrk antibody. After 4 6-minute washes in TBS-T, blots were incubated for 1 hr at room temperature in HRP-conjugated secondary antibodies in TBS-T with 5% nonfat milk powder at a dilution of 1:6,000 for donkey anti-rabbit antibody and 1:10,000 for sheep anti-mouse antibody. For analysis of phosphorylated trks, the more sensitive HRP-dextran-labeled anti-rabbit secondary was used at a dilution 1:200 in TBS-T with 5% milk powder for 1 hr at room temperature.

Following Trk analysis, blots containing homogenates were reblocked in 5% nonfat milk powder and reprobed with anti-β-actin antibody at a 1:40,000 dilution for 50 min, followed by incubation with HRP-conjugated sheep anti-mouse antibody at 1:80,000, both at room temperature in TBS-T. An ECL chemiluminescence system (Amersham Pharmacia Biotech) was used for detection, according to the manufacturer's instructions.

Densitometry and Statistical Analysis. Developed films were scanned using a Microtek Scanner and the bands were quantified using Scion Image Beta 4.01 Acquisition and Analysis software (Scion Corporation, Frederic, MD). Each Western blot contained a standard rat hippocampal sample to allow normalization between blots. Both raw density values and values normalized to β-actin were analyzed. Each Western blot was repeated at least twice.

4.2.5 Histology

Two weeks following the last kindling stimulation, the remaining animals were perfused and sectioned for Timm and cresyl violet staining. The methods for perfusion, sectioning and staining were described in the Methods section of Chapter 1. The relative optical density of IML and stratum oriens as well as the area of the hilus and the total number of hilar cells per section were measured and calculated. In addition, the cell density for each section was calculated as the total cell number within the hilus divided by the area of the entire hilus.

4.2.6 Statistical Analyses

Statistical analyses were performed using Statistica software (Statsoft, Tulsa, Oklahoma). A two-way analysis of variance (ANOVA) was used to evaluate the behavioral progression of seizures and differences in afterdischarge durations. A two-way ANOVA was also used to evaluate relative levels of Trk protein and Trk phosphorylation, with one between variable (groups) and one within variable (Western blotting). For analysis of hilar area and hilar neuronal number, a three-way ANOVA [4 × (2 × 6)] with one between variable (group) and two within variables [brain hemisphere (left or right) and brain section depth (1-6, ventral to dorsal)] was used. A four-way ANOVA [4 × (2 × 6 × 16/9)] with one between variable (group) and three within variables [section (1-6 ventral to dorsal), brain hemisphere (left or right) and cursor position (1–16, in CA3; 1–9, in IML)] was conducted for the analysis of Timm density in the CA3 or IML regions. The ANOVA was followed by Tukey *post hoc* comparisons. A

probability of < 0.05 was considered significant. All measures reported in the present study are expressed as mean ± standard error of the mean (SEM).

4.3 Results

4.3.1 Progression of Behavioral Seizures and Afterdischarge Measurement

Post hoc Tukey tests revealed no differences in behavioral seizure or afterdischarge duration (AD) measurements between cytochrome C-infused kindled, PBS kindled, or histidine buffer kindled groups ($p>0.05$, data not shown). Therefore, results from these groups were pooled as one control kindled group (n=23). There was no significant difference between results using NT-3 purified in our lab and NT-3 from Regeneron Pharmaceuticals on the progression of behavioral seizures or AD duration (*post hoc* Tukey test, $p=0.65$, data not shown), hence these two groups were pooled as one NT-3-infused non-kindled group (n=23) and one NT-3-infused kindled group (n=16). Continuous infusion of NT-3 significantly retarded the development of behavioral seizures compared to the control kindled group (two-way ANOVA, $p<0.001$, Figure 4.1A). Among the sixteen NT-3-infused kindled rats, seven of them (43.75%) failed to develop any stage 5 seizures during the kindling procedure. In contrast, only two animals from the control group (8.70%) failed to show stage 5 seizures. NT-3-infused rats required more electrical stimulations (mean +/- SEM, 17.7 +/- 1.2) to reach the first stage 5 seizure when compared with the control kindled group (11.1 +/- 1.2) (two-tailed *t*-test, $p<0.0005$, Figure 4.1B). No difference in AD duration was observed between groups (two-way ANOVA, $p>0.05$, data not shown).

4.3.2 Mossy Fiber Sprouting

A four-way ANOVA [groups (4) X Sections (6) X hemispheres (2) X cursor positions (9 for dentate gyrus, 16 for CA3 region)] was conducted for the analyses of Timm granule density. *Post hoc* Tukey tests revealed no difference between animals infused with different vehicles (PBS or histidine buffer) on Timm granule density measures ($p>0.05$, data not shown). In addition, no difference was found between the cytochrome C-infused kindled group and the vehicle-infused (PBS or histidine buffer) kindled group, nor was there a difference between cytochrome C-infused non-kindled animals and vehicle-infused non-kindled animals (*post hoc* Tukey test, $p>0.05$, data not shown). The results demonstrate that infusion of a protein that has a similar molecular weight and charge as NT-3 does not affect kindling-induced mossy fiber sprouting. Therefore, in the following analysis, the cytochrome C-infused groups and vehicle-infused groups are pooled as one control kindled group and one control non-kindled group for comparison purposes.

Continuous infusion of NT-3 (12 μg/day) in the absence of kindling induced mossy fiber sprouting in both the inner molecular layer of the dentate gyrus (*post hoc* Tukey test, $p<0.005$) and the stratum oriens of CA3 region (*post hoc* Tukey test, $p<0.05$, Figure 4.2 and 4.3B).

Consistent with our previous studies (Adams et al., 1997; Rashid et al., 1995; van der Zee et al., 1995), current experiments demonstrate kindling-induced mossy fiber sprouting in both the dentate gyrus (*post hoc* Tukey test, $p<0.01$) and CA3 region (*post hoc* Tukey test, $p<0.001$, Figures 4.3C and 4.4A). Continuous intraventricular infusion of NT-3, however, significantly inhibits this kindling-induced sprouting effect in IML (four-

Figure 4.1 NT-3 inhibits kindling epileptogenesis. (A) Continuous infusion of NT-3 significantly retards the development of behavioral seizures (two-way ANOVA, $p<0.001$). (B) NT-3-infused rats require more electrical stimulations (mean +/- SEM, 17.7 +/- 1.2) to reach the first stage 5 seizure when compared with control kindled group (11.1 +/- 1.2) (two-tailed *t*-test, $p<0.0005$).

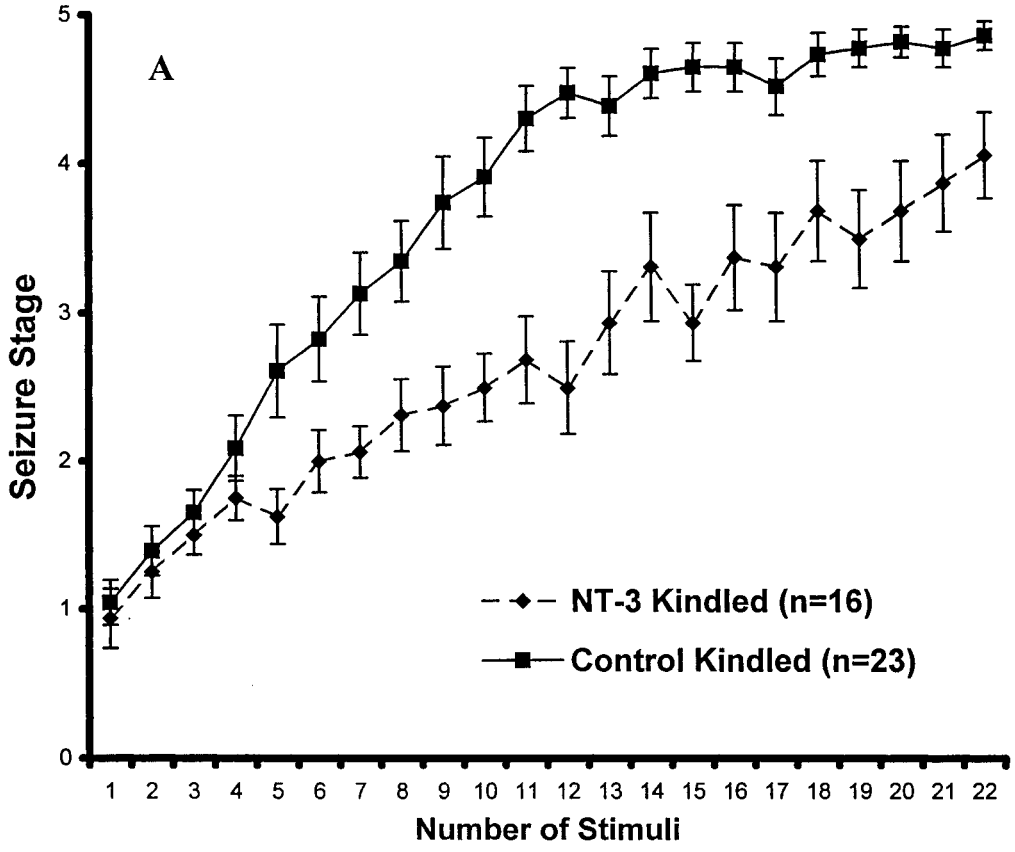
A
Seizure Stage
0
1
2
3
4
5
1 2 3 4 5 6 7 8 9 10 11 12 13 14 15 16 17 18 19 20 21 22
Number of Stimuli
NT-3 Kindled (n=16)
Control Kindled (n=23)

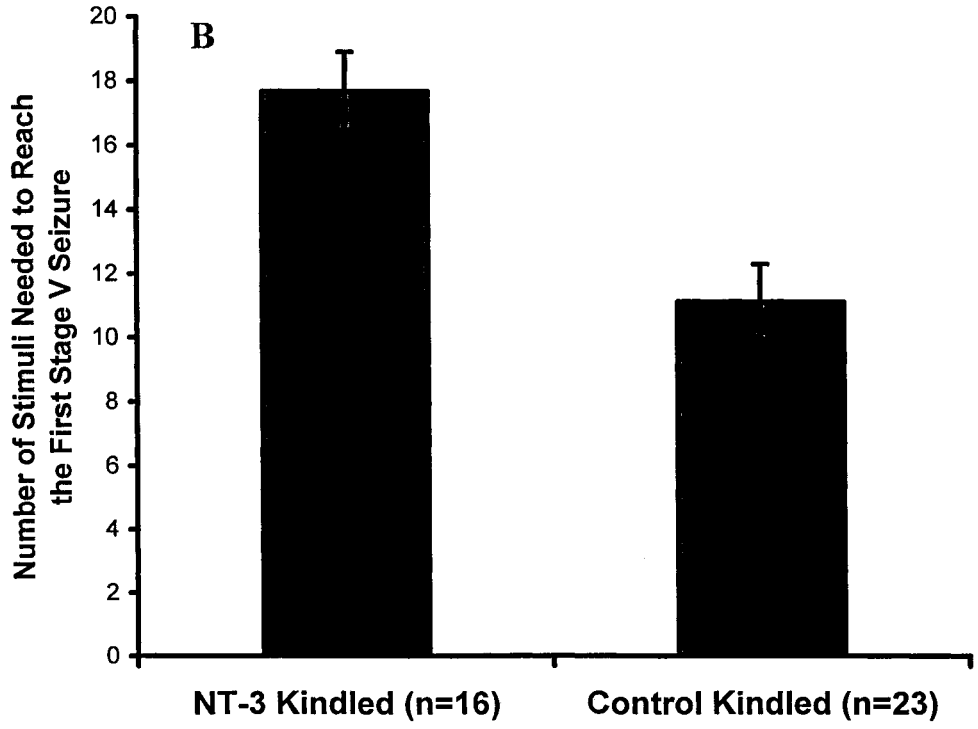
B
Number of Stimuli Needed to Reach the First Stage V Seizure
0
2
4
6
8
10
12
14
16
18
20
NT-3 Kindled (n=16)
Control Kindled (n=23)

Figure 4.2 NT-3 infusion in the absence of kindling induced mossy fiber sprouting in the inner molecular layer of the dentate gyrus (*post hoc* Tukey test, $p<0.005$) **and stratum oriens of the CA3 region** (*post hoc* Tukey test, $p<0.05$).

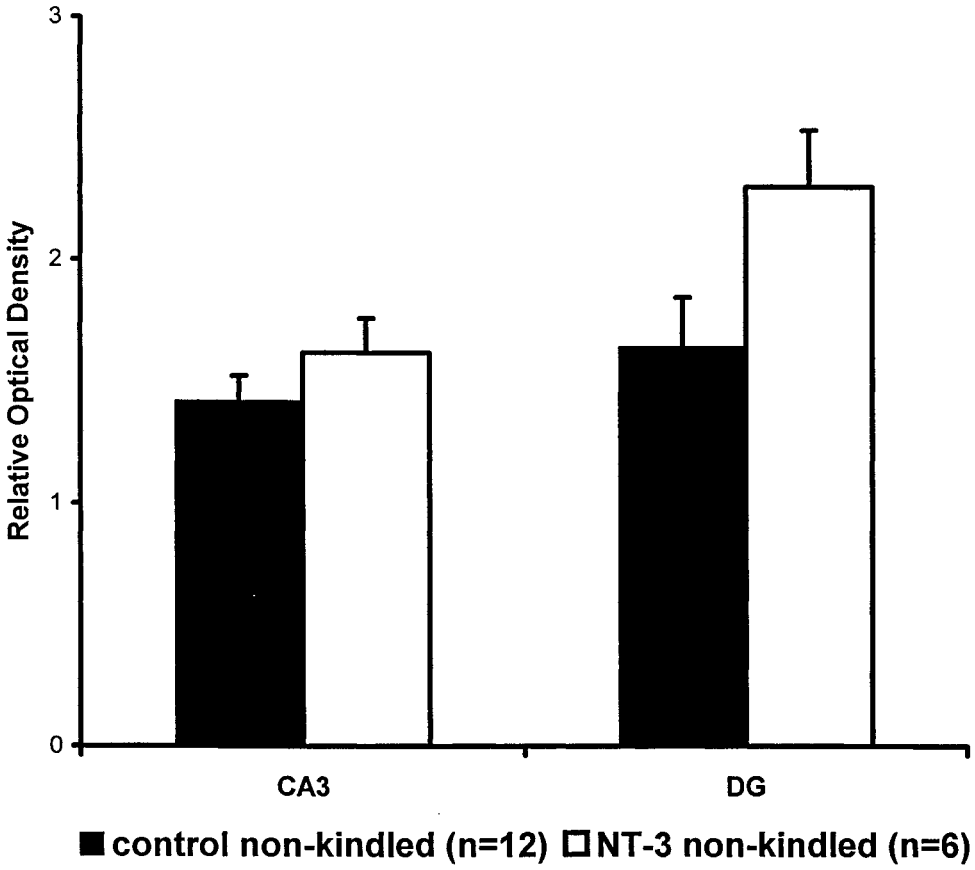
3
2
1
0
Relative Optical Density
CA3
DG
control non-kindled (n=12)
NT-3 non-kindled (n=6)

Figure 3. Timm staining in IML. NT-3-infused, non-kindled animals showed significantly more Timm granules than control non-kindled animals. NT-3-infused kindled animals had less sprouted mossy fibers when compared with control-kindled animals. Arrows indicate Timm granules. NK: non-kindled animals, K: kindled animals. Scale bar, 500 μm.

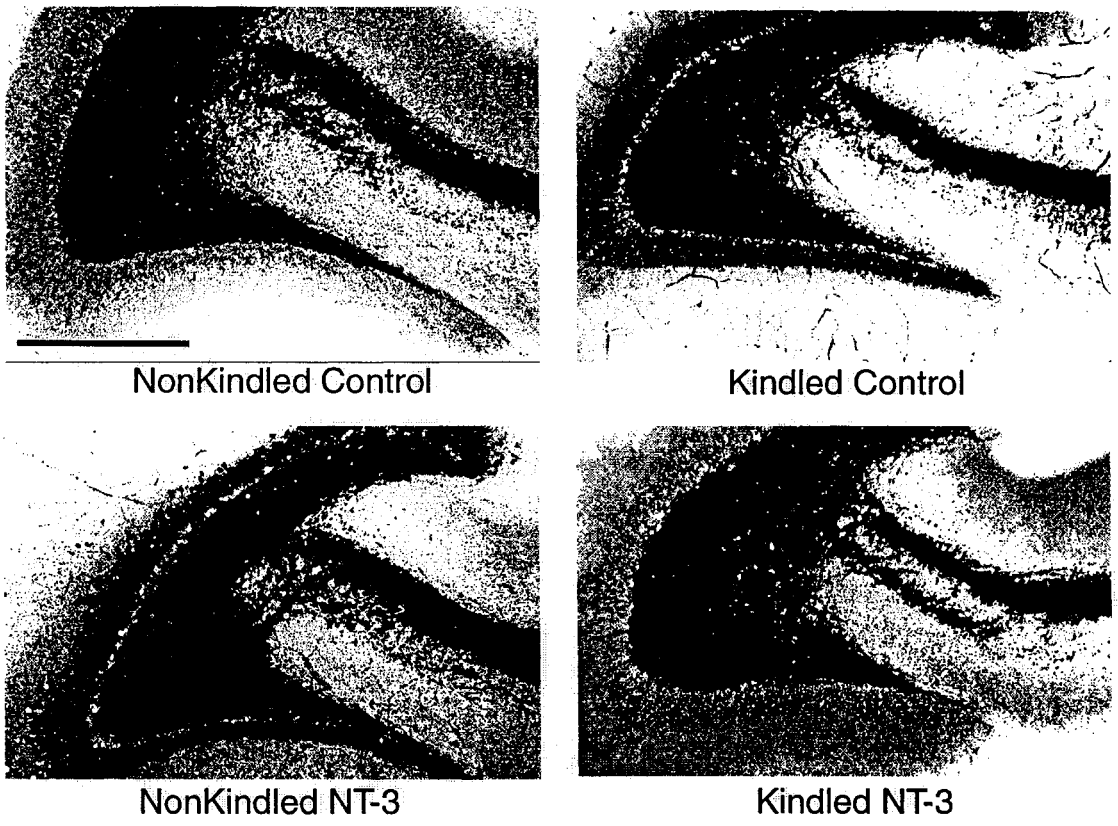
NonKindled Control
Kindled Control
NonKindled NT-3
Kindled NT-3

Figure 4.4 Timm density in the dentate gyrus (DG) and the CA3 region. (A) Kindling-induced mossy fiber sprouting in both the dentate gyrus (*post hoc* Tukey test, $p<0.01$) and CA3 regions (*post hoc* Tukey test, $p<0.001$). **(B)** Continuous intraventricular infusion of NT-3 significantly inhibited this kindling-induced sprouting effect in IML (four-way ANOVA, $F(8,128)=5.14$, $p<0.001$).

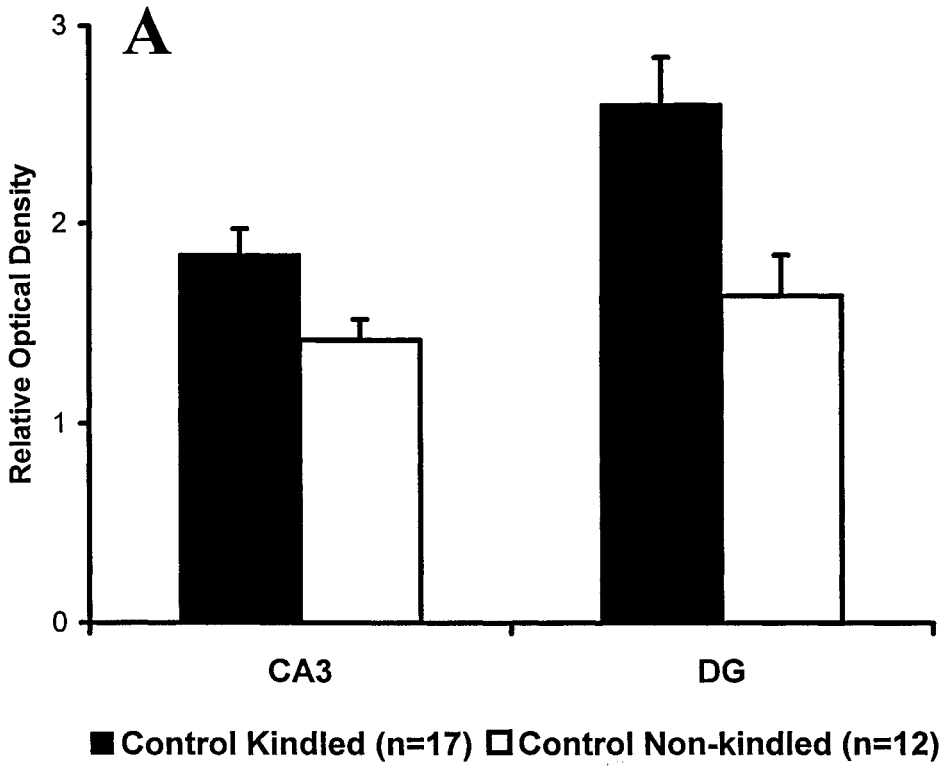
A
Relative Optical Density
3
2
1
0
CA3
DG
Control Kindled (n=17)
Control Non-kindled (n=12)

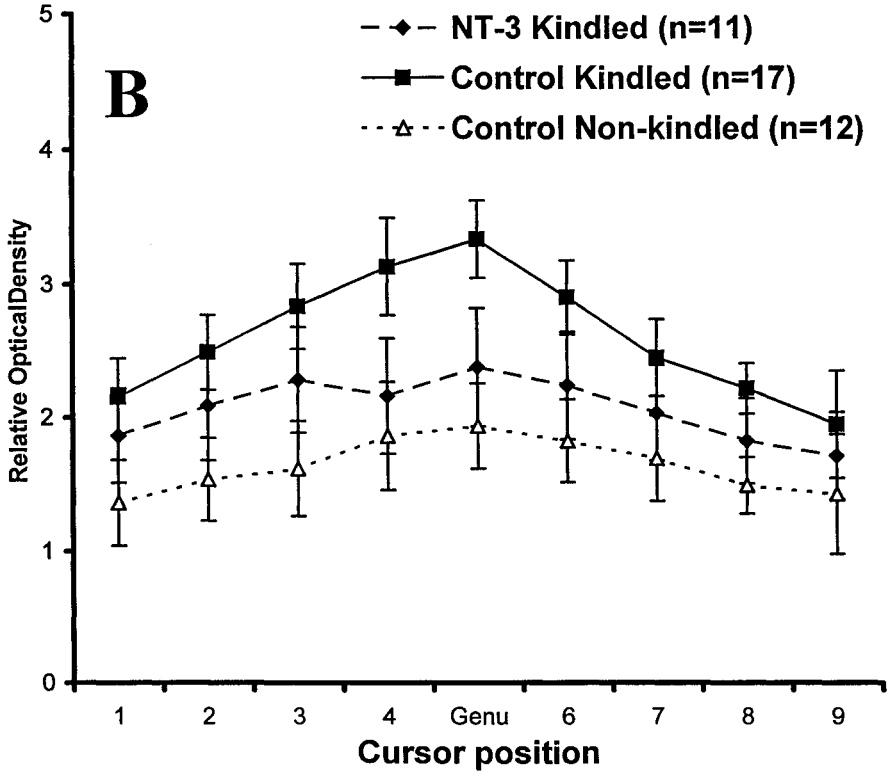
B
NT-3 Kindled (n=11)
Control Kindled (n=17)
Control Non-kindled (n=12)
Relative OpticalDensity
5
4
3
2
1
0
1
2
3
4
Genu
6
7
8
9
Cursor position

way ANOVA, $F(8,128)=5.14$, $p<0.001$, Figures 3D and 4B), but not in the stratum oriens (four-way ANOVA, $p>0.05$, data not shown). No difference was found between NT-3 kindled and NT-3 non-kindled groups in either region (*post hoc* Tukey test, $p>0.05$, data not shown).

4.3.3 Measurement of Hilar Area and Hilar Cell Number

A thee-way ANOVA [groups (4) X sections (6) X hemispheres (2)] was conducted for the analyses of hilar area, hilar cell number per section, and hilar cell density. No significant difference was found between the two vehicles (PBS and histidine buffer) in the measurement of hilar area or hilar cell density (*post hoc* Tukey test, $p>0.05$, data not shown). Furthermore, there was no significant difference between the vehicle-infused kindled group and the cytochrome C kindled group, nor was there a difference between the vehicle-infused non-kindled group and the cytochrome C kindled group (*post hoc* Tukey test, $p>0.05$, data not shown). Therefore, these groups were combined as a control non-kindled group and a control kindled group.

Consistent with our previous studies (Adams et al., 1997), kindling results in a significant increase in hilar area (*post hoc* Tukey test, $p<0.05$, Figure 4.5A), and a decrease in hilar cell density (*post hoc* Tukey test, $p<0.01$, Figure 4.5B). Although the average cell density was lower in the control kindled group when compared with the control non-kindled group, the total hilar cell number per section did not differ between these two groups (mean ± SEM, 98.5 ± 13.2 cells/section for control-kindled animals, 118 ± 10.3 cell/section for control non-kindled animals, *post hoc* Tukey test, $p>0.05$).

These results indicate that the enlargement of the hilar area after kindling might contribute to the observed decrease in hilar cell density.

No differences were found between NT-3-infused non-kindled animals and control non-kindled animals (*post hoc* Tukey test, $p>0.05$, Figure 4.5), suggesting NT-3 infusion alone did not alter the size of the hilus or the hilar cell number. The average hilar cell density and the average size of the hilar area in NT-3-infused, kindled animals were slightly higher than those of NT-3-infused non-kindled animals, and lower than those of control kindled animals (Figure 4.5). However, none of these differences was significant (*post hoc* Tukey test, $p>0.05$). The total hilar cell number per section did not differ between groups (*post hoc* Tukey test, $p>0.05$, data not shown).

4.3.4 Trk Protein and Phosphorylation

To assess whether infusion of NT-3 or kindling or both influence levels of Trk receptors or their phosphorylation in rat hippocampus, Western blot analysis was used. A pan-Trk antibody exhibiting reactivity against the C-terminus of all three Trk receptors was used to immunoprecipitate full-length forms of these proteins. Specific antibodies against each Trk receptor as well as the phospho-TrkA(Tyr490) antibody, which detects all Trks phosphorylated at Tyr 490, were used for analysis of immunoprecipitates. The TrkA and TrkB antibodies were also used on blots containing crude homogenates, the latter in order to detect and distinguish truncated from full-length TrkB.

TrkA. Kindling did not significantly influence TrkA protein levels for either cytochrome C-infused or NT-3-infused rats (*post hoc* Tukey test, $p>0.05$, Figure 4.6A). However, the NT-3-infused, non-kindled animals exhibited a 43% decrease in TrkA

compared to cytochrome C-infused non-kindled controls (*post hoc* Tukey test, p=0.005). When TrkA pixel values were normalized to β-actin pixel values, the difference was still statistically significant (*post hoc* Tukey test, p<0.01). There was no difference in β-actin levels between groups. Both experiments (immunoprecipitates and homogenates) also suggested a tendency towards decreased TrkA levels in the NT-3- infused, kindled group compared to cytochrome C-infused, kindled animals, although there was no statistical significance (*post hoc* Tukey test, p >0.05).

Full-length and truncated TrkB. There were no differences in levels of full-length or truncated TrkB between any of the groups in either immunoprecipitated material or in crude homogenates, in two independent evaluations (*post hoc* Tukey test, p>0.05, Figure 4.6B). The same result was obtained when TrkB pixel values were normalized to pixel values for β-actin. There were no differences in β-actin protein levels between any of the groups (data not shown; *post hoc* Tukey test, p>0.05).

TrkC full-length. In controls, kindling did not affect full-length TrkC protein levels; values were equivalent in cytochrome C-infused non-kindled versus kindled rats (*post hoc* Tukey test, p>0.05) (Figure 4.6C). NT-3 infused, non-kindled animals, however, similarly to TrkA, contained 40% less full-length TrkC protein than cytochrome C non-kindled animals (*post hoc* Tukey test, p<0.05) or than NT-3-infused kindled animals (*post hoc* Tukey test, p<0.05). However, NT-3 did not reduce TrkC protein levels in kindled animals, as there was no difference in levels of full-length TrkC between NT-3 kindled and the two cytochrome C groups (*post hoc* Tukey test, p>0.05).

Phosphorylated Trks. Kindling resulted in a 20% increase in Trk phosphorylation in cytochrome C-infused groups (*post hoc* Tukey test, p=0.029) (Figure 4.6D). The level

Figure 4.5 Hilar area and hilar cell density measurements. (A) Kindling results in a significant increase in hilar area (*post hoc* Tukey test, $p<0.05$). No difference was found between NT-3-infused kindled or non-kindled animals and control-non-kindled animals (*post hoc* Tukey test, $p>0.05$). **(B)** Average cell density in the hilus. The cell density for each section was calculated as the total cell number within the hilus divided by the area of the entire hilus per section. Kindling elicited a decrease in hilar cell density (*post hoc* Tukey test, $p<0.01$). No difference was found between NT-3-infused non-kindled animals and control non-kindled animals (*post hoc* Tukey test, $p>0.05$). The average hilar cell density of NT-3-infused kindled animals was slightly higher than that of NT-3-infused non-kindled animals, and lower than that of control kindled animals. However, none of these differences was significant (*post hoc* Tukey test, $p>0.05$).

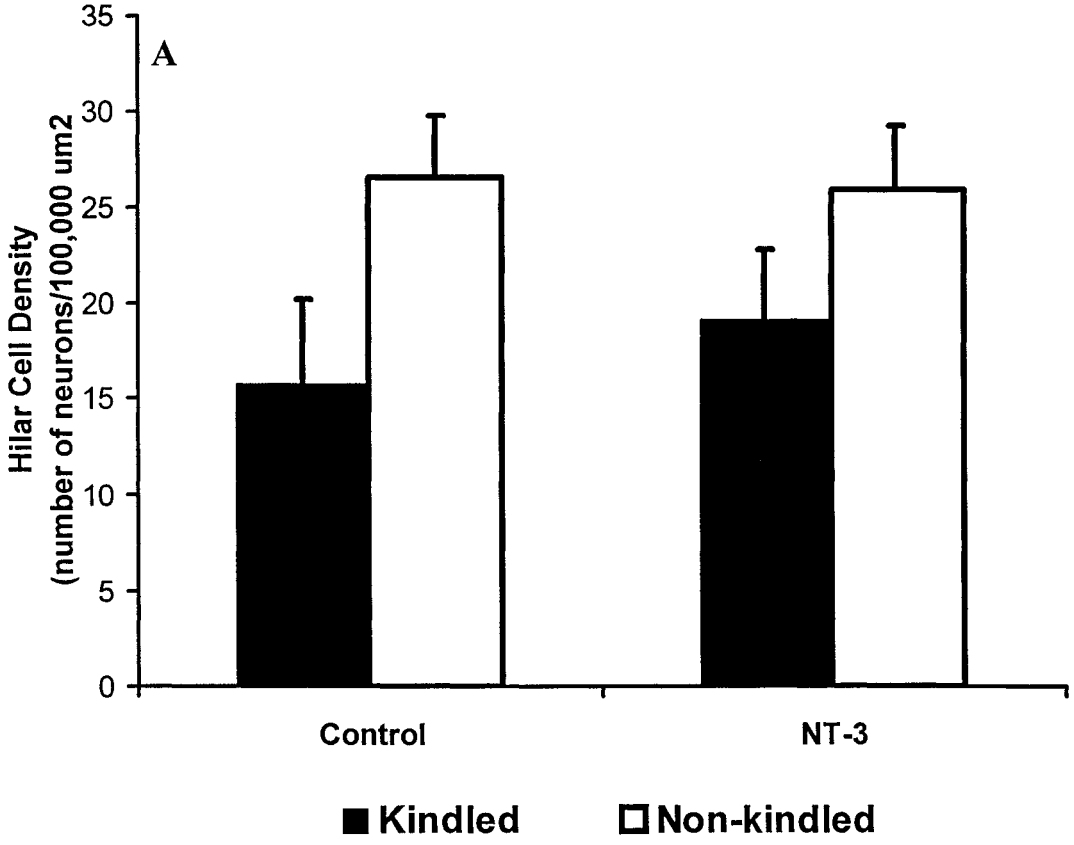
A
Hilar Cell Density
(number of neurons/100,000 um2
35
30
25
20
15
10
5
0
Control
NT-3
Kindled
Non-kindled

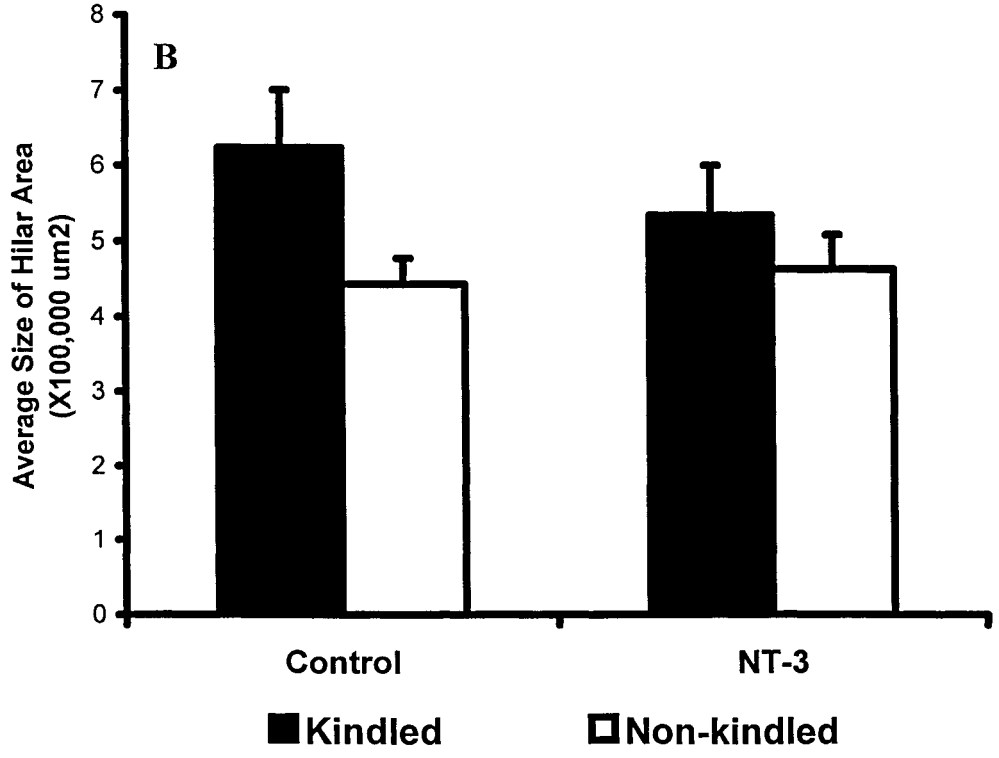
B
Average Size of Hilar Area
(X100,000 um2)
8
7
6
5
4
3
2
1
0
Control
NT-3
Kindled
Non-kindled

Figure 4.6 Relative levels of Trk proteins and Trk phosphorylation in hippocampus determined by Western blotting. **(A)** TrkA is decreased in non-kindled, NT-3-infused animals compared to non-kindled, cytochrome C-treated animals (*post hoc* Tukey test, $p<0.01$). **(B)** No differences were detected in either full-length or truncated TrkB (*post hoc* Tukey test, $p>0.05$). **(C)** Full-length TrkC is decreased in non-kindled, NT-3-infused animals compared to non-kindled, cytochrome C-treated animals (*post hoc* Tukey test, $p<0.01$). **(D)** Trk phosphorylation is increased by kindling (*post hoc* Tukey test, $p<0.05$), but there is no difference between either of the NT-3-infused groups and the cytochrome C-infused groups (*post hoc* Tukey test, $p>0.05$). At least two Western blots were carried out for each antibody and the results averaged. Both immunoprecipitates and homogenates were analyzed for TrkA and TrkB, and the results were combined.

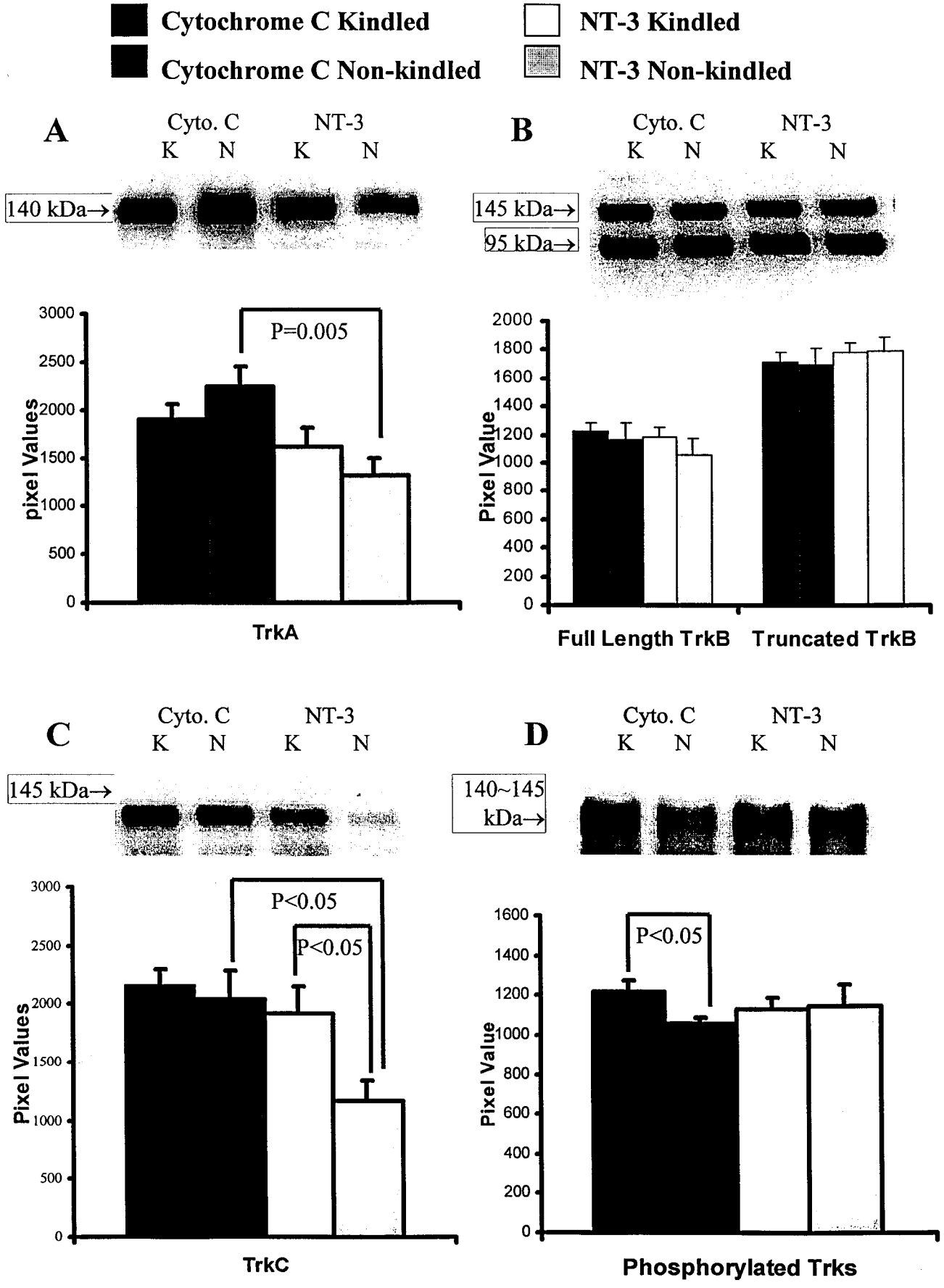
Cytochrome C Kindled
Cytochrome C Non-kindled
NT-3 Kindled
NT-3 Non-kindled
A
Cyto. C
NT-3
K N K N
140 kDa→
3000
2500
2000
1500
1000
500
0
pixel Values
P=0.005
TrkA
B
Cyto. C
NT-3
K N K N
145 kDa→
95 kDa→
2000
1800
1600
1400
1200
1000
800
600
400
200
0
Pixel Value
Full Length TrkB
Truncated TrkB
C
Cyto. C
NT-3
K N K N
145 kDa→
3000
2500
2000
1500
1000
500
0
Pixel Values
P<0.05
P<0.05
TrkC
D
Cyto. C
NT-3
K N K N
140~145 kDa→
1600
1400
1200
1000
800
600
400
200
0
Pixel Value
P<0.05
Phosphorylated Trks

of Trk phosphorylation in both NT-3-infused groups was slightly but reproducibly higher than in cytochrome C-infused non-kindled rats, although the differences were not statistically significant. In contrast to the cytochrome C groups, there was no significant change in Trk phosphorylation following kindling in NT-3-infused groups (*post hoc* Tukey test, $p>0.05$).

4.4 Discussion

We demonstrate in this study that (1) continuous infusion of NT-3 retards the development of behavioral seizures, (2) NT-3 infusion inhibits kindling-induced mossy fiber sprouting in the dentate gyrus, whereas chronic infusion of NT-3 in the absence of electrical activation results in sprouting of mossy fibers in the inner molecular layer of the dentate gyrus and the stratum oriens of the CA3 region, (3) prolonged infusion of NT-3 leads to down-regulation of the high-affinity Trk receptors, TrkA and TrkC, whereas NT-3 infusion has no effect on Trk receptor protein levels in kindled animals, and (4) continuous infusion of NT-3 attenuates kindling-induced Trk receptor phosphorylation.

4.4.1 Decreased Epileptogenesis Following Continuous Infusion of NT-3

We demonstrate here that increasing the levels of NT-3 within the CNS by continuous infusion of NT-3 into the ventricles retards the development of electrical kindling and generalized seizures. Similar phenomena were also found in BDNF studies, wherein continuous BDNF infusions resulted in an inhibition of epileptogenesis and a decrease in the kindling rate (Larmet et al., 1995; Osehobo et al., 1999; Reibel et al., 2000a,b). In contrast, single, acute injections of either NT-3 or BDNF into the brain have

been shown to induce epileptiform activity (Berzaghi et al., 1997), and acute administration of BDNF or NT-3 in hippocampal slice culture increases excitability (Kang and Schuman, 1995). These latter data are supported by transgenic mouse knockout studies demonstrating that reduction of endogenous BDNF or NT-3 by gene mutation inhibits the development of generalized seizures in the kindling model (Kokaia et al., 1995; Elmer et al., 1997). It is tempting to conclude that, in contrast to acute application of BDNF or NT-3 which increases excitability, prolonged infusion of BDNF (Frank et al., 1996, 1997) or NT-3 (this study) may result in a decrease in neuronal responsiveness. However, the mechanism for kindling inhibition by BDNF and NT-3 remains unclear.

4.4.2 Regulation of Seizure-Induced Mossy Fiber Sprouting by Continuous Infusion of NT-3

In this study we demonstrate that infusion of NT-3 in the absence of activation induces axonal sprouting in the mossy fiber network. This tropic effect of NT-3 has previously been reported in cultured embryonic hippocampal neurons (Labelle and Leclerc, 2000; Morfini et al., 1994), and in explants of neonatal neocortex (Back et al., 1998). *In vivo,* NT-3 is known to enhance peripheral nerve regeneration (Oudega and Hagg, 1999; Zhang *et al.*, 1998), but our results provide the first evidence that NT-3 also promotes axonal outgrowth in adult CNS. Interestingly, NT-3 infusion, combined with kindling, inhibits rather than enhances kindling-induced mossy fiber sprouting, suggesting an interaction between NT-3, neuronal activation, and axonal growth. However, the underlying mechanism of such an interaction is still poorly understood.

4.4.3 Effects of NT-3 on Neuronal Density and Hilar Area

In agreement with our previous studies (Adams et al., 1996; Osehobo et al., 1999), we show here that kindling results in an enlargement of the hilar area. No significant cell loss or expansion of the hilar area is found in NT-3-infused kindled animals compared with NT-3-infused non-kindled animals, demonstrating that NT-3 can at least partially ameliorate the effects of kindling on the hilus. However, there is no statistically significant decrease in hilar area between the kindled NT-3-infused animals and the kindled control animals, suggesting that the effects of NT-3 on hilar area are weaker than NGF's effects.

Consistent with previous studies (Adams et al., 1996; Bertram and Lothman, 1993), our results fail to support the hypothesis that kindling produces hilar cell loss. More likely, the observed decrease of hilar cell density is a consequence of kindling-induced hilar area expansion. Our previous study suggests that kindling induces reactive gliosis within the hilus, and such a reactive gliosis might serve as the underlying mechanism of the kindling-induced increase in hilar area (Adams et al., 1998). Additional experiments investigating the effects of NT-3 on reactive gliosis are required to clarify the effects of NT-3 on kindling-induced hilar area expansion.

4.4.4 Chronic Infusion of NT-3 Results in Down-Regulation of TrkA and TrkC in the Absence of Activation

NT-3 is the most promiscuous of the known neurotrophins, and although the preferred receptor for NT-3 is TrkC, it can also bind to TrkA and TrkB (Barbacid, 1995;

Ryden & Ibanez, 1996). The down-regulation of Trk receptor proteins upon chronic exposure to BDNF or NT-3 has been previously reported in cultured hippocampal and cortical neurons and in adult brain (Frank et al., 1996, 1997; Knüsel et al., 1997; Sommerfeld et al., 2000). In the present study, we find that continuous infusion of NT-3 down-regulates both TrkA and TrkC protein, without influencing the levels of TrkB. Our results are supported by *in vitro* experiments demonstrating no changes in TrkB protein levels in response to NT-3 administration (Frank et al., 1996).

Neurotrophins and their Trk receptors are dynamically regulated in a wide range of epilepsy models (for review see Gall et al., 1991, 1993). In the present study, we find that after 11 days of chronic kindling, there is no change in the amounts of any of the Trk receptor proteins in hippocampus compared to non-kindled controls. Unlike the non-kindled situation, infusion of NT-3 during kindling does not alter Trk receptor protein levels. Although our chronic kindling model differs from the acute models prevalent in the literature, our results are consistent with previous reports. No changes in TrkA mRNA expression have been noted following rapid kindling (Bengzon et al., 1993; Merlio et al., 1993), while TrkC mRNA reportedly remains unchanged (Merlio et al., 1993) or is increased (Bengzon et al., 1993; Elmer et al., 1996) following electrical stimulation. We also find no change in either full-length or truncated TrkB protein levels following chronic kindling, which is consistent with a report demonstrating no change in full-length TrkB protein and a transient increase in truncated TrkB protein 12-24 hours only following kainic acid administration (Rudge et al., 1998). Furthermore, whereas TrkB mRNA is upregulated during pentylenetetrazol kindling, TrkB mRNA levels are unchanged in fully kindled rats following the last pentylenetetrazol injection (Humpel et

al., 1993). This suggests that chronic kindling models may regulate Trk receptors differently than acute seizure models that generally report large increases in TrkB mRNA and protein levels (Bengzon et al., 1993; Elmer et al., 1996; Inoue et al., 1998; Merlio et al., 1993; Mudo et al., 1996). It also suggests that Trk receptors may be regulated early in the kindling process, but these effects may dwindle as kindling progresses. A complete time course will be essential to investigate these possibilities more fully.

4.4.5 NT-3 Infusion Dampens Kindling-Induced Trk Activation

In the present study, consistent with the literature, we find that chronic kindling induces a moderate increase in phosphorylation of Trk receptors. Binder et al. (1998, 1999) also reported enhanced Trk phosphorylation following partial, rapid electrical kindling and kainic acid-induced seizures. In contrast to kindled control animals, however, we found no significant change in Trk phosphorylation following kindling in NT-3-infused groups. This suggests that NT-3 infusion is at least partly able to suppress the responsiveness of Trk phosphorylation to electrical activation. Pretreatment with NT-3 is known to reduce tyrosine phosphorylation of Trks in response to BDNF (Frank et al., 1996; Knüsel et al., 1997), and since kindling is known to upregulate BDNF levels (Rocamora et al., 1992; Katoh-Semba et al., 1999), this may account for our results.

Taken together, the data presented here indicate that chronic exposure to NT-3 *in vivo* may alter the responsiveness of neurons to other neurotrophins such as NGF and BDNF.

4.4.6 Possible mechanisms

Our results suggest two possible mechanisms for NT-3's effects on kindling and on kindling-induced sprouting and hilar area changes: down-regulation of TrkA and TrkC, and decreased activation-induced Trk phosphorylation. Chronic administration of NGF increases TrkA levels (Gibbs & Pfaff, 1994), and our previous studies demonstrate that NGF enhances epileptogenesis (Adams et al., 1997). Therefore, the down-regulation of TrkA receptors after prolonged NT-3 infusion should result in a loss of responsiveness to NGF, and lead to decreased kindling development and decreased sprouting. Similarly, NT-3 enhances synaptic transmission in the Schaffer collateral-CA1 pathway (Kang and Schuman, 1995; Kim et al., 1994), increases paired-pulse facilitation in the perforant path-dentate gyrus pathway (Asztely et al., 2000; Kokaia et al., 1998), and attenuates GABAergic inhibition (Kim et al., 1994). Thus, down-regulation of TrkC receptors after prolonged NT-3 infusion should result in a loss of responsiveness to NT-3, and lead to decreased synaptic excitability and kindling development.

Evidence suggests that prolonged treatment with BDNF or NT-3 can lead to a significant reduction of neurotrophin-related c-Fos activation (Frank et al., 1996), decreased Trk phosphorylation (Frank et al., 1996; Knüsel et al., 1997), and a complete loss of Ras activation (Carter et al., 1995). In the current study, the fact that kindling-induced increase in Trk receptor phosphorylation is suppressed in the presence of continuous NT-3 infusion provides further evidence that chronic NT-3 treatment leads to a decrease in neurotrophin responsiveness. The differential effects of kindling on NT-3-

induced mossy fiber sprouting and Trk receptor regulation only serve to emphasize the interplay between electrical activity and neurotrophic factor action.

4.5 Conclusions

In summary, we find that continuous infusion of NT-3 inhibits kindling epileptogenesis, mossy fiber sprouting, and increases in hilar area. Such inhibitory effects might result from decreases in neuronal responsiveness induced by down-regulation of TrkA and TrkC protein and attenuation of Trk phosphorylation. NT-3 by itself induces axonal outgrowth in the mossy fiber system, while, when combined with kindling, it decreases kindling-induced mossy fiber sprouting, suggesting an interaction between neurotrophins and activation.

CHAPTER 5: REGULATION OF EPILEPTOGENESIS AND KINDLING INDUCED MOSSY FIBER SPROUTING BY THE AXON GUIDANCE MOLECULES EPHA5 RECEPTOR AND EPHRIN A5 LIGAND

5.1 Introduction

Previous studies in our lab have shown that neurotrophic factors, which play an important role in neuronal growth during development, also affect activity-dependent axonal sprouting in adult CNS (Adams et al., 1997; Li et al., in preparation). Such evidence raises the possibility that these axon-guidance molecules might also preserve their functions into adulthood. Thus, we started to look at the effect of one particular family of axonal guidance molecules, the Eph receptors, and their ligands, ephrins, on adult neuronal plasticity and activity-dependent axonal growth.

The Eph receptors belong to the family of tyrosine kinase receptors. It has been shown that Eph receptors and ephrins serve as molecular guidance cues for axon targeting. They are involved in the development of the topography of innervation during neuronal development (for review see Tessier-Lavigne, 1995; Flanagan and Vanderhaeghen, 1998). Most of the Eph receptors and ephrins are widely distributed in the developing central nervous system (CNS) and are involved in the formation of retinotectal and hippocamposeptal topographic maps and in the development of segmental organization in the spinal cord (Tessier-Lavigne, 1995; Flanagan and Vanderhaeghen, 1998). Although the spatial and temporal distribution of most Eph receptors and ephrins has not been well addressed, evidence suggests that several members of this family, including EphB2, EphA4, ephrinA2, ephrinA3 and ephrinA5, are

also detected in the *adult* central nervous system (Zhou et al., 1994; Winslow et al, 1995; Martone et al., 1997; Gao et al., 1998; Moreno-Flores and Wandosell, 1999; Gerlai et al., 1999). Detailed in situ hybridization studies in the adult show that the mRNA for EphA5, one member of the Eph tyrosine kinase receptor family, is expressed mainly in hippocampus and piriform cortex, structures that exhibit a high degree of neuronal plasticity and are involved in epilepsy (Zhou et al., 1994; Gao et al., 1998; Gerlai et al., 1999). Moreover, it has been shown that infusion of immunoadhesins for EphA5 and its ligand ephrinA5 altered the generation and/or maintenance of long-term potentiation (LTP) in Schaffer collaterals. These immunoadhesins also affected performance on several hippocampus-dependent behavioral tasks, including the T-maze continuous spontaneous alternation task and context-dependent fear conditioning (Gao et al., 1998; Gerlai et al., 1999). The evidence indicates that the functions of Eph receptors and their ligands are not limited to the developing nervous system. They may also modulate neuronal plasticity and axonal reorganization in the adult brain.

Pilot studies in our lab show that a wide range of EphA receptors and ephrinA ligands are expressed in adult CNS. Among the EphA receptors tested in our lab, the hybridization signal for EphA5 is significantly stronger than for other family members, including EphA2, EphA4 and EphA6 (unpublished data). Therefore, in the present study, the distribution and the functions of EphA5 receptors were examined in detail. We manipulated the functions of EphA receptors by continuous intraventricular infusion of immunoadhesin agonists and antagonists of EphA5 receptors and examined the effects on the development of kindling-induced behavioral seizures and the pattern of mossy fiber sprouting.

5.2 Material and Methods

5.2.2 Animals and Surgery

A total of 104 male Long-Evans hooded rats (250 to 400 g) were used in this study. All the animals were housed individually, maintained on an *ad lib* feeding schedule, and kept on a 12 hr on/12 hr off light cycle.

The surgery procedure was described in Chapter 4. Briefly, a teflon-coated, stainless steel bipolar electrode was implanted into the right perforant pathway. A cannula was implanted into the right lateral ventricle of those rats receiving continuous infusion of immunoadhesins or PBS. A flow-regulated osmotic minipump (Alzet model 2000, flow rate 0.5μl/hr, effective maximally 18 days) was connected to the cannula via polyethylene tubing. The minipump delivered either EphA5-IgG, ephrinA5-IgG (Genentech Inc., San Francisco CA), NUK-IgG (Regeneron Pharmaceuticals, Tarrytown, NY), or PBS as shown in Table 5.1. Animals were given 7 d recovery after surgery before the kindling protocol was initiated.

5.2.3 Kindling Procedure

The kindling protocol used in this study was the same as that described in Chapter 4. The intensity of each kindling stimulation ranged from 500 to 700 μA, which was sufficient to trigger an afterdischarge after each stimulation. Animals were stimulated twice daily for 11 day. Both the behavioral progression of kindling-induced seizures and the duration of the ADs was recorded. Animals that failed to reach stage 5 after 22 stimulations were assigned a value of 22 for the purpose of calculating kindling rate.

Table 5.1 Experimental Groups

Groups		Number of Animals
In situ hybridization	Kindled	5
	Non-kindled	5
EphrinA5-IgG (0.5 mg/rat)	Kindled	7
	Non-kindled	7
EphrinA5-IgG (0.125 mg/rat)	Kindled	14
	Non-kindled	14
EphA5-IgG (1.25 mg/rat)	Kindled	13
	Non-kindled	6
NUK-IgG (0.175mg/rat)	Kindled	12
	Non-kindled	7
PBS	Kindled	7
	Non-kindled	7
Total		104

5.2.4 In situ hybridization

Immediately after the last kindling stimulation, 5 non-kindled animals and 5 kindled animals were perfused transcardially with 4% paraformaldehyde in phosphate buffered saline. The brains were removed and immediately frozen in isopentane cooled to -40°C and stored at -70°C until sectioning. Horizontal, serial, 16-μm sections were taken from dorsal, middle and ventral parts of the hippocampus (~4.3 mm, ~5.9 mm, ~7.5 mm ventral to bregma) using a cryostat, and mounted on chromium potassium sulfate-coated slides. Each slide contained a pair of sections from the same coordinates from kindled and control non-kindled animals. Adjacent sections taken from the same coordinates were separated into two groups, and two independent *in situ* hybridization procedures were performed. The density readings from these two hybridizations were combined for statistical tests.

^{35}S-RNA *in situ* hybridization was carried out according to the protocol of Hogan et al. (1986), with minor modifications. The radiolabeled ([^{35}S]UTP and [^{35}S]CTP) antisense EphA5 riboprobe was prepared from an RT-PCR fragment (from nucleotide 329 to nucleotide 1235) of the mouse EphA5 gene subcloned into pGEM-T Easy (Promega Biotech, Madison, WI). Hybridizations were carried out at 55°C for 16 hours, using approximately 20 μl of probe (5 X 10^7cpm/ml) per section. A high-stringency wash in 2X SSC (17.53 g of NaCl and 8.82 g of sodium citrate in 800 ml of H_2O, pH=7.0), 50% formamide, and 10mM dithiothreitol (DTT) was performed at 65°C for 45 minutes. RNAse digestions were performed for 15 minutes in buffer prewarmed to 37°C. The final wash was 0.2X SSC for 5 minutes at room temperature. Emulsion-dipped

slides were exposed for 2 weeks prior to developing, and counterstaining was done with Hoechst stain.

EphA5 mRNA expression in the dentate gyrus of the dorsal, middle and ventral hippocampus were examined at 100× magnification by creating a digitized image using Bioquant True Color Windows 98 software (R&M Biometrics Inc., Nashville, TN, U.S.) attached to a light microscope (Zeiss Axioskop, Oberkochen, Germany). The densities of fluorescent signals were measured by placing 9 open circle cursors (diameter 50μm) within the granule cell layer of the dentate gyrus as shown in Figure 2A. To control for non-specific binding, 9 background density readings were taken from the molecular layer. Relative optical densities (RODs) were calculated as follows

$$\text{ROD} = \frac{\text{density reading in the granule cell layer}}{\text{average of 9 background readings taken from the molecular layer}}$$

5.2.5 Timm stain for mossy fiber sprouting

Two weeks following the last kindling stimulation, animals were perfused and sectioned for Timm staining. The method of perfusion, sectioning and Timm staining were described in Chapter 2. Six horizontal sections at 4.5, 5.1, 5.7, 6.3, and 6.9 ventral to the Bregma were examined. The relative optical density was calculated.

5.3 Results

5.3.1 Graded Distribution of EphA5 Receptors within Adult Hippocampus along the Dorsal-Ventral Axis

Intense hybridization signals for EphA5 mRNAs were detected in the cerebellum, piriform cortex and hippocampus of the rat brain. Within the hippocampus, strong hybridization signals for EphA5 were detected in the granule cell layer of the dentate gyrus, in the pyramidal cell layer of all the CA fields, and within the hilar region (Figure 5.1).

Further analysis of horizontal sections taken from different regions of hippocampus (dorsal, middle and ventral) revealed a graded distribution of EphA5 receptors along the dorsal-ventral axis. The expression of EphA5 receptor mRNA was highest in the granule cell layer of the dorsal dentate gyrus and decreased dramatically in the granule cell layer of the middle dentate gyrus (Figure 5.2). In the ventral hippocampus, hybridization signals in the granule cell layers could not be distinguished from background, and therefore were not included in statistical tests.

A four-way ANOVA [hybridization (2) X sections (dorsal or middle) (2) X hemispheres (2) X cursor positions (9)] was conducted. The density readings from the two independent hybridization procedures did not significantly differ from each other (four-way ANOVA, $p>0.05$). The fluorescent signals detected in the granule cell layer of the dorsal hippocampus were significantly stronger than those of the middle hippocampus (four-way ANOVA, $p<0.005$, Figure 5.3).

There was a tendency towards decreased expression of EphA5 mRNA levels in the dentate gyrus of kindled animals compared to controls. However, the difference failed to reach statistical significance (four way ANOVA, $p>0.05$).

Figure 5.1 Distribution of EphA5 mRNA in adult CNS. Shown are representative examples of EphA5 mRNA distribution in the dentate gyrus (DG), the CA3 region, the CA1 region, cerebellum, and piriform cortex. Within the hippocampus, EphA5 mRNA is detected in the granule cell (GC) layer of the dentate gyrus and the pyramidal cell layer of the CA3/CA1 region.

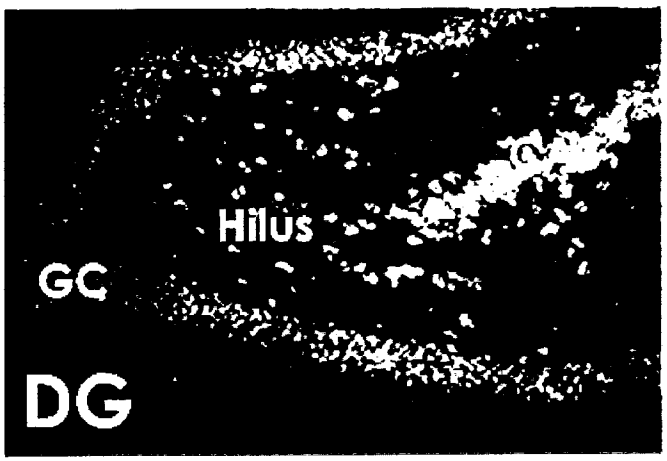
Hilus
GC
DG

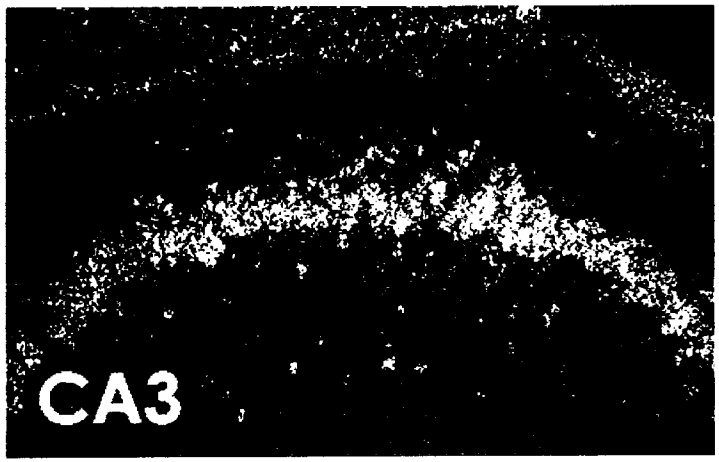
CA3

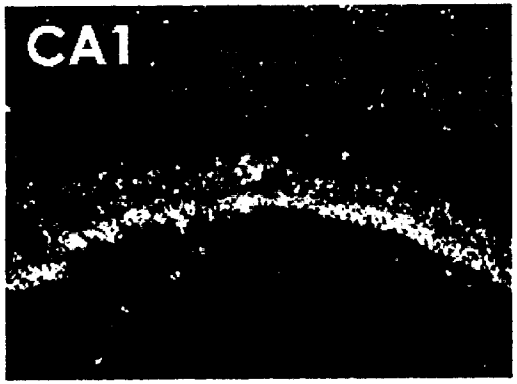
CA1


Cerebellum

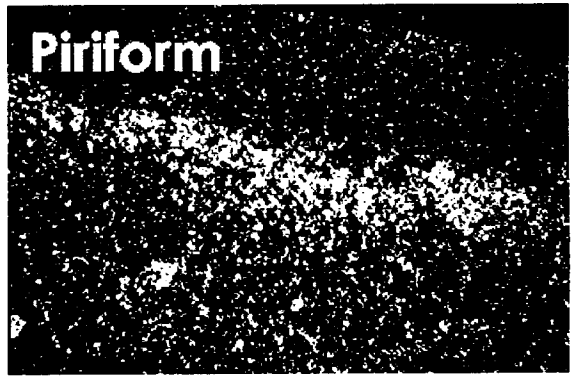
Piriform

Figure 5.2 The expression of EphA5 mRNA in the dentate gyrus. (A) hybridization signals were measured by placing 9 adjacent cursors (cursors 1 to 9) within the granule cell layer of the dentate gyrus. 9 background density readings (cursors A to I) were taken from the molecular layer of the dentate gyrus. (B) The relative optical density of the dorsal and middle dentate gyrus. The RODs of the dorsal sections are significantly higher than those of the middle sections.

A

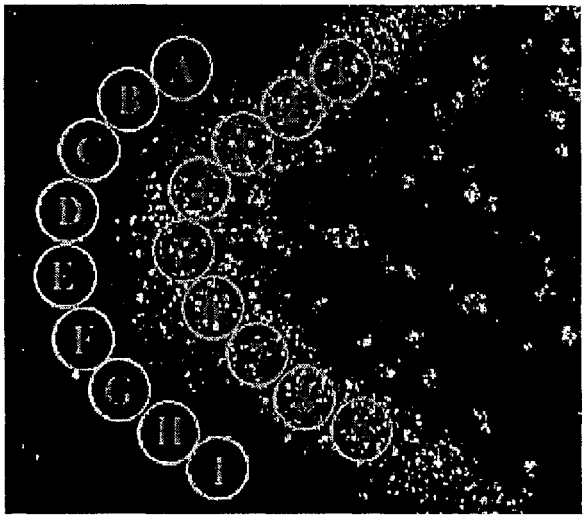
A
B
C
D
E
F
G
H
I

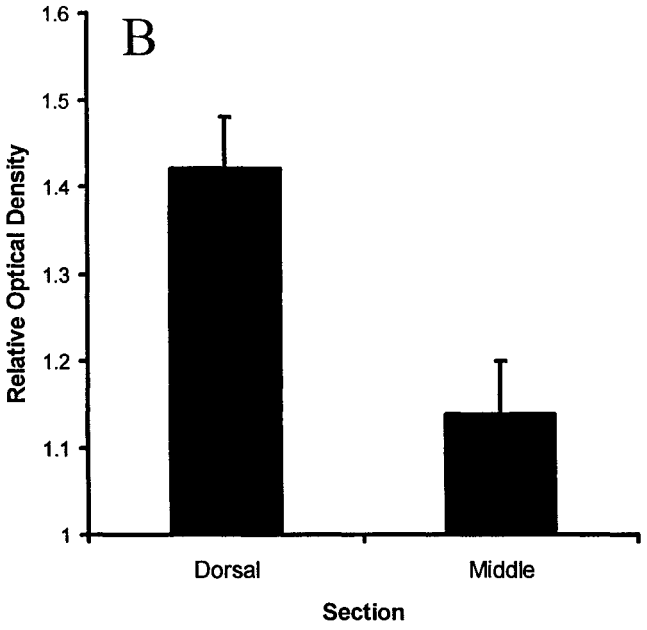
B
1.6
1.5
1.4
1.3
1.2
1.1
1
Relative Optical Density
Dorsal
Middle
Section

Figure 5.3 Gradient distribution of EphA5 receptors within dentate gyrus. The EphA5 hybridization signal (red) is shown for dorsal and middle sections of the dentate gyrus (left panels, 100X) and for dorsal and middle sections of the hilus (right panels, 400X). Blue represents 4',6-diamidino-2-phenylindole (DAPI)-stained cell bodies. Note the increased clustering of EphA5 signal around selected cells, which is most clear at the higher magnification in the hilus.

Granule Cells Dorsal

Hilar Cells Dorsal

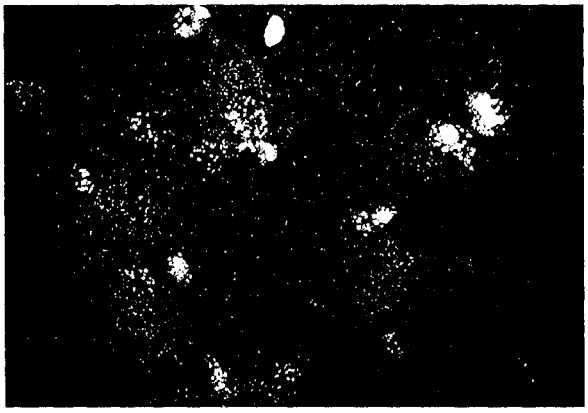

Granule Cells Middle

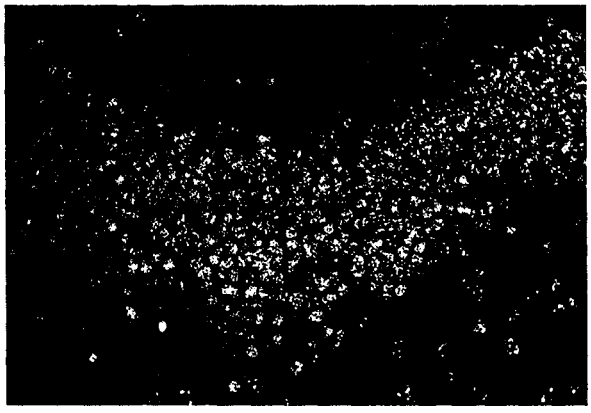

Hilar Cells Middle

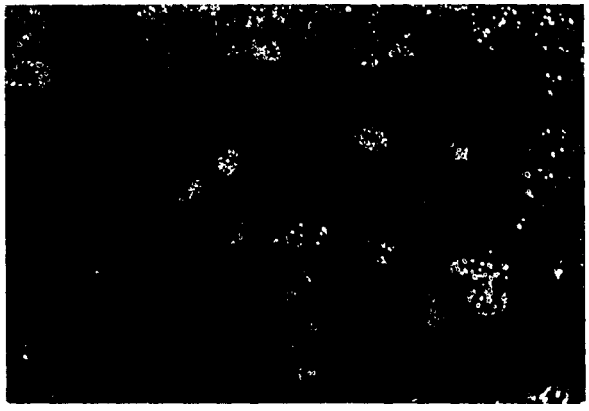

5.3.2 EphA5 Receptors Modulate the Development of Kindling-Induced Behavioral Seizures

A previous study suggested that receptor dimerization or clustering is required for the activation of Eph receptors (Davis et al., 1994). A soluble ephrinA5 immunoadhesin was constructed by fusing two extracellular receptor-binding domains of ephrinA5 to an IgG Fc domain (Gao et al., 1998). This ephrinA5-IgG has been shown to dimerize and activate EphA5 receptors, and therefore serves as an agonist of endogenous EphA5 receptors (Gerlai et al., 1999; Figure 5.4). The EphA5 immunoadhesin, in contrast, contains two extracellular ligand-binding domains of EphA5 receptor linked to the IgG Fc arm (Gao et al., 1998). It has been shown to compete with endogenous EphA5 receptors for the binding of ephrinA5 ligand, and act as an antagonist of endogenous EphA5 receptor (Gerlai et al., 1999). Another group of animals received infusions of EphB immunoadhesin, NUK-IgG.

Intraventricular infusion of EphA5-IgG, an antagonist of endogenous EphA receptors, significantly retarded the development of behavioral seizures (n=13; *post hoc* test, $p<0.05$). Infusion of EphrinA5-IgG, an agonist of endogenous EphA5 receptors (Figure 5.5), either had no effect on the progression of behavioral seizures (at low concentration -- 0.125mg/rat, n=14; *post hoc* test, $p>0.05$, data not shown), or showed a non-significant tendency to accelerate seizure development (at high concentration – 0.5mg/rat, n=7; *post hoc* test, $p=0.062$) (Figure 2). No significant difference was found between an EphB immunoadhesin (NUK-IgG) infused kindled group (n=12) and PBS controls (n=7). Therefore, the NUK-IgG and PBS groups were combined to form one control kindled group (n=19) and one control non-kindled group (n=14). There were no

significant differences between any of the above groups in afterdischarge duration (*post hoc* Tukey test, $p>0.05$, data not shown).

5.3.3 EphA5 Receptors Modulate Kindling-Induced Mossy Fiber Sprouting

Infusion of EphB immunoadhesin (NUK-IgG) did not alter kindling-induced mossy fiber sprouting. Therefore, the NUK-IgG and PBS kindled groups were combined into a single control-kindled group (n=19). No significant difference in Timm labeling was found among the four non-kindled groups (ephrinA5-IgG high concentration non-kindled group, n=7; ephrinA5-IgG low concentration non-kindled group, n=14; EphA5-IgG non-kindled group, n=6; and control non-kindled group, n=14) in either IML of the dentate gyrus or in area CA3. Therefore, these four groups were combined for analysis of mossy fiber sprouting. No significant difference in mossy fiber sprouting measures was detected between ephrinA5-IgG low concentration (0.125mg/rat) and ephrinA5-IgG high concentration (0.5mg/rat) kindled groups. Therefore, these two groups were also combined to form one ephrinA5-IgG kindled group (n=21).

Consistent with our previous experiments (van der Zee et al., 1995; Rashid et al., 1995; Adams et al., 1997), kindling itself resulted in increased Timm labeling in both the IML of dentate gyrus and area CA3 when compared with non-kindled control animals (*post hoc* test, $p<0.001$ and $p<0.005$, respectively) (Figure 5.6). EphA5-IgG infusion significantly decreased kindling-induced Timm granule density in the IML of the dentate gyrus (*post hoc* test, $p<0.05$), but not in area CA3 (*post hoc* test, $p=0.80$). EphrinA5-IgG infusion increased kindling-induced mossy fiber sprouting in both the IML and stratum oriens of area CA3 (*post hoc* test, $p<0.01$) (Figure 5.6).

Figure 5.4 Receptor dimerization is required for the activation of EphA5 receptors. (A) EphrinA5 exists in CNS as a membrane-bound protein that can dimerize the EphA5 receptor and activate its intrinsic tyrosine kinase domain. (B) Soluble ephrinA5, which contains only the receptor-binding domain of ephrinA5 ligand, can bind to the endogenous EphA5 receptors without activating them. (C) Soluble ephrinA5-IgG consists of two receptor-binding domains fused to an IgG Fc arm. It activates the EphA5 receptor, probably by dimerizing it. (D) By binding to ephrinA5 ligands and preventing them from combining with the intrinsic EphA5 receptors, the soluble EphA5-IgG acts as an antagonist for endogenous EphA5 receptors.

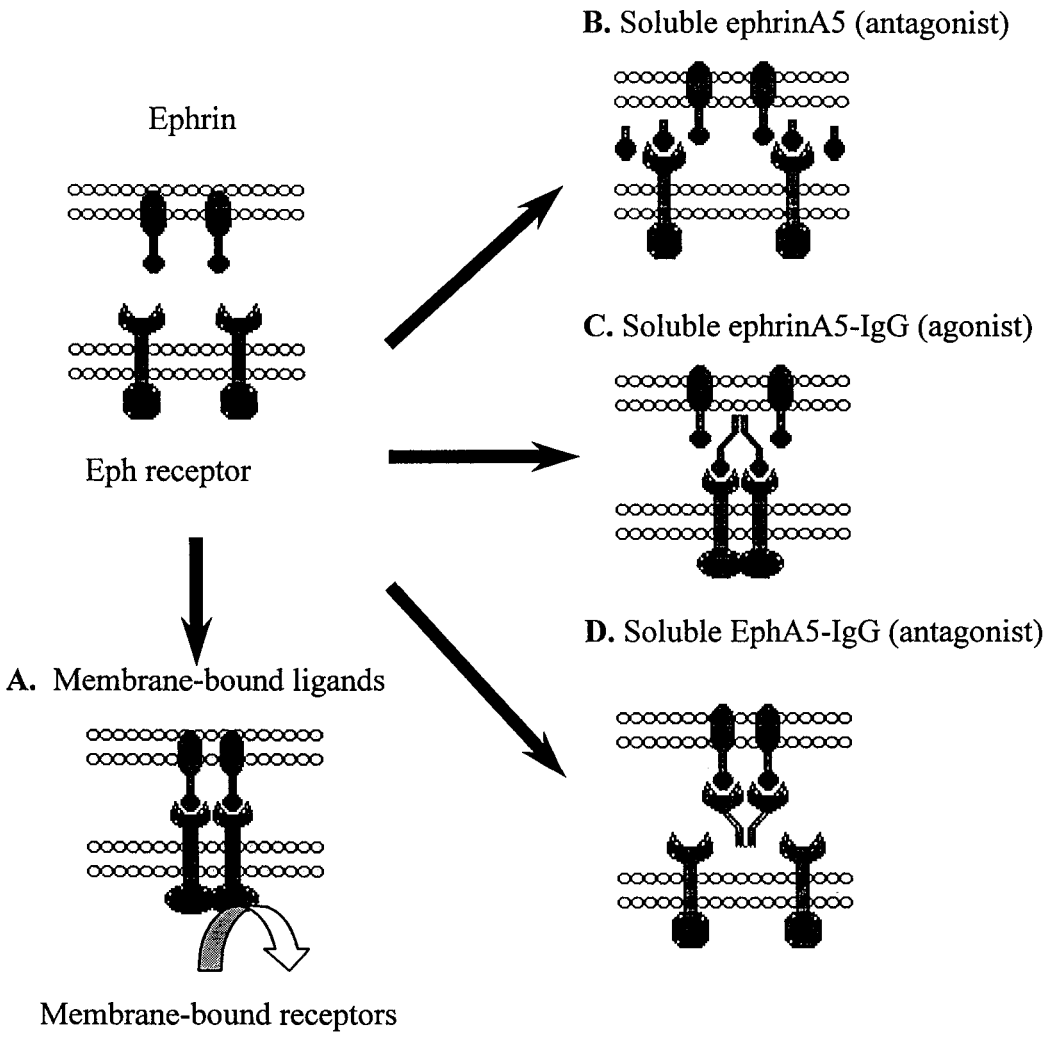
B. Soluble ephrinA5 (antagonist)
Ephrin
C. Soluble ephrinA5-IgG (agonist)
Eph receptor
D. Soluble EphA5-IgG (antagonist)
A. Membrane-bound ligands
Membrane-bound receptors

Figure 5.5 Intraventricular infusion of EphA5-IgG retards the development of behavioral seizures (*post hoc* Tukey test, $p<0.05$). No significant difference was found between ephrinA5-IgG (n=21) group and control group (n=19; *post hoc* Tukey test, $p>0.05$). Error bars represent SEM.

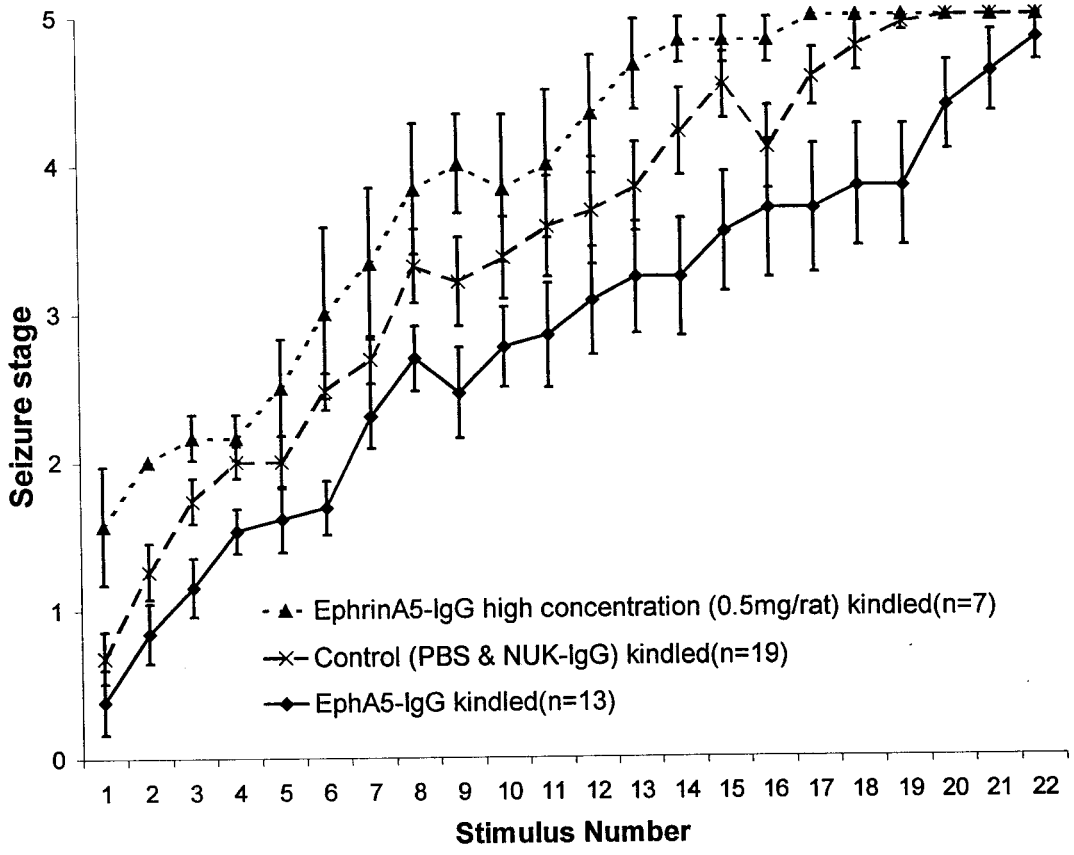
Seizure stage
0
1
2
3
4
5
1 2 3 4 5 6 7 8 9 10 11 12 13 14 15 16 17 18 19 20 21 22
Stimulus Number
EphrinA5-IgG high concentration (0.5mg/rat) kindled(n=7)
Control (PBS & NUK-IgG) kindled(n=19)
EphA5-IgG kindled(n=13)

Figure 5.6 Intraventricular infusion of EphA5-IgG and ephrinA5-IgG alters the amount of mossy fiber sprouting. EphrinA5-IgG infused kindled group (n=21) exhibited an enhancement of kindling-induced mossy fiber sprouting in the dentate gyrus and in the CA3 region when compared with control-kindled group (n=19), at two weeks following the last kindling stimulation (*post hoc* Tukey test, $p<0.01$). EphA5-IgG infusion (n=13) inhibited mossy fiber sprouting in the dentate gyrus (*post hoc* Tukey test, $p<0.05$). **A**) IML of dentate gyrus and **B**) stratum oriens of area CA3. Error bars represent SEM.

A. Dentate Gyrus

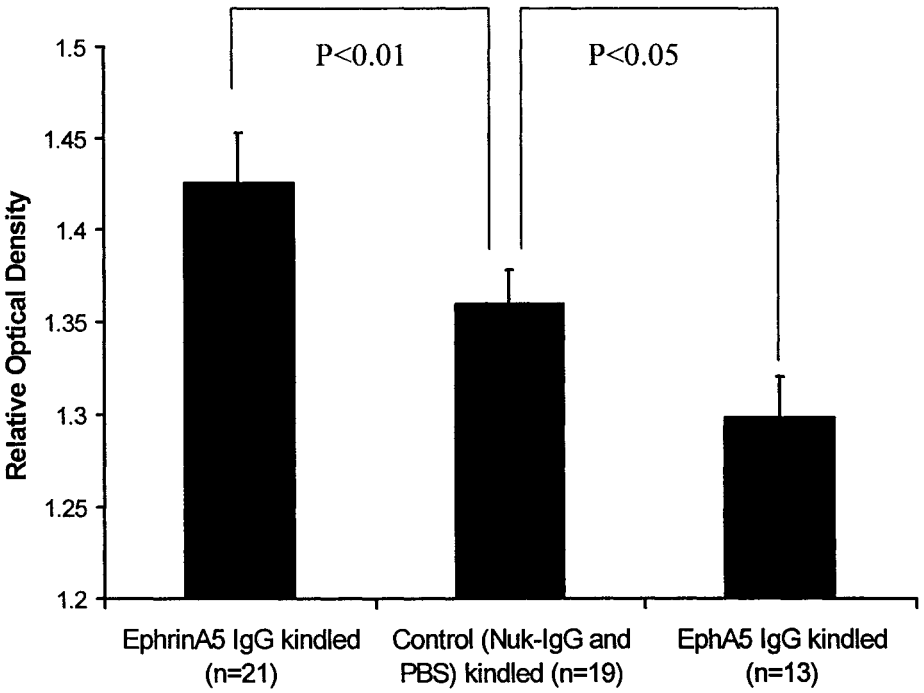

B. Area CA3

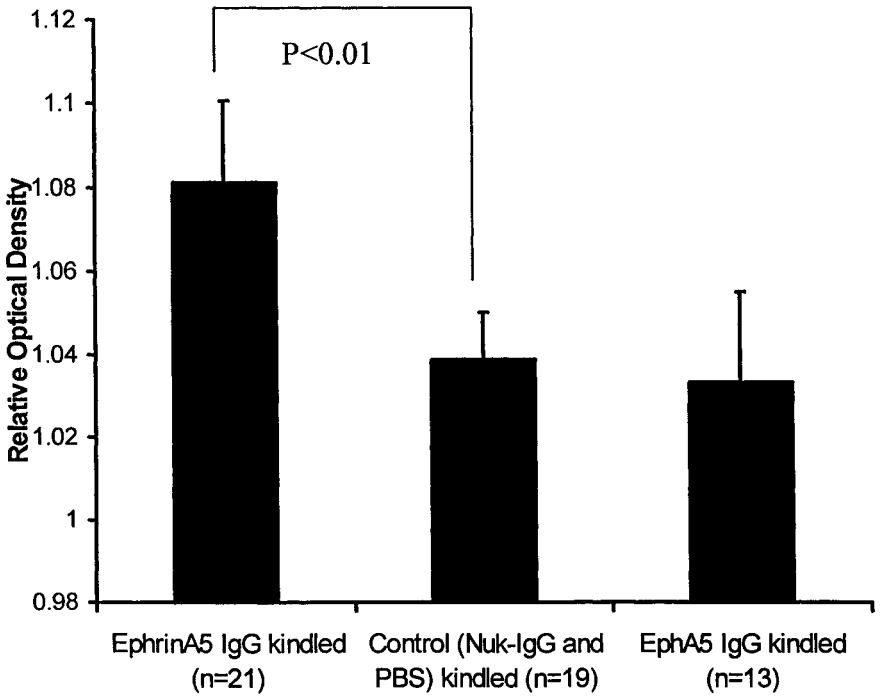

5.3.4 Continuous Infusion of EphrinA5-IgG Alters the Distribution of Sprouted Mossy Fibers Within CA3 Area Along the Dorsal-Ventral Axis and Along the Stratum Oriens

Infusion of ephrinA5-IgG significantly altered the pattern of mossy fiber distribution within area CA3 along the dorsal-ventral axis (Figure 5.7) as well as along the stratum oriens from the hilus to the CA2 transitional zone (Figure 5.8). Previous studies in our lab have shown a reliably stronger sprouting effect in the dorsal CA3 area when compared to the ventral CA3 area (Adams et al., 1997). Also, within the same horizontal section, mossy fiber sprouting is generally more prominent in areas close to the hilus (CA3c) than areas close to CA2 (CA3a) (Adams et al., 1997). The same gradient of sprouting was observed in control (combined PBS and NUK-IgG) kindled (n=19) and control non-kindled groups (n=14) in this experiment (four-way ANOVA, group-cursor interaction, $p<0.001$; group-section interaction, $p<0.01$). Continuous intraventricular infusion of ephrinA5-IgG, at both concentrations tested, elicited a rearrangement of the axonal sprouting patterns within area CA3. EphrinA5-IgG infused kindled rats (n=21) showed a significant increase in sprouting in the ventral hippocampus and a slight decrease in Timm labeling in the dorsal hippocampus when compared with the control kindled group (n=19) (four-way ANOVA, group-cursor interaction, $p<0.001$, Figure 5.9A). A similar rearrangement of sprouted mossy fibers was also observed along the stratum oriens of CA3 (Figure 5.9B). EphrinA5-IgG infusion induced a small decrease in Timm labeling in area CA3c near the hilus (cursor positions 1 and 2), and a dramatic increase in Timm labeling in area CA3b and CA3a (cursor positions 4 to 16) (group-section interaction, $p<0.005$, Figure 5.9B).

Figure 5.7 Intraventricular infusion of ephrinA5-IgG alters the dorsal-ventral pattern of mossy fiber sprouting. Kindling increases mossy fiber sprouting in both dorsal and ventral hippocampus, but the effects are strongest in the dorsal hippocampus (compare top two panels, *Nonkindled Control*(s), and middle two panels, *Kindled Control*(s)). Infusion of ephrinA5-IgG had either no effect or reduced sprouting in **Dorsal CA3** (compare bottom left panel, *Kindled Ephrin*, with middle left panel, *Kindled Control*). However, ephrinA5-IgG greatly enhanced mossy fiber sprouting within **Ventral CA3** (compare bottom right panel, *Kindled Ephrin*, with middle right panel, *Kindled Control*). Arrows indicate sprouted mossy fibers.

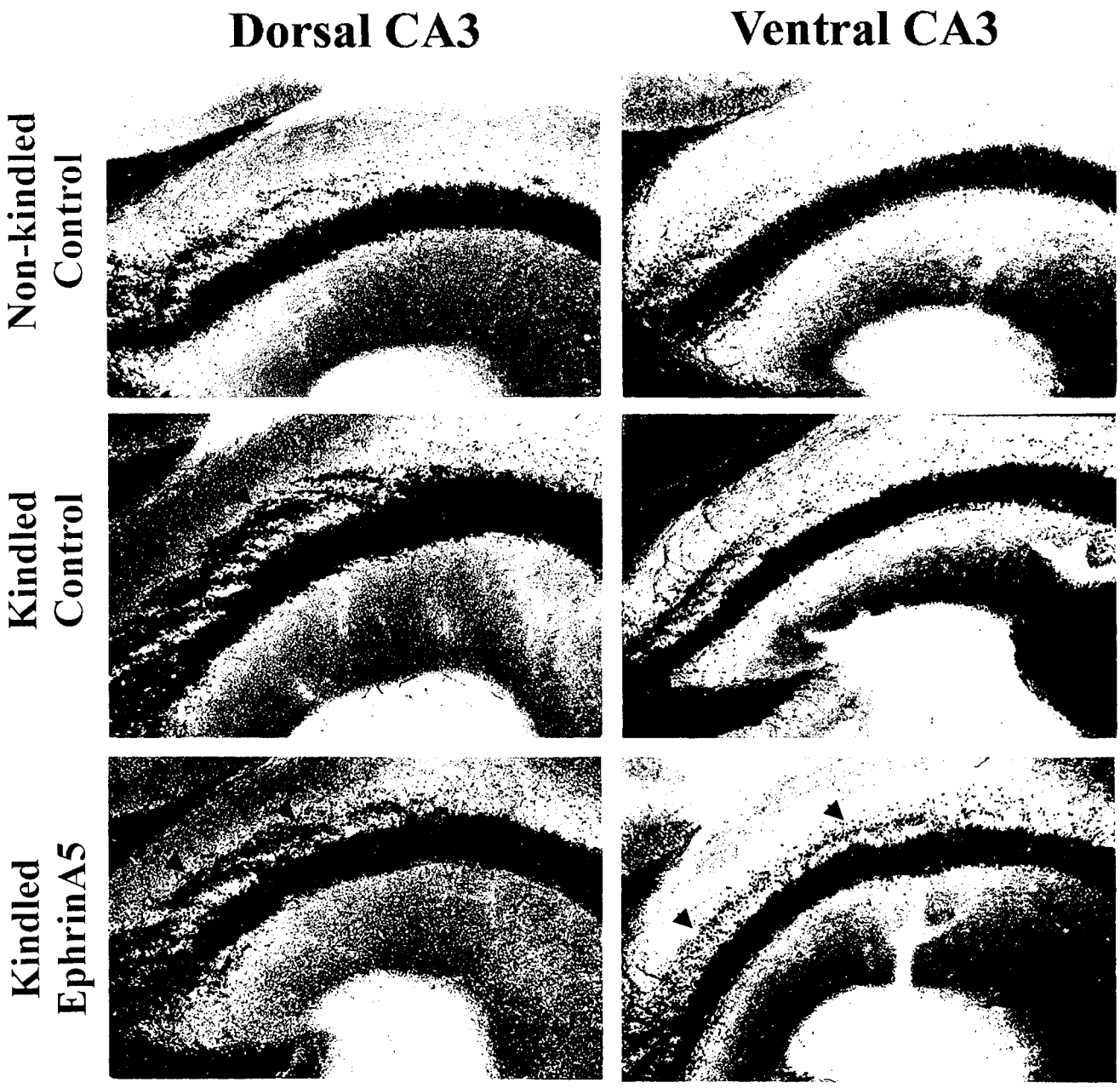
Dorsal CA3
Ventral CA3
Non-kindled Control
Kindled Control
Kindled EphrinA5

Figure 5.8 EphrinA5-IgG elicited a rearrangement of kindling-induced sprouted mossy fibers within area CA3 along the stratum oriens (four-way ANOVA, group-cursor interaction, $F(15,570)=2.70$, $p<0.001$). In ephrinA5-IgG-infused animals (*Kindled Ephrin*), mossy fiber sprouting was greatly enhanced in area CA3a (near the CA2 transition zone). Arrows indicate sprouted mossy fibers.

Kindled Control

Kindled EphrinA5

Figure 5.9 Infusion of EphrinA5-IgG elicited a rearrangement of the axonal sprouting patterns within the area CA3. (A) EphrinA5-IgG infused kindled rats showed a significant increase in sprouting in the ventral hippocampus and a slight decrease in Timm labeling in the dorsal hippocampus when compared with the control kindled group (n=19) (four-way ANOVA, group-cursor interaction, $p<0.001$). **(B)** EphrinA5-IgG infusion induced a small decrease in Timm labeling in area CA3c near the hilus (cursor positions 1 and 2), and a dramatic increase in Timm labeling in area CA3b and CA3a (cursor positions 4 to 16) (group-section interaction, $p<0.005$).

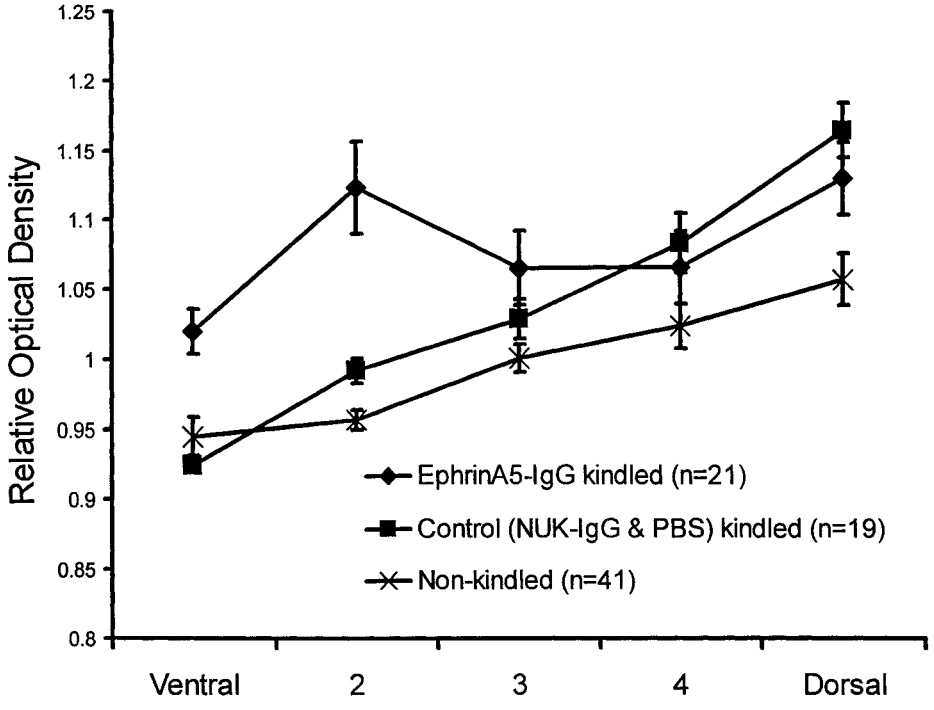
Relative Optical Density
1.25
1.2
1.15
1.1
1.05
1
0.95
0.9
0.85
0.8
Ventral
2
3
4
Dorsal
EphrinA5-IgG kindled (n=21)
Control (NUK-IgG & PBS) kindled (n=19)
Non-kindled (n=41)

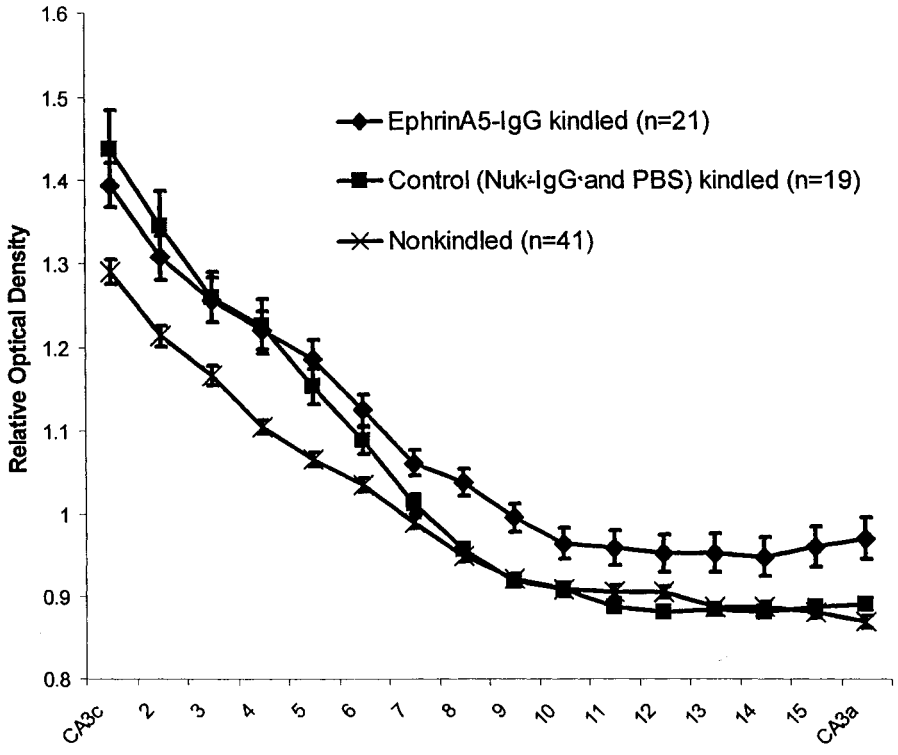
Relative Optical Density
1.6
1.5
1.4
1.3
1.2
1.1
1
0.9
0.8
CA3c
2
3
4
5
6
7
8
9
10
11
12
13
14
15
CA3a
EphrinA5-IgG kindled (n=21)
Control (Nuk-IgG and PBS) kindled (n=19)
Nonkindled (n=41)

EphA5-IgG infusion, on the other hand, did not detectably alter the distribution of sprouted mossy fibers in area CA3 (data not shown).

5.4 Discussion

We demonstrate in this study that the axonal guidance molecule EphA5 receptor is expressed in the adult CNS. Intraventricular administration of the EphA5 immunoadhesin, EphA5-IgG (an EphA5 receptor antagonist), retards kindling development and inhibits mossy fiber sprouting in area CA3. Conversely, continuous infusion of the EphA5 receptor agonist, ephrinA5 immunoadhesin, accelerates kindling and increases mossy fiber sprouting in IML and CA3. These results indicate that activation of the EphA5 tyrosine kinase receptor can contribute to the development of kindling and kindling-induced morphological changes. The EphB receptor antagonist, NUK-IgG, had no effect on kindling or mossy fiber sprouting. These results indicate that activation of EphA tyrosine kinase receptors can contribute to the development of kindling and kindling-induced morphological changes. Finally, infusion of ephrinA5-IgG alters the pattern of kindling-induced mossy fiber reorganization in CA3 area, indicating that Eph receptors may modulate activity-dependent axonal growth and targeting in the mature central nervous system.

5.4.1 Expression of EphA Receptors and Ephrins in Adult CNS

Several studies suggest that the expression of Eph receptors and ephrins, including EphB2, EphA4, EphA5, ephrinA2, ephrinA3 and ephrinA5, persist into adulthood (Zhou

et al., 1994; Zhang et al., 1996; Martone et al., 1997; Gao et al., 1998, and Gerlai et al., 1999). Among them, the mRNA for EphA4, EphA5 and EphB2 are mainly expressed in the hippocampal region of adult brain, a region exhibiting a high degree of plasticity (Morono-Flores and Wandosell, 1999; Gerlai et al., 1999; Gao et al, 1998). Consistent with these findings, pilot studies in our lab show that several EphA receptors and ephrins, including EphA3, EphA4, EphA5, EphA6, ephrinA2 and ephrinA5, are expressed in various regions of adult CNS, particularly in the hippocampal area. The highest level of expression of EphA receptors tested is for EphA5. In the present study, we demonstrate that EphA5 mRNA is widely distributed in adult brain, especially in regions that are associated with a high degree of plasticity and epileptogenesis. Such structures include hippocampus, piriform cortex, entorhinal cortex, and cerebellum. Within the hippocampus, EphA5 mRNA is detected in the granule cell layer of the dentate gyrus and the pyramidal cell layer of the CA3/CA1 region.

Moreno-Flores and Wandosell (1999) demonstrated that intraventricular injection of kainate induces an up-regulation of mRNA expression for several Eph receptors, including EphA4, EphA5 and EphB2, in surviving CA1 neurons in adult animals. The continued expression and the dynamic modulation of EphA receptors in adult CNS raises the probability that Eph receptors and ephrins may regulate neuronal plasticity and axonal patterning in adult CNS.

5.4.2 Activation of Eph Receptors and Adult CNS Plasticity

Recent studies have shown that infusion of soluble EphA5-IgG impairs the induction (Gao et al., 1998) or the maintenance (Gerlai et al., 1999) of LTP in area CA1

of hippocampal slices. In contrast, the EphA5 receptor agonist, ephrin-IgG, improves LTP (Gerlai et al, 1999) or induces a sustained increase of normal synaptic transmission (Gao et al., 1998). Moreover, infusion of EphA5-IgG enhances the performance of rats on two hippocampally-dependent behavioral tasks, spontaneous alternation in the T-maze and context-dependent fear conditioning, while infusion of ephrinA5-IgG retards performance (Gerlai et al, 1999).

Although there exist clear differences between kindling and LTP, it has been suggested that LTP and kindling share common features, such as the involvement of N-methyl-D-aspartate (NMDA) glutamate receptors, the activation of protein kinases, phosphatases and neurotrophic factors, the synthesis of proteins and the sprouting of mossy fibers. Once induced, both phenomena result in a long-lasting increase of synaptic efficacy (For review see Cain, 1989, McEachern and Shaw, 1999). Moreover, induction of LTP in the perforant path has been shown to facilitate subsequent kindling induction (Sutula and Steward, 1987).

Given the striking similarities between LTP and kindling, and the observation that infusion of EphA5 and ephrinA5 immunoadhesins significantly alters the development of LTP, we examined the effects of EphA receptors and their ligands on kindling. Immunoadhesins for EphA5 receptors and ephrinA5 were chosen in this study because (1) within hippocampus, the amount of EphA5 mRNA is significantly higher than that of EphA3, A4 and A6; (2) previous studies showed that activation of EphA5 receptors is involved in LTP, which raises the possibility that it might also modulate kindling and kindling-induced morphological changes.

In agreement with the effects of EphA5 and ephrinA5 immunoadhesins on LTP, we have shown that continuous infusion of EphA5-IgG retards the development of kindling and inhibits kindling-induced mossy fiber sprouting, while infusion of ephrinA5-IgG accelerates the progression of kindling-induced behavioral seizures and increases mossy fiber sprouting in CA3.

Eph receptors contain PDZ binding domains that may allow them to interact with cytoskeletal proteins (Torres *et al.;* 1998). EphrinA5-IgG mediates actin depolymerization and axonal growth cone collapse, consistent with repulsive effects of Eph receptors and ligands, and decreases tubulin and MAP2 expression, while EphA5-IgG has the opposite effects (Gerlai et al.,1999; Meima et al., 1997). This suggests that alteration of cytoskeletal protein expression and function may be a mechanism common to synaptic and/or structural modifications such as sprouting and LTP.

Together, these results indicate that EphA receptors not only contribute to axonal growth and pathway guidance during development, but also play a role in neuroplasticity in adulthood.

5.4.3 Eph Receptors, Ephrins and Kindling-Induced Mossy Fiber Reorganization

All the known members of the ephrin ligand family are membrane-associated. It is proposed that the membrane-bound ephrins may serve as location signals for the formation of topographic maps (for review see Flanagan and Vanderhaeghen, 1999). In brief, the Eph receptors are found in the source regions of the axons, while ephrins, the ligands, can be detected in target regions of the axons (Zhang et al., 1996). There is usually a complementary gradient distribution of Eph receptors and ephrins in the source

and target region. Since the ligands are suggested to serve as repellent signals for axons expressing Eph receptors (Meima et al., 1997), axons that contain high levels of Eph receptors can only project to the target regions that have little or no ephrins. Only axons that do not express Eph receptors can project to target regions where ligand expression is high (for review see Flanagan and Vanderhaeghen, 1999). It has been shown that such a complementary gradient distribution of Eph receptors and ephrins within the source and target regions is important for axonal targeting during neuronal development. However, whether such a gradient distribution of Eph receptors and ligands persists into adulthood, and the possible functions of Eph receptors and ephrins in adult CNS, have not yet been well-addressed.

Here we show that the mRNA for EphA5 receptors is not equally distributed within the granule cell layer of the dentate gyrus across the dorsal-ventral axis. The expression of EphA5 mRNA is highest in the dorsal dentate gyrus, with a dramatic decrease in the middle dentate gyrus, and no EphA5 mRNA detected in the ventral dentate gyrus. This gradient distribution of EphA5 receptor mRNA in dentate gyrus raises the possibility that EphA5 receptors may serve as axonal guidance cues for the axons of dentate gyrus granule cells (mossy fibers) in the adult CNS. In order to test this possibility, high concentrations of exogenous EphA5 receptors or one of its ephrin ligands was introduced into adult animals in order to disturb the gradient of EphA5 receptors. Our hypothesis was that if EphA5 receptors serve as axonal guidance cues in the adult CNS, infusion of exogenous EphA5 receptors or EphrinA5 ligands would disrupt the functions of endogenous Eph receptors, resulting in axonal rearrangement. Our results suggest that continuous infusion of ephrinA5-IgG alters the distribution of kindling-induced mossy

fiber sprouting along the dorsal-ventral axis as well as along the stratum oriens of area CA3, providing the first evidence for the function of Eph receptors and ephrins in adult axonal reorganization.

Consistent with previous results from our lab (Adams et al., 1997), we show that the kindling-induced sprouted mossy fiber collaterals are more prominent in the area CA3a than in area CA3c, and in the dorsal hippocampus than in the ventral hippocampus. However, ephrinA5-IgG infused kindled rats exhibit a strong sprouting effect in the ventral hippocampus and in area CA3c, and a slight decrease in Timm labeling in the dorsal hippocampus and area CA3a, when compared with the control kindled group. These site-dependent effects indicate that EphA receptors and their ligands may continue to serve as axonal guidance cues in adult CNS, and may play a role in epileptogenesis and mossy fiber reorganization.

The lack of effect of NUK-IgG, an EphB receptor antagonist, on kindling or mossy fiber sprouting may reflect a preferential role for EphA receptors in kindling and synaptic plasticity in the adult CNS. However, we cannot rule out that the NUK-IgG was infused at an insufficient dose, or that it is relatively less stable *in vivo* than the EphA5 immunoadhesin.

Based on the distribution of EphA receptors and ephrins in hippocampus and the effects of ephrinA5-IgG on kindling and kindling-induced axonal growth, we present a model to explain the possible roles of EphA5 receptors on activity-induced axonal targeting in adult CNS. As shown in Figure 10, under normal conditions, EphA5 receptors are located in the granule cell layer of the dentate gyrus. The expression of EphA5 receptor mRNAs is higher in the dorsal dentate gyrus and lower in the middle

dentate gyrus. No EphA5 mRNA is detected in the ventral hippocampus. Consequently, mossy fibers, the axons of dentate gyrus granule cells, express different amounts of EphA5 receptors. While the mossy fibers derived from ventral granule cells usually express few or no EphA receptors, axons from dorsal dentate gyrus express relatively high numbers of EphA receptors. Pilot studies in our lab suggest that ephrinA2, one ligand of EphA5 receptors (Flanagan and Vanderhaeghen, 1999), is expressed in area CA3, the target region of mossy fibers. Based on the results from previous studies, which usually suggest a complementary graded distribution of the ligands within the target area (Flanagan and Vanderhaeghen, 1999), we propose that the concentration of ephrins, the ligands of the EphA5 receptors, should be higher in the ventral CA3 region than in the dorsal CA3 region. Axons of the granule cells from dorsal hippocampus, which express high levels of EphA5 receptors, therefore, project to dorsal CA3 pyramidal cells, that contain few or no ephrins. Axons of the granule cells from the ventral dentate gyrus, which do not express EphA5 receptors, on the other hand, project to the ventral CA3 region, which expresses high numbers of ephrins (Figure 9A).

It is well-established that kindling can induce sprouting in the mossy fiber pathway (Sutula et al., 1988; Cavazos et al., 1991; Represa and Ben-Ari, 1992). Experiments in our lab consistently show that the sprouted mossy fiber collaterals are more prominent in the dorsal CA3 region than in the ventral CA3 region (unpublished data) (Figure 9B), and more prominent in the CA3a region than in the CA3c region (Adams et al, 1997).

Figure 5.10 Hypothetical effects of Eph receptors and ephrins on kindling-induced mossy fiber reorganization. In the normal non-kindled condition (TOP), EphA receptors are detected at higher concentration in the granule cell layer (GC) of the dorsal dentate gyrus (DG), while ephrinA expression is higher in the ventral part of area CA3. Kindling induces a stronger sprouting effect in the dorsal hippocampus than in the ventral hippocampus (MIDDLE). Infusion of high amounts of ephrin-IgGs (BOTTOM) activates the repellent effects of EphA receptors, and results in a reversal of mossy fiber distribution across the dorsal-ventral axis.

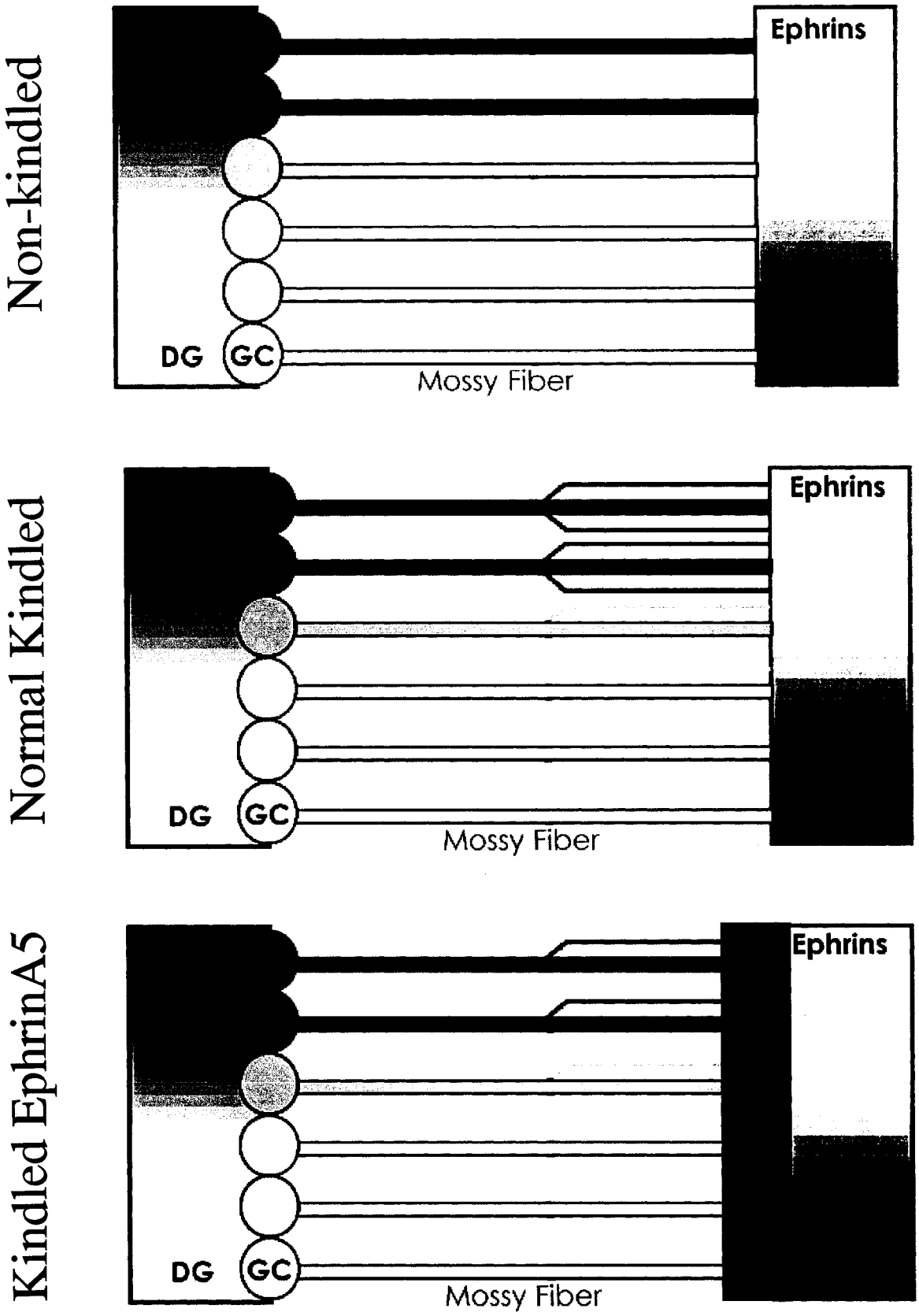
Non-kindled
Ephrins
DG
GC
Mossy Fiber
Normal Kindled
Ephrins
DG
GC
Mossy Fiber
Kindled EphrinA5
Ephrins
DG
GC
Mossy Fiber

Continuous infusion of ephrinA5-IgG into the brain disrupts the effects of spatial axonal guidance molecules and results in a disturbance of mossy fiber patterns across the dorsal-ventral axis. Introducing high amounts of exogenous ephrinA5-IgG into adult brain results in a slight inhibition of kindling-induced mossy fiber sprouting in the dorsal hippocampus and in the CA3a region, and an increase of kindling-induced mossy fiber sprouting in the ventral hippocampus and in the CA3c region. Our hypothesis is that such a high concentration of exogenous ligand blocks the endogenous ephrins from binding to their receptors, disrupts the effects of Eph and ephrins as spatial axonal guidance molecules, and results in a disturbance of mossy fiber sprouting. Several studies suggest that ephrinA5 can modulate axonal growth and pruning in a bi-directional way (Castellani et al., 1998; Gao et al, 1999). For example, ephrinA5 functions as a repellent signal for the axons of layer 2/3 cortical neurons, which normally express EphA5 receptors. On the other hand, ephrinA5 selectively promotes axonal sprouting of layer 6 neurons, which do not express EphA5 receptors (Castellani et al., 1998). Infusion of ephrinA5-IgGs, then, may exert an inhibitory effect on dorsal mossy fibers, which express a higher level of EphA5 receptors, while promoting the axonal sprouting effect of dorsal mossy fibers, which normally have few or no EphA5 receptors (Figure 9C).

Worth noticing is that the effects of EphA5 receptors on axonal patterning in adult CNS appears to be activity-dependent. Infusion of EphA5-IgG or ephrinA5-IgG alone does not produce any visible effect on mossy fiber distribution, suggesting that activation or blockage of EphA5 receptors alone is not sufficient to alter the pattern of axonal growth.

Surprisingly, our data show that EphA5-IgG does not induce any detectable change in the mossy fiber sprouting pattern. There are several possible explanations for the apparent difference between the effects of EphA5-IgG infusion and ephrinA5-IgG infusion on the redistribution of mossy fibers. First, we infused both immunoadhesins intraventricularly. It is possible that these two IgGs penetrated and diffused differently, resulting in a difference in concentration achieved within the hippocampal CA3 area. Second, the EphA5-IgG exerts it antagonistic effects on the EphA receptors by blocking ligand binding to endogenous EphA receptors. The concentration of EphA5-IgG used in this study may not be sufficient to block all the ligands that are involved. On the other hand, the ephrinA5-IgG serves as an agonist by binding to and activating EphA receptors. A small amount of ephrinA5-IgGs may activate endogenous EphA receptors and elicit EphA-dependent axonal reorganization.

5.5 Conclusions

EphA5 receptors continue to be expressed throughout adulthood. Infusion of EphA5-IgG and ephrinA5-IgG significantly alter kindling-induced epileptogenesis and mossy fiber sprouting, suggesting that Eph receptors and their ligands play an important role in adult neuronal plasticity and activity-induced axonal reorganization.

CHAPTER 6 GENERAL DISCUSSION

The main objectives of this thesis were to study (1) the relationship of epileptogenesis, neuronal damage and axonal growth; and (2) the modulation of seizure induction and MFS in adult CNS.

Using a variety of animal models, including genetic models, kindling, and both KA- and pilocarpine-induced SE, I found that seizure activity and the extent of MFS were not always correlated with the gross neuronal loss in the hilar region. The Long-Evans strain, which is resistant to seizure-related neuronal damage, developed status-induced mossy fiber sprouting and spontaneous seizure activity to the same extent as the Wistar strain, which more reliably shows such damage (Chapter 2). Similar results were found for kindling (Chapter 4). In addition, although short-duration status epilepticus does not elicit any cell damage within the hilar area, it is sufficient to trigger spontaneous seizures and mossy fiber sprouting in several rat strains, including the Long-Evans hooded, Wistar, and kindling-prone or kindling-resistant strains (Chapters 2 and 3). Hence, I have dissociated neuronal damage from the induction of seizures and mossy fiber sprouting. Such results argue against the "dormant basket cell hypothesis" (Houser, 1999), which suggests a casual relationship between epileptogenesis and neuronal damage within the hilar area. Instead, my results clearly indicate that epilepsy and axonal growth can be induced independently of gross cell loss. However, it is likely that neuronal damage contributes to the development of mossy fiber sprouting. The highest levels of sprouting are seen in animals with neuronal loss, and there is often a correlation between MFS and hilar cell loss (Chapter 2).

The fact that the extent of MFS and the development of acute or recurrent seizures are positively correlated (Chapters 2 and 3) indicates that axonal growth may be associated with epileptogenesis. It has been suggested that the sprouted mossy fiber collaterals form recurrent synapses onto the dendrites of other DG granule cells, contributing to the abnormal hyperexcitability observed in the epileptic brain ("the mossy fiber sprouting hypothesis") (Babb et al., 1991; Mathern et al., 1995). Although it is clear that mossy fiber sprouting is not the only cause of seizures, since blocking MFS with protein synthesis inhibitors does not hamper the development of seizure activity (Longo and Mello, 1997, 1998, 1999; Covolan, 2000), it is possible that MFS contributes to epileptogenesis.

In an effort to study the regulatory mechanisms of activity-induced MFS in adult CNS, we have introduced exogenous proteins such as neurotrophins into the brain. Such molecules regulate axonal growth during neuronal development. Neurotrophins and their high affinity receptors, Trks, have been shown to be dynamically regulated during epilepsy and in animal models of epilepsy (Rocamora et al., 1992, 1994; Rudge et al., 1998; Schmidt-Kaster & Olson, 1995). Infusion of exogenous NGF, BDNF, or TrkB receptorbodies significantly modulates the development of seizures and/or the extent of MFS in adult CNS (Adams et al., 1997; Larmet et al., 1995; Osehobo et al., 1999; Binder et al., 1999). In the present study, we have found that another neurotrophin, NT-3, also regulates the kindling development and the extent of kindling-induced MFS. Taken together, these results show that many proteins that affect neurite outgrowth during neuronal development also modulate activity-dependent axonal sprouting in adult CNS.

These factors continue to play a role in neuronal plasticity and synaptic reorganization in adult brain. They may also play a role in epileptogenesis.

The reverse dorsal/ventral gradients for mossy fiber sprouting in the CA3 region and in the IML of the dentate gyrus has been a very reliable finding in the Racine laboratory. Sprouting in the stratum oriens is much denser in the dorsal hippocampus, while sprouting in the IML is denser in the ventral hippocampus (Adams et al., 1997; Chapter 5). These results suggest that there might be molecular cues guiding the growth of these collaterals. Thus, we have expanded our investigation to include one family of axon guidance factors, Eph receptors and ephrins. Pilot experiments have shown that several Eph receptors and ephrins are expressed in adult rat CNS, particularly in the hippocampus. In addition, EphA5 receptors distribute in the dentate gyrus in a graded manner (Chapter 5). Exposure to agonists and antagonists of EphA5 receptors not only modulates the extent of axonal growth, but also alters the gradient of kindling-induced MFS along the dorsal-ventral axis of CA3 and along the stratum oriens. Hence, we have proven that Eph receptors function as signalling cues for the gradient distribution of MFS.

Using *in situ* hybridization techniques, we are currently examining the expression of several other Eph receptors and ephrins in adult rats, and the regulation of their patterns of expression following kindling. We also plan to investigate the function of Eph receptors on activity-induced axonal growth by combining the manipulation of Eph receptors with mild, focal electrical stimulation. Delivering non-epileptigenic electrical stimulation, such as LTP-inducing stimulation, into the dorsal, middle or ventral hippocampus, might selectively activate the mossy fiber pathways in a focused manner.

In conclusion, our results suggest a complex regulatory mechanism of epileptogenesis and related morphological changes. Apparently, seizure-related neuropathological alterations such as neuronal loss, axonal sprouting, and the alteration of gene and protein expression contribute to epileptogenesis. However, the present results suggest that it is possible to produce an increase in epileptic reactivity (kindling) or to develop spontaneous seizures (status) in the absence of either hilar cell loss or mossy fiber sprouting. Any one of these neurological changes, by itself, does not appear to be sufficient to account for the development of seizures.

REFERENCES

Acsady L, Kamondi A, Sik A, Freud T, and Gyorgy B (1998) GABAergic cells are the major postsynaptic target of mossy fibers in the rat hippocampus. J. Neurosci 18(9): 3386-3403.

Acsady L, Katona I, Martinez-Guijarro FJ, Buzsaki G, and Freud T (2000) Unusual target selectivity of perisomatic inhibitory cells in the hilar region of the rat hippocampus J. Neurosci 20(18): 6917-6919.

Adams B, Lee M, Fahnestock M, Racine RJ (1997) Long-term potentiation trains induce mossy fiber sprouting. Brain Res. 775(1-2): 193-197.

Adams B, Sazgar M, Osehobo P, Van der Zee CEEM, Diamond J, Fahnestock M, and Racine RJ. (1997), Nerve growth factor accelerates seizure development, enhances mossy fiber sprouting, and attenuates seizure-induced decreases in neuronal density in the kindling model of epilepsy. J. Neurosci. 17(14): 5288-5296.

Adams B, Von Ling E, Vaccarella L, Ivy GO, Fahnestock M, Racine RJ. (1998) Time course for kindling-induced changes in the hilar area of the dentate gyrus: reactive gliosis as a potential mechanism. Brain Res. 804(2):331-6.

Adams B, Vaccarella L, Fahnestock M and Racine RJ. The cholinergic system is involved in kindling-induced mossy fiber sprouting. Submitted to Synapse.

Ajmone-Marsan C., and Abraham K., (1965) Epilepsy. Prog Neurol Psychiatry. 20:286-351.

Amural DG, Ishizuka N, and Claiborne B (1990) Neurons, numbers and the hippocampal network. In Progress in Brain Research (Eds).

Arnold PS, Racine RJ and Wise RA (1973) Effects of atropine, reserpine, 6-hydroxydopamine and handling on seizure development in the rat. Exp Neurol. 40: 457-470.

Asztely, F., Kokaia, M., Olofsdotter, K., Ortegren, U., Lindvall, O.R. (2000) Afferent-specific modulation of short-term synaptic plasticity by neurotrophins in dentate gyrus. Eur. J. Neurosci. 12, 662-669.

Babb TL, Kupfer WR, Pretorius JK, Crandall PH, Levesque MF (1991) Synaptic reorganization by mossy fibers in human epileptic fascia dentate. Neuroscience 42: 351-363.

Babb TL, Pretorius JK, Kupfer WR et al. (1989) Glutamate decarboxylase-immunoreactive neurons are preserved in human epileptic hippocampus. J Neurosci 9(7): 2562-2574.

Baker, R.E., Dijkhuizen, P.A., Van Pelt, J., Verhaagen, J. (1998) Growth of pyramidal, but not non-pyramidal, dendrites in long-term organotypic explants of neonatal rat neocortex chronically exposed to neurotrophin-3. Eur. J. Neurosci. 10, 1037-1044.

Barbacid, M. (1995) Structural and functional properties of the TRK family of neurotrophin receptors. Ann. N. Y. Acad. Sci. 766, 442-458.

Becker A, Krug M, Schroder H. (1997) Strain differences in pentylenetetrazol-kindling development and subsequent potentiation effects. Brain Res 763(1):87-92.

Ben-Ari Y, Tremblay E, and Ottersen OP (1980a) Injections of kainic acid into the amygdaliod complex of the rat: an electrographic, clinical and histological study in relation to the pathology of epilepsy. Neuroscience 5: 515-528.

Ben-Ari Y, Tremblay E, Ottersen OP, and Meldrum BS (1980b) The role of epileptic activity in hippocampal and "remote"cerebral lesions induced by kainic acid. Brain Res 191: 79-97.

Ben-Ari Y, Tremblay E, Riche D, Chilini G and Naquet R (1981) Electrographic, clinical and pathological alternations following systemic administration of kainic acid, bicuculline and pentetrazole: metabolic mapping using the deoxyglucose method with special reference to the pathology of epilepsy. Neuroscience 6: 1361-1391.

Bengzon, J., Kokaia, Z., Ernfors, P., Kokaia, M., Leanze, G., Nilsson, O.G., Persson, H., Lindvall, O. (1993) Regulation of neurotrophin and TrkA, TrkB and TrkC tyrosine kinase receptor messenger RNA expression in kindling. Neuroscience 53, 433-466.

Bengzon J, Kokaia Z, Elmer E, Nanobashvili A, Kokaia M, Lindvall O. Free in PMC , (1997) Apoptosis and proliferation of dentate gyrus neurons after single and intermittent limbic seizures. Proc Natl Acad Sci U S A. 1997 Sep 16;94(19):10432-7.

Berger M and Ben-Ari Y (1983) Autoradiographic visulization of ^{3}H kainic acid receptor subtypes in the rat hippocampus. Neurosci. Lett. 39: 237-242.

Bertram, E.H. & Lothman, E.W. (1993) Morphometric effects of intermittent kindled seizures and limbic status epilepticus in the dentate gyrus of the rat. Brain Res. 603, 25-31.

Berzaghi, M.P., Gutierrez, R., Heinemann, U., Lindholm, D., Thoenen, H. (1995) Neurotrophins induce acute transmitter-mediated changes in brain electrical activities. Soc. Neurosci. Abstr. 21, 545.

Binder, D.K., Routbort, M.J., McNamara, J.O., (1999) Immunohistochemical evidence of seizure-induced activation of trk receptors in the mossy fiber pathway of adult rat hippocampus. J. Neurosci. 19(1), 4616-4626.

Bliss T. and Collingridge, (1993) A synaptic model of memory: long-term potentiation in the hippocampus, Nature, 361: 31-39.

Bouchet C and Cazauvielh Y. (1825) De l'epilepsie consideree dans ses rapports avec l'alenation mentale. Arch Gen Med par 9: 510-542.

Bratz E. (1899) Ammonshornbefunde bei epileptikern. Arch Psychiatr Neuvekr 32: 820-835.

Broca P (1878) Anatomie comparee des circonvolutions cerebrales. Le grand lobe limbique et la scissure limbique dans le serie des mammiferes. Rev Anthropol, Ser 2 1: 385-498.

Brooks-Kayal AR, Shumate MD, Jin H, Rikhter TY, Coulter DA (1998) Selective changes in single cell GABAA receptor subunit expression and function in temporal lobe epilepsy. Nat Med 4:1166-1172.

Burnham WM., (1989) The GABA hypothesis of kindling: recent assay studies. Neurosci. Biobehav. Rev. 13: 281-288.

Cain D., (1989) Long-term potentiation and kindling: how similar are the mechanism? TINS, 12: 6-10.

Cantallops I, Routtenberg A. (2000) Kainic acid induction of mossy fiber sprouting: dependence on mouse strain. Hippocampus 10(3):269-73.

Carter, B.D., Zirrgiebel, U., Barde, Y.A. (1995) Differential regulation of p21ras activation in neurons by nerve growth factor and brain-derived neurotrophic factor. J.

Biol. Chem. 270, 21751-21757.

Casterllani V., Yue Y., Gao P.P., Zhou R., and Bolz J. (1998) Dual action of a ligand for Eph receptor tyrosine kinases on specific populations of axons during the development of cortical circuits. J Neurosci. 18(12): 4663-4672.

Cavalheiro EA. (1995) The pilocarpine model of epilepsy. Ital J Neurol Sci. 16(1-2):33-7.

Cavazos JE, Das I, and Sutala TP (1994) Neuronal loss induced in limbic pathways by kindling: evidence for induction of hippocampal sclerosis by repeated brief seizures. J Neurosci 14(5): 3106-3121.

Cavazos, J.E., Das, Igolarai, G., and Sutula, T.P., (1991) Mossy fiber synaptic reorganization induced by kindling: time course for development progression and permanence, J. Neurosci., 11: 2795-2803.

Chen AC, Shin KH, Duman RS, Sanacora G. (2001) ECS-Induced mossy fiber sprouting and BDNF expression are attenuated by ketamine pretreatment. J ECT. 17(1):27-32.

Claiborne BJ, Amaral DG and Cowan WM (1986) A light and electron microscopic analysis of the mossy fibers of the rat dentate gyrus. J. Comp Neurol 246: 435-458.

Clark M, Massenburg GS, Weiss SR, Post RM (1994) Analysis of the hippocampal $GABA_A$ receptor system in kindled rats by autoradiographic and in situ hybridization techniques: contingent tolerance to carbamazepine. Mol Brain Res 26:309-319.

Clifford DB, Olney JW, Maniotis A, Collins RC and Zorumski CF (1987) The functional anatomy and pathology of lithium-pilocarpine and high-dose pilocarpine seizures. Neuroscience, 23: 953-968.

Coggeshall RE, Lekan HA. (1996) Methods for determining numbers of cells and synapses: a case for more uniform standards of review. J Comp Neurol. 364(1):6-15.

Coulter DA. (2001) Epilepsy-associated plasticity in gamma-aminobutyric acid receptor expression, function, and inhibitory synaptic properties. Int Rev Neurobiol 2001;45:237-52.

Covolan L, Ribeiro LT, Longo BM, Mello LE. R (2000) Cell damage and neurogenesis in the dentate granule cell layer of adult rats after pilocarpine- or kainate-induced status epilepticus. Hippocampus. 10(2):169-80.

Croll, S.D., Chesnutt, C.R., Rudge, J.S., Acheson, A., Ryan, T.E., Siuciak, J.A., DiStefano, P.S., Wiegand, S.J., Lindsay, R.M. (1998) Co-infusion with a TrkB-Fc receptor body carrier enhances BDNF distribution in the adult rat brain. Exp. Neurol. 152, 20-33.

Cruz-Orive LM (1993) Discussion of topic IN22: Stereology. Bull. Intern. Statis. Inst., Proceedings 49th Session, Florence 1993. 55(4): 162, 1993.

Dailey J.W., Reigel C.E., Mishra P.K., and Jobe P.C., (1989) Neurobiology of seizure predisposition in the genetically epilepsy-prone rat. Epilepsy Res. 3(1): 3-17.

Davenport CJ, Brown WJ, and Babb TL (1990) GABAergic neurons are spared after intrahippocampal kainite in the rat. Epilepsy Res. 5:28-42.

Davies, A.M. (1994) The role of neurotrophins in the developing nervous system. J. Neurobiol. 25, 1334-1349.

Davis S., Gale N.W., Aldrich T.H., maisonpierre P.C., lhotak V., Pawson T., Goldfarb M., and Yancopoulos G.D., (1994) Ligands for Eph-related receptor tyrosine kinases that require membrane attachment or clustering for activity. Science 266: 816-819.

De Bonnel G and De Montigny C (1983) Benzodiazepines selectively antagonize kainite-induced activation in the rat hippocampus. Eur. J. Pharmac. 93: 45-54.

Dreyfus CF, (1989) Trends in Pharmacol. Sciences 10:145-149.

Ebendal, T. (1992) Function and evolution in the NGF family and its receptors. J. Neurosci. Res. 32, 461-470.

El Bahh B, Lespinet V, Lurton D, Coussemacq M, Le Gal La Salle G, and Rougier A (1999), Correlations between granule cell dispersion, mossy fiber sprouting, and hippocampal cell loss in temporal lobe epilepsy. Epilepsia 40(10): 1393-401.

Elmer E, Kokaia M, Kokaia Z, Ferencz I, Lindvall O. (1996) Delayed kindling development after rapidly recurring seizures: relation to mossy fiber sprouting and neurotrophin, GAP-43 and dynorphin gene expression. Brain Res. 712: 19-34.

Elmer, E., Kokaia, M., Ernfors, P., Ferencz, I., Kokaia, Z., Lindvall, O. (1997) Suppressed kindling epileptogenesis and perturbed BDNF and TrkB gene regulation in NT-3 mutant mice. Exp. Neurol. 145, 93-103.

Elmer, E., Kokaia, Z., Kokaia, M., Carnahan, J., Nawa, H., Lindvall, O. (1998) Dynamic changes of brain-derived neurotrophic factor protein levels in the rat forebrain after single and recurring kindling-induced seizures. Neuroscience 83, 351-362.

Elmer E., Kokaia M., Kokaia Z., McIntyre D.C., Lindvall O., (1998) Epileptogenesis induced by rapidly recurring seizures in genetically fast- but not slow-

kindling rats. Brain Res. 789(1):111-117.

Ernfors, P., Bengzon, J., Kokaia, Z., Persson, H., and Lindvall, O. (1991) Increased levels of messenger RNA for neurotrophic factors in the brain during kindling epileptogenesis. Neuron 7, 165-176.

Ernfors, P., Wetmore, C., Olson, L. and Persson, H. (1990) Identification of cells in rat brain and peripheral tissues expressing mRNA for members of the nerve growth factor family. Neuron 5, 511-526.

Fahnestock, M. & Zhu, W. (1999) Expression of human prohormone convertase PC2 in a baculovirus-insect cell system. DNA Cell Biol. 18, 409-417.

Ferencz, I., Kokaia, M., Keep, M., Elmer, E., Metsis, M., Kokaia, Z., Lindvall, O. (1997) Effects of cholinergic denervation on seizure development and neurotrophin messenger RNA regulation in rapid hippocampal kindling. Neuroscience 80, 389-399.

Flanagan J. G., & Vanderhaeghen P., (1998) The ephrins and Eph receptors in neural development.Annu. Rev. Neurosci. 21, 309.

Franck JE, Pokorny J, Kunkel DD et al (1995) Physiologic and morphologic characteristics of granule cell circuity in human epileptic hippocampus. Epilepsia 36: 543-558.

Frank, L., Ventimiglia, R., Anderson, K., Lindsay, R.M., Rudge, J.S. (1996), BDNF down-regulates neurotrophin responsiveness, TrkB protein and TrkB mRNA levels in cultured rat hippocampal neurons. Eur. J. Neurosci. 8, 1220-1230.

Frank, L., Wiegand, S.J., Siuciak, J.A., Lindsay, R.M., Rudge J.S. (1997), Effects of BDNF infusion on the regulation of TrkB protein and message in adult rat brain. Exp. Neurol. 145, 62-70.

Frankel WN, Taylor L, Beyer B, Tempel BL, White HS. (2001) Electroconvulsive thresholds of inbred mouse strains. Genomics 74(3):306-12.

Freund RK, Marley RJ, Wehner JM. (1987) Differential sensitivity to bicuculline in three inbred mouse strains. Brain Res Bull 1987 May;18(5):657-62.

Frotscher M, Soriano E, and Misgeld U (1994) Divergence of hippocampal mossy fibers. Synapse 16: 148-160.

Gall, C., Lauterborn, J., Bundman, M., Murray, K., Isackson (1991) Seizures and the regulation of neurotrophic factor and neuropeptide gene expression in brain. Epilepsy Res. Suppl. 4, 225-245.

Gall, C.M. & Isackson, P.J. (1989) Limbic Seizures increase neuronal production of messenger RNA for nerve growth factor. Science 24, 758-761.

Gall, C.M. (1993) Seizure-induced changes in neurotrophin expression; implication for epilepsy. Exp. Neurol. 124, 150-166.

Gao P.P., Yue Y., Cerretti D. P., Deryfus C., and Zhou R., (1999) Ephrin-dependent growth and pruning of hippocampal axons. Pro. Natl. Acad. Sci. USA 96: 4073-77.

Gao W. Q., Shinsky N., Armanini M.P., Moran P., Zheng J.L., Mendoza-Ramirez J. L., Phillips H.S., Winslow J.W., and Caras I.W., (1998) Regulation of hippocampal synaptic plasticity by the tyrosine kinase receptor, REK7/EphA5 and its ligand, AL-1/ephrin-A5. Mol. Cell. Neurosci. 11: 247-259.

Gerlai R., Shinsky N., Shih A., Williams P., Winer J., Armanini M., Cairns B., Winslow J., Gao W.Q., and Phillips H. S., (1999) Regulation of learning by EphA receptors: a protein targeting study. J. Neurosci. 19(21): 9538-9549.

Gibbs, R.B., & Pfaff, D.W. (1994) In situ hybridization detection of trkA mRNA in brain: distribution, colocalization with p75NGFR and up-regulation by nerve growth factor. J. Comp. Neurol. 341, 324-339.

Goddard G.V., and Douglas R.M., (1975) Does the engram of kindling model the engram of normal long-term memory? Can J Neurological Sci.: 385-398.

Goddard G.V., McIntyre D., and Leech C., (1969) A permanent change in brain function resulting from daily electrical stimulation. Exp. Neurol. 25: 295-330.

Goddard, G. V., (1967) Development of epileptic seizures through brain stimulation at low intensity, Nature, 214:1020-1021.

Goddard, G. V., and Maru, E., (1986): Forces for and against the kindled state as revealed by EEG and field potential analysis in the hippocampal dentate area of perforant path kindled rats. In: Kindling III, edited by J. A. Wada, pp. 1-13, Raven Press. New York.

Golden G.T., Smith G.G., Ferraro T.N., Reyes P.F., Kulp J.K., Fariello R.G. (1992) Strain differences in convulsive response to the excitotoxin kainic acid. Neuroreport 2(3):141-144.

Golden G.T., Ferraro T.N., Smith G.G., Snyder R.L., Jones N.L., Berrettini W.H. (2001) Acute cocaine-induced seizures: differential sensitivity of six inbred mouse strains. Neuropsychopharmacology 24(3):291-299.

Guillery RW, Herrup K. (1997) Quantification without pontification: choosing a method for counting objects in sectioned tissues. J Comp Neurol. 386(1):2-7.

Gundersen HJ, Bagger P, Bendtsen TF, Evans SM, Korbo L, Marcussen N, Moller A, Nielsen K, Nyengaard JR, Pakkenberg B (1988) The new stereological tools: Disector, fractionator, nucleator, and point sampled intercepts and their use in pathological research and diagnosis. APMIS 96: 857-881.

Hogan B, Costantini F, Lacy E (1986). Manipulating the mouse embryo: A laboratory manual, 2nd edition., Cold Spring Harbor Press, Cold Spring Harbor, NY.

Holtzman, D.M., Li, Y., Parada, L.F., Kinsman, S., Chen, C.K., Valletta, J.S., Zhou, J., Long, J.B., Mobley, W.C. (1992) p140trk mRNA marks NGF-responsive forebrain neurons: evidence that trk gene expression is induced by NGF. Neuron 9, 465-478.

Houser CR, Miyashiro JE, Sweartz BE, Walsh GO, Rich JR and Delgado-Escueta AV (1990) Altered patterns of dynorphin immonoreactivity suggest mossy fiber reorganization in human hippocampal epilepsy. J. Neurosci. 10: 267-282.

Hughes, P.E., Young, D., Preston, K.M., Yan, Q., Dragunow, M. (1998) Differential regulation by MK801 of immediate-early genes, brain-derived neurotrophic factor and trk receptor mRNA induced by a kindling after-discharge. Mol. Brain Res. 53(1-2), 138-151.

Humpel, C., Wetmore, C. and Olson, L. (1993) Regulation of brain-derived neurotrophic factor messenger RNA and protein at the cellular level in pentylenetetrazol-induced epileptic seizures. Neuroscience 53(4), 909-918.

Ikegaya Y, Nishiyama N, Matsuki N. (2000) L-type Ca(2+) channel blocker inhibits mossy fiber sprouting and cognitive deficits following pilocarpine seizures in immature mice. Neuroscience 98(4):647-59.

Inoue, T., Hirai, H., Onteniente, B., Suzuki, F. (1998) Correlated long-term increase of brain-derived neurotrophic factor and Trk B proteins in enlarged granule cells of mouse hippocampus after kainic acid injection. Neuroscience 86, 723-728.

Jankowsky JL, Patterson PH. (2001) The role of cytokines and growth factors in seizures and their sequelae. Prog Neurobiol 63(2):125-49.

Jean-Pierre Wuarin and F. Edward Dudek Electrographic seizures and new recurrent excitatory circuits in the dentate gyrus of hippocampal slices from kainate-treatment epileptic rats. J Neurosci 16:4438-4448.

Jensen, E.B. and Gundersen, H.J.G. (1985) The stereological estimation of moments of particle volume. J. Appl. Prob. 22: 82--98.

Kamphuis W, De Rijk TC, Lopes da Silva FH (1994) GABAA receptor 1-3 subunit gene expression in the hippocampus of kindled rats. Neurosci Lett 174:5-8.

Kang, H. & Schuman, E.M. (1995) Long-lasting neurotrophin-induced enhancement of synaptic transmission in the adult hippocampus. Science 267, 1658-1662.

Katoh-Semba, R., Kaisho, Y., Shintani, A., Nagahama, M., Kato, K. (1996) Tissue distribution and immunocytochemical localization of neurotrophin-3 in the brain and peripheral tissues of rats. J. Neurochem. 66, 330-337.

Katoh-Semba, R., Takeuchi, I.K., Inaguma, Y., Ito, H., Kato, K. (1999) Brain-derived neurotrophic factor, nerve growth and neurotrophin-3 selected regions of the rat brain following kainic acid-induced seizure activity. Neurosci. Res. 35, 19-29.

Khurgel M, Ivy GO. (1996) Astrocytes in kindling: relevance to epileptogenesis. Epilepsy Res. 26(1):163-75.

Kiessling M, Gass P. (1993) Immediate early gene expression in experimental epilepsy. Brain Pathol. 3(4):381-93.

Kim, H.G., Wang, T., Olafsson, P., Lu, B. (1994) Neurotrophin 3 potentiates neuronal activity and inhibits gamma-aminobutyratergic synaptic transmission in cortical neurons. Proc. Natl. Acad. Sci. U.S.A. 91, 12341-12345.

Kleinrok Z and Turski L. (1980) Kanic acid-induced wet dog shakes in rat: the relation to central neurotransmitters. Naunyn Schmiedebergs Arch Pharmacol 314: 37-46.

Klioueva IA, van Luijtelaar EL, Chepurnova NE, Chepurnov SA. (2001) PTZ-induced seizures in rats: effects of age and strain. Physiol Behav 72(3):421-6.

Knusel, B., Beck, K.D., Winslow, J.W., Rosenthal, A., Burton, L.E., Widmer, H.R., Nikolics, K., and Hefti, F., (1992) Brain-derived neurotrophic factor administration protects basal forebrain cholinergic but not nigral dopaminergic neurons from degenerative changes after axotomy in the adult rat brain. J. Neurosci. 12:4391-4402.

Knüsel, B., Gao, H., Okazaki, T., Yoshida, Y., Mori, N., Hefti, F., Kaplan, D.R. (1997) Ligand-induced down-regulation of TRK messenger RNA, protein and tyrosine phosphorylation in rat cortical neurons. Neuroscience 78, 851-862.

Kokaia Z, Kelly ME, Elmer E, Kokaia M, McIntyre DC, Lindvall O. (1996) Seizure-induced differential expression of messenger RNAs for neurotrophins and their receptors in genetically fast and slow kindling rats. Neuroscience 75(1):197-207.

Kokaia, M., Asztely, F., Olofsdotter, K., Sindreu, C.B., Kullmann, D.M., Lindvall, O. (1998) Endogenous neurotrophin-3 regulates short-term plasticity at lateral perforant path-granule cell synapses. J. Neurosci. 18,8730-9.

Kokaia, M., Ernfors, P., Kokaia, Z., Elmer, E., Jaenisch, R., Lindvall, O. (1995)

Suppressed epileptogenesis in BDNF mutant mice. Exp. Neurol. 133, 215-224.

Kokaia, Z., Bengzon, J., Metsis, M., Kokaia, M., Persson, H., Lindvall, O. (1993) Coexpression of neurotrophins and their receptors in neurons of the central nervous system. Proc. Natl. Acad. Sci. U.S.A. 90, 6711-6715.

Kokaia, Z., Kelly, M.E., Elmer, E., Kokaia, M., McIntyre, D.C., Lindvall, O. (1996) Seizure-induced differential expression of messenger RNAs for neurotrophins and their receptors in genetically fast and slow kindling rats. Neuroscience 75(1), 197-207.

Kosobud AE, Cross SJ, Crabbe JC. Neural sensitivity to pentylenetetrazol convulsions in inbred and selectively bred mice. Brain Res 1992 Oct 2;592(1-2):122-8.

Labelle, C. & Leclerc, N. (2000) Exogenous BDNF, NT-3 and NT-4 differentially regulate neurite outgrowth in cultured hippocampal neurons. Dev. Brain Res. 123, 1-11.

Larmet, Y., Reibel, S., Carnahan, J., Nawa, H., Marescaux, C., Depaulis, A. (1995) Protective effects of brain-derived neurotrophic factor on the development of hippocampal kindling in the rat. NeuroReport 6(14), 1937-1941.

Laurie DJ, Wisden W, Seeburg PH (1992) The distribution of thirteen GABAA receptor subunit mRNAs in the rat brain. III. Embryonic and postnatal development. J Neurosci 12:4151-4172.

Lehmann TN, Gabriel S, Kovacs R, Eilers A, Kivi A, Schulze K, Lanksch WR, Meencke HJ, Heinemann U. (2000) Alterations of neuronal connectivity in area CA1 of hippocampal slices from temporal lobe epilepsy patients and from pilocarpine-treated epileptic rats. Epilepsia. 41 Suppl 6:S190-4.

Lehmann T.N., Gabriel S., Eilers A., Njunting M., Kovacs R., Schulze K., Lanksch W.R., Heinemann U., (2001) Fluorescent tracer in pilocarpine-treated rats shows widespread aberrant hippocampal neuronal connectivity. Eur J Neurosci. 14(1):83-95.

Li S, Xu B, Martin D, Racine R. J., and M. Fahnestock. Glial cell line-derived neurotrophic factor (GDNF) retards seizure development, prevents kindling-induced hilar area increases and blocks mossy fiber sprouting in kindled rats. Neuroscience (submitted).

Lindsay, R.M., Wiegand, S.J., Altar, C.A., DiStefano, P.S. (1994) Neurotrophins and brain insults. Trends Neurosci. 17, 490-496.

Liu Z, Nagao T, Desjardins GC, Gloor P, and Avoli M. (1994) Quantitative evaluation of neuronal loss in the dorsal hippocampus in rats with long-term pilocarpine seizures. Epilepsy Res 17: 237-247.

Lloyd K.G., Scatton B., Voltz C., Bryere P., Valin A., and Naquet R., (1986) Cerebrospinal fluid amino acid and monoamine metabolite levels of Papio papio: correlation with photosensitivity. Brain Res. 363(2): 390-394.

Longo BM, Mello LE. (1997) Blockade of pilocarpine- or kainate-induced mossy fiber sprouting by cycloheximide does not prevent subsequent epileptogenesis in rats. Neurosci Lett. 226(3):163-6.

Longo BM, Mello LE. (1998) Supragranular mossy fiber sprouting is not necessary for spontaneous seizures in the intrahippocampal kainate model of epilepsy in the rat. Epilepsy Res. 32(1-2):172-82.

Longo BM, Mello LE. (1999) Effect of long-term spontaneous recurrent seizures or reinduction of status epilepticus on the development of supragranular mossy fiber sprouting. Epilepsy Res. 36(2-3):233-41.

Loscher W, Cramer S, Ebert U. (1998) Differences in kindling development in seven outbred and inbred rat strains. Exp Neurol 154(2):551-9.

Lothman EW, Williamson JM. (1993) Rapid kindling with recurrent hippocampal seizures. Epilepsy Res. 14(3):209-20.

Lynch M, Sutula T. (2000) Recurrent excitatory connectivity in the dentate gyrus of kindled and kainic acid-treated rats. J Neurophysiol. 83(2):693-704.

Maclean PD (1952) Some psychiatric implications of physiological studies on frontotemporal portion of limbic system (Visceral brain). EEG Clin Neurophysiol 4: 286-290.

Macnamara J.O., Byrne M.C., Dashieff R.M. and Fritz J.G., (1980) The kindling model of epilepsy: a review. Prog Neurobiol, 15: 139-159.

Martone M.E., Holash J.A., Bayardo A., Pasquale E.B., Ellisman M.H., (1997) Immunolocalization of the receptor tyrosine kinase EphA4 in the adult rat central nervous system. Brain Res. 771 (1997): 238-250.

Masukawa LM, O'Connor WM, Lynott J et al. (1995) Longitudinal variation in cell density and mossy fiber reorganization in the dentate gyrus from temperal lobe epileptic patients. Bran Res 678: 65-75.

Mathern GW, Cifuentes F, Leite JP, Pretorius JK, and Babb TL (1993) Hippocampal EEG excitability and chronic spontaneous seizures are associated with

aberrant synaptic reorganization in the rat intrahippocampal kainite model. Electroencephalogr Clin Neurophysiol 87: 326-339.

Mathern GW, Pretorius JK, Babb TL. (1995) Quatified patterns of mossy fiber sprouting and neuron densities in hippocampal and lesional seizures. J Neurosurg 82: 211-219.

McAllister, A.K., Katz, L.C., Lo, D.C. (1999) Neurotrophins and synaptic plasticity. Annu. Rev. Neurosci. 22, 295-318.

McEachern J.C. and Shaw C. A., (1999) The plasticity-pathology continuum: defining a role for the LTP phenomenon. J. Neurosci. Res. 58: 42-61.

McIntyre DC, Racine RJ. (1986) Kindling mechanisms: current progress on an experimental epilepsy model. Prog Neurobiol. 27(1):1-12.

McIntyre DC, Edson N. (1989) Kindling-based status epilepticus: effect of norepinephrine depletion with 6-hydroxydopamine. Exp Neurol 104(1):10-4.

McIntyre DC, Kelly ME, Dufresne C. (1999a) FAST and SLOW amygdala kindling rat strains: comparison of amygdala, hippocampal, piriform and perirhinal cortex kindling. Epilepsy Res 35(3):197-209.

McIntyre DC, Kent P, Hayley S, Merali Z, Anisman H. (1999b) Influence of psychogenic and neurogenic stressors on neuroendocrine and central monoamine activity in fast and slow kindling rats. Brain Res 840(1-2):65-74.

McNamara RK, Lenox RH. (2000) Differential regulation of primary protein kinase C substrate (MARCKS, MLP, GAP-43, RC3) mRNAs in the hippocampus during kainic acid-induced seizures and synaptic reorganization. J Neurosci Res. 62(3):416-26.

Meima L., Kljavin I.J., moran P., Shih A., Winslow J.W., and Caras I.W., (1997) Al-1-induced growth cone collapse of rat cortical neurons is correlated with REK expression and rearrangement of the actin cytoskeleton. Euro. J Neurosci. 9: 177-188.

Mello LE, Cavalheiro EA, Tan AM, Kupfer WR, Pretorius JK, Babb TL, Finch DM. (1993) Circuit mechanisms of seizures in the pilocarpine model of chronic epilepsy: cell loss and mossy fiber sprouting. Epilepsia. 34(6):985-95.

Merlio, J.P., Ernfors, P., Kokaia, Z., Middlemas, D.S., Bengzon, J., Kokaia, M, Smith, M.L., Siesjo, B.K., Hunter, T., Lindvall, O., Persson, H. (1993) Increased production of the TrkB protein tyrosine kinase receptor after brain insults. Neuron 10, 151-164.

Michael O. Poulter, Leslie A. Brown, Stephen Tynan, Gordon Willick, Ross William, and Dan C. McIntyre Differential Expression of α1, α2, α3, and α5 GABAA Receptor Subunits in Seizure-Prone and Seizure-Resistant Rat Models of Temporal Lobe Epilepsy J. Neurosci. 1999 19: 4654-4661.

Mohapel P, McIntyre DC. (1998) Amygdala kindling-resistant (SLOW) or -prone (FAST) rat strains show differential fear responses. Behav Neurosci 112(6):1402-13.

Moreno-Flores M. T. and Wandosell F., (19??) Up-regulation of Eph tyrosine kinase receptors after excitotoxic injury in adult hippocampus. Neuroscience 91(1): 193-201.

Morfini, G., DiTella, M.C., Feiguin, F., Carri, N., Caceres, A. (1994) Neurotrophin-3 enhances neurite outgrowth in cultured hippocampal pyramidal neurons. J. Neurosci. Res. 39, 219-232.

Morgan JI, Curran T. (1991) Proto-oncogene transcription factors and epilepsy.Trends Pharmacol Sci. 12(9):343-9.

Morimoto, K., Sato, K., Sato, S., Yamada, N., Hayabara, T. (1998) Time-dependent changes in neurotrophic factor mRNA expression after kindling and long-term potentiation in rats. Brain Research Bull. 45, 599-605.

Mudo G, Jiang XH, Timmusk T, Bindoni M, Belluardo N. (1996) Change in neurotrophins and their receptor mRNAs in the rat forebrain after status epilepticus induced by pilocarpine. Epilepsia 37, 198-207.

Nadler JV (1981) Kainic acid as a tool for the study of temporal lobe epilepsy. Life Sci. 29: 289-300.

Naquet R., Silva-Barrat C., and Menini C. (1995) Reflex epilepsy in the Papio-papio baboon, particularly photosensitive epilepsy. Ital J Neurol Sci. 16(1-2):119-25.

Noebels J.L. (1995) Single locus mutations in mice expressing generalized spike-wave absence epilepsies. Ital J Neurol Sci. 16(1-2):107-11.

Noebels J.L., (1999) Single-gene models of epilepsy. Adv Neurol. 79:227-238.

O'Reilly R.C. and McClelland JL (1994) Hippocampal conjunctive encoding, storage and recall: Avoiding a trade-off. Hippocampus 4(6):661-82.

Okazaki MM and Nadler JV (1988) Protective effects of mossy fiber lesions against kainic acid induced seizures and neuronal degeneration. Neuroscience 26: 763-781.

Olney JW, Collins RC, Sloviter RS (1986) Excitotoxic mechanisms of epileptic brain damage. In: Delgado-Escueta AV, Ward AA, Woodbury DM, Porter RJ. Eds. Basic

Mechanisms of the epilepsies: molecular and cellular approaches, Vol 44. New York: Raven Press: 857-877.

Osehobo, P., Adams, B., Sazgar, M., Xu, Y., Racine, R.J., Fahnestock, M. (1999) Brain-derived neurotrophic factor infusion delays amygdala and perforant path kindling without affecting paired-pulse measures of neuronal inhibition in adult rats. Neuroscience 92, 1367-1375.

Oudega, M. & Hagg, T. (1999) Neurotrophins promote regeneration of sensory axons in the adult rat spinal cord. Brain Res. 818, 431-438.

Papaz JW. (1937) A proposed mechanism of emotion. Arch Neurol Psychiat 38: 725-743.

Parent JM, and Lowenstein DH. (1997) Mossy fiber reorganization in the epileptic hippocampus. Curr Opin Neurol. 10(2):103-9.

Parent JM, Janumpalli S, McNamara JO, Lowenstein DH. (1998) Increased dentate granule cell neurogenesis following amygdala kindling in the adult rat. Neurosci Lett, 247(1):9-12.

Parent JM, Tada E, Fike JR, Lowenstein DH. (1999) Inhibition of dentate granule cell neurogenesis with brain irradiation does not prevent seizure-induced mossy fiber synaptic reorganization in the rat. J Neurosci. 19(11):4508-19.

Parent JM, Yu TW, Leibowitz RT, Geschwind DH, Sloviter RS, Lowenstein DH.(1997) Dentate granule cell neurogenesis is increased by seizures and contributes to aberrant network reorganization in the adult rat hippocampus. J Neurosci. 17(10):3727-38.

Poulter MO, Ohannesian L, Larmet Y, Feltz P (1997) Evidence that $GABA_A$ receptor subunit mRNA expression during development is regulated by $GABA_A$ receptor stimulation. J Neurochem 68:631-639.

Proper EA, Jansen GH, van Veelen CW, van Rijen PC, Gispen WH, de Graan PN. (2001) A grading system for hippocampal sclerosis based on the degree of hippocampal mossy fiber sprouting. Acta Neuropathol (Berl). 101(4):405-9.

Racine R.J. (1972) Modification of seizure activity by electrical stimulation. II. Motor seizure. Electroencephalogr Clin Neurophysiol. 32(3): 281-294.

Racine R. (1978) Kindling: the first decade.Neurosurgery. 3(2):234-52.

Racine R, Steigert MO, IcIntyre DC (1999) Development of kindling-prone and kindling-resistant rats: selective breeding and electrophysiological studies. Epilepsy Res, 35:183-195.

Ramirez-Amaya V, Sandoval J, Mejia J, Escobar ML, Bermudez-Rattoni F (2000) NMDA antagonist blocks the acquisition of Morris water maze and mossy fiber sprouting. Soc. Neurosci. 26: 196.

Reibel, S., Larmet, Y., Le, B., Carnahan, J., Marescaux, C., Depaulis, A. (2000a) Brain-derived neurotrophic factor delays hippocampal kindling in the rat. Neuroscience 100, 777-788.

Reibel, S., Larmet, Y., Carnahan, J., Marescaux, C., Depaulis, A. (2000b) Endogenous control of hippocampal epileptogenesis: a molecular cascade involving brain-derived neurotrophic factor and neuropeptide Y. Epilepsia 41 Suppl 6, S127-S133.

Represa A, Ben-Ari Y. (1997) Molecular and cellular cascades in seizure-induced neosynapse formation. Adv Neurol. 72:25-34.

Represa A, Jorquera I, Le Gal La Salle G, Ben-Ari Y. (1993) Epilepsy induced collateral sprouting of hippocampal mossy fibers: Does it induce the development of ectopic synapses with granule cell dendrites? Hippocampus 3(3): 257-268.

Represa A, Robain O, Tremblay E, and Ben-Ari Y. (1989) Hippocampal plasticity in childhood epilepsy. Neurosci. Lett. 99: 351-355.

Represa A, Tremblay E and Ben-Ari Y (1987) Kainate binding sites in the hippocampal mossy fibers; localization and plasticity. Neurosci. 20: 739-748.

Represa A. and Ben-Ari Y., (1992) Kindling is associated with the formation of novel mossy fiber synapses in the CA3 region. Exp. Brain Res. 92: 69-78.

Rocamora, N., Massieu, L., Boddeke, H.W., Palacios, J.M., Mengod, G. (1994) Differential regulation of the expression of nerve growth factor, brain-derived neurotrophic factor and neurotrophin-3 mRNAs in adult rat brain after intrahippocampal injection of quinolinic acid. Mol. Brain Res. 26, 89-98.

Rocamora, N., Palacios, J.M. Mengod, G. (1992) Limbic seizures induce a differential regulation of the expression of nerve growth factor, brain-derived neurotrophic factor and neurotrophin-3, in the rat hippocampus. Mol. Brain Res. 13, 27-33.

Rosahl T.W., Spillane D., Missler M., Herz J., Selig D.K., Wolff J.R., Hammer R.E., Malenka R.C., Sudhof T.C., (1995) Essential functions of synapsins I and II in synaptic vesicle regulation. Nature. 375(6531): 488-493.

Rudge, J.S., Mather, P.E., Pasnikowshi, E.M., Cai, N., Corcoran, T., Acheson, A., Anderson, K., Lindsay, R.M., Weigand, S.J. (1998) Endogenous BDNF protein is increased in adult rat hippocampus after a kainic acid induced excitotoxic insult but

exogenous BDNF is not neuroprotective. Exp. Neurol. 149, 398-410.

Ryden, M. & Ibanez, C.F. (1996) Binding of neurotrophin-3 to p75LNGFR, TrkA, and TrkB mediated by a single functional epitope distinct from that recognized by trkC. J. Biol. Chem. 271, 5623-5627.

Sankar R, Shin D, Liu H, Katsumori H, Wasterlain CG. (2000) Granule cell neurogenesis after status epilepticus in the immature rat brain. Epilepsia. 2000;41 Suppl 6:S53-6.

Saper CB. (1996) Any way you cut it: a new journal policy for the use of unbiased counting methods. J Comp Neurol. 364(1):5.

Schmidt-Kastner, R. & Olson, L. (1995) Decrease of neurotrophin-3 mRNA in adult rat hippocampus after pilocarpine seizures. Exp Neurol. 136(2), 199-204.

Schwarzer C, Tsunashima K, Wanzenbock C, Fuchs K, Sieghart W, Sperk G. GABA(A) receptor subunits in the rat hippocampus II: altered distribution in kainic acid-induced temporal lobe epilepsy. Neuroscience 80(4):1001-17.

Scott BW, Wojtowicz JM, Burnham WM. Related Articles (2000) Neurogenesis in the dentate gyrus of the rat following electroconvulsive shock seizures. Exp Neurol. 165(2):231-6.

Shinozaki H and Konishi S (1970) Actions of several antihelminthics and insecticides on rats cortical neurons. Brain Res. 24: 368-371.

Sloviter R.S., Dempster D.W. (1985) "Epileptic" brain damage is replicated qualitatively in the rat hippocampus by central injection of glutamate or aspartate but not by GABA or acetylcholine. Brain Res Bull. 15(1): 39-60.

Sloviter RS. (1992) Possible functional consequences of synaptic reorganization in the dentate gyrus of kainite-treated rats. Neurosci Lett 137: 91-96.

Sloviter, RS (1999) Epilepsia, 40 (Suppl. 1):S34-S39.

Sommerfeld, M.T., Schweigreiter, R., Barde, Y.A., Hoppe, E. (2000) Down-regulation of the neurotrophin receptor TrkB following ligand binding. J. Biol. Chem. 275, 8982-8990.

Sommor W. (1880) Erkrankung des ammonshorns als aetiologisches moment der epilepsie Arch Psychiatr Nervenkr 10:631-675.

Sperk G, Schwarzer C, Tsunashima K, Fuchs K, Sieghart W. (1997) GABA(A) receptor subunits in the rat hippocampus I: immunocytochemical distribution of 13 subunits. Neuroscience 80(4):987-1000.

Spiller AE, Racine RJ. (1994) The effect of kindling beyond the 'stage 5' criterion on paired-pulse depression and hilar cell counts in the dentate gyrus. Brain Res. 635(1-2):139-47.

Sutula T, He XX, Cavazos J, Scott G (1988) Synaptic reorganization in the hippocampus induced by abnormal functional activity. Science 239: 1147-1150.

Sutula T., and Steward O, (1986) Quantitative analysis of synaptic potentiation during kindling of the perforant path. J. Neurophysiol 56: 732-746.

Sutula, T., Cascino, G., Cavazos, J., Parada, I., &Ramirez, L. (1989). Mossy fiber synaptic reorganization in the epileptic human temporal lobe. Ann of Neurol, 26, 321-330.

Sutula, T., Xiao-Xian, H, Cavazos, J. and Scotte, G., (1988) Synaptic reorganization in the hippocampus induced by abnormal functional activity. Science, 239: 1147-1150.

Suzuki J., Nakamoto Y., (1977) Seizure patterns and electroencephalograms of E1 mouse.

Electroencephalogr Clin Neurophysiol. 43(3): 299-311.

Tailairach J, and Bancaud J (1974) Stereotoxic exploration and therapy in epilepsy in Vinken PJ, Bruyn CW eds. Handbook of clinical neurology Vol 15. The epilepsies. Msterdan North Holland: 758-782.

Tecott L.H., Sun L.M., Akana S.F., Strack A.M., Lowenstein D.H., Dallman M.F., and Julius D., (1995) Eating disorder and epilepsy in mice lacking 5-HT2c serotonin receptors. Nature. 374(6522):542-546.

Tessier-Lavigne M. (1995) Eph receptor tyrosine kinases, axon repulsion, and the development of topographic maps. Cell, 82: 345-348.

Teter B, Harris-White ME, Frautschy SA, Cole GM. (1999) Role of apolipoprotein E and estrogen in mossy fiber sprouting in hippocampal slice cultures. Neuroscience 91(3): 1009-16.

Tsunashima K, Schwarzer C, Kirchmair E, Sieghart W, Sperk G. (1997) GABA(A) receptor subunits in the rat hippocampus III: altered messenger RNA expression in kainic acid-induced epilepsy. Neuroscience 80(4):1019-32.

Turski WA, Cavalheiro EA, Schwarz M, Czuczwar SJ, Kleinrok Z, Turski L.(1983a) Limbic seizures produced by pilocarpine in rats: behavioral, electroencephalographic and neuropathological study. Behav Brain Res 9: 315-335.

Turski WA, Czuczwar SJ, Kleinrok Z, Turski L. (1983) Cholinominetics produce seizures and brain damage in rat. Experientia 39: 1408-1411.

Tuunanen J, Pitkanen A. (2000) Do seizures cause neuronal damage in rat amygdala kindling? Epilepsy Res. 39(2):171-6.

Van der Zee, C.E.E.M, Rashid, K., Le, K., Moore, K.A., Stanisz, J., Diamond, J., Racine, R.J., Fahnestock, M. (1995) Intraventricular administration of antibodies to NGF retards kindling and blocks mossy fiber sprouting in adult rats. J. Neurosci. 15, 5316-5323.

Van Luijtelaar, and Coenen A.M., (1986) Two types of electrocortical paroxysms in an inbred strain of rats. Neurosci Lett. 70(3):393-7.

West MJ. (1993) New stereological methods for counting neurons. Neurobiol Aging. 14(4):275-85.

West MJ. (1999) Stereological methods for estimating the total number of neurons and synapses: Issues of precision and bias. Trends Neurosci. 22(2):51-61.

Winslow J.W., Moran P., Valverde J., Shih A., Yuan J.Q., Wong S. C., Tsai S.P., Goddard A., Henzel W. J., Hefti F., Beck K., and Caras I.W., (1995) Cloning of AL-1, a ligand for an Eph-related tyrosine kinase receptor involved in axon bundle formation. Neuron, 14: 973-981.

Wuarin J, Dudek FE (1996) Electrographic seizures and new recurrent excitatory circuit in the dentate gyrus of hippocampal slices from kainite-treated epileptic rats. J Neurosci 15(4): 4438-4448.

Wuarin JP, Dudek FE. (2001) Excitatory synaptic input to granule cells increases with time after kainate treatment. J Neurophysiol. 85(3):1067-77.

Zhang J.H., Cerretti D.P., Yu T., Flanagan J.G., Zhou R.P., (1996) Detection of ligands in regions anatomically connected to neurons expressing the Eph receptor Bsk: potential roles in neuron-target interaction. J. Neurosci. 16(22): 7182-7192.

Zhang N, and Houser CR. (1999), Ultrastructural localization of dynorphin in the dentate gyrus in human temporal lobe epilepsy: a study of reorganized mossy fiber synapses. J Comp Neurol. 1999 405(4):472-90.

Zhang, Y., Dijkhuizen, P.A., Anderson, P.N., Lieberman, A.R., Verhaagen, J. (1998) NT-3 delivered by an adenoviral vector induces injured dorsal root axons to regenerate into the spinal cord of adult rats. J. Neurosci. Res. 54, 554-562.

Zhou R., Copeland T.D., Kromer L.F., and Schulz N.T., (1994) Isolation and characterization of BSK, a growth factor receptor-like tyrosine kinase associated with the limbic system. J. Neurosci. Res. 37: 129-143.

Zhou, X.F. & Rush, R.A. (1994) Localization of neurotrophin-3-like immunoreactivity in the rat central nervous system. Brain Res. 643, 162-172.